21:40:53 OCA PAD AMENDMENT - PROJECT HEADER INFORMATION 06/10/91

Active

Project #: E-18-609 Cost share #: E-18-322 Rev #: 1
Center # : 10/24-6-R6996-0A0 Center shr #: 10/22-1-F6996-00 OCA file #:
Work type : RES
Contract#: DMR-9013098 Mod #: AMEND 01 Document : GRANT
Prime #: Contract entity: GTRC

Subprojects ? : N CFDA:
Main project #: PE #:

Project unit: MAT ENGR Unit code: 02.010.112
Project director(s):
GOKHALE A M MAT ENGR (404)894-2887
UNDERWOOD E E MAT ENGR (404)-

Sponsor/division names: NATL SCIENCE FOUNDATION / GENERAL
Sponsor/division codes: 107 / 000

Award period: 900715 to 921231 (performance) 940331 (reports)

Sponsor amount	New this change	Total to date
Contract value	0.00	291,300.00
Funded	97,100.00	194,200.00
Cost sharing amount		19,412.00

Does subcontracting plan apply ?: N

Title: QUANTITATIVE ANALYSIS OF FRACTURE SURFACES USING STEREOLOGICAL METHODS

PROJECT ADMINISTRATION DATA

OCA contact: Mildred S. Heyser 894-4820

Sponsor technical contact

KRISHAN K. CHAWLA
(202)357-9789

NATIONAL SCIENCE FOUNDATION
1800 G STREET, N.W.
WASHINGTON, D.C. 20550

Sponsor issuing office

JEFFREY S. LEITHEAD
(202)357-9843

NATIONAL SCIENCE FOUNDATION
1800 G STREET, NW
WASHINGTON, D.C. 20550

Security class (U,C,S,TS) : U ONR resident rep. is ACO (Y/N): N
Defense priority rating : N/A NSF supplemental sheet
Equipment title vests with: Sponsor GIT X

Administrative comments -
AMEND 1 ADDS $97,100 AND EXTENDS PERIOD OF PERFORMANCE THROUGH 12/31/92.

GEORGIA INSTITUTE OF TECHNOLOGY
OFFICE OF CONTRACT ADMINISTRATION

NOTICE OF PROJECT CLOSEOUT

Closeout Notice Date 03/03/95

Project No. E-18-609 Center No. 10/24-6-R6996-0A0

Project Director GOKHALE A M School/Lab MSE

Sponsor NATL SCIENCE FOUNDATION/GENERAL

Contract/Grant No. DMR-9013098 Contract Entity GTRC

Prime Contract No.

Title QUANTITATIVE ANALYSIS OF FRACTURE SURFACES USING STEREOLOGICAL METHODS

Effective Completion Date 931231 (Performance) 940331 (Reports)

Closeout Actions Required:	Y/N	Date Submitted
Final Invoice or Copy of Final Invoice	N	
Final Report of Inventions and/or Subcontracts	N	
Government Property Inventory & Related Certificate	N	
Classified Material Certificate	N	
Release and Assignment	N	
Other	N	

Comments
LETTER OF CREDIT APPLIES. 98A SATISFIES PATENT REQUIREMENT.

Subproject Under Main Project No.

Continues Project No.

Distribution Required:

Project Director	Y
Administrative Network Representative	Y
GTRI Accounting/Grants and Contracts	Y
Procurement/Supply Services	Y
Research Property Managment	Y
Research Security Services	N
Reports Coordinator (OCA)	Y
GTRC	Y
Project File	Y
Other	N
	N

RENEWAL RESEARCH PROSAL
ON

QUANTITATIVE ANALYS OF FRACTURE SURFACES UNG STEREOLOGICAL METDS

Submitted to

National Science Fouration
Division of Materials search

by

School of Materials Engiering and
Mechanical Properties Rearch Lab
Georgia Institute of Tchnology
Atlanta, Georgia 303-0245

A.M. Gokhale
Principal Investigor

Approved by

S.D. Antolovich,
Director
School of Materials Engineering

W.M. Sangster
Dean
College of Engineering

Contracting Offier

TABLE OF CONTENTS

Copies of five recent papers on stereology, by the P.I., are enclosed (these papers are extensively referred to in the project description).

PROJECT SUMMARY

The objective of this research is to develop general and practical stereological techniques for the geometric characterization of the fracture surfaces and the microstructural features in three dimensional space. The proposed research is based on the solid foundation developed in the areas of theoretical stereology, computer simulations, and experimental measurement techniques during the research work on the present NSF sponsored project "Quantitative Analysis of Fracture Surfaces Using Stereological Methods" at Georgia Tech. The following research efforts are proposed for the next three years.

(1) Development of the stereological techniques for the estimation of the spatial distribution of the microstructural features (for example, inclusions, voids, etc.) in three-dimensional microstructure and in the fracture surfaces, from the measurements performed on the plane sections.

(2) Development of efficient stereological procedures for the quantification of anisotropy of fracture surfaces and microstructural features, from the measurements performed on the plane sections. It is also proposed to devote a part of the effort for the development of design based stereological procedures for reliable estimation of the global microstructural properties of anisotropic microstructures from the measurements performed on a few sectioning planes or projected images.

(3) Quantification of the fractal characteristics and surface roughness behavior of the fracture surfaces in three dimensional space from the measurements performed on the fracture profiles, without any assumptions whatsoever.

(4) Experimental measurements of the stereological attributes in the microstructures and fracture surfaces of 4340 steel, metal matrix composite having continuous unidirectional fibers of Al_2O_3 in Al-Li matrix, and creep test specimens of copper, to demonstrate the practical applications of the new stereological procedures.

RESULTS FROM PRIOR NSF SUPPORT

Title: Quantitative Analysis of Fracture Surfaces Using Stereological Methods

Grant Number: DMR-8504167
Funding Period: 8/15/85 to 7/31/90
Amount of Support: $332,300
P.I.: A.M. Gokhale (from July, 1989)

The basic objective of this research is to develop general and efficient stereological procedures for the geometric quantification of fracture surfaces and microstructural features. Such rigorous quantification can provide important input concerning the role of microstructure in the deformation and fracture processes, evolution of microstructural damage, interpretation of fracture toughness and fatigue crack growth data, etc. The techniques are equally applicable to biological structures. The stereological techniques are also useful for the characterization of microstructural evolution during solid state transformations and materials processing.

This project is vital for the development of quantitative fractography and stereology; Georgia Tech has received significant recognition in these areas, particularly due to the results from this project. Significant new results have emerged during the past two years, and there is an excellent potential for fruitful developments in the future. The progress during the last two years is discussed briefly; the earlier results are reported in a number of publications (the list is enclosed).

(I) Geometric Quantification of Fracture Surfaces: Vertical section profilometry and digital image analysis techniques have been established for the quantification of the fracture profiles; the feasibility of these methods has been demonstrated via extensive experimental measurements. These results are given in a chapter in ASM Handbook (1987, 9th ed., vol. 12) and a number of other publications.

Recently, we have developed a geometrically general, statistically exact, unambiguous, and assumption-free stereological relationship for the estimation of fracture surface roughness parameter R_s from the measurements of profile roughness parameter R_L and the angular orientation distribution function of the line elements in the vertical section fracture profiles, $f(\alpha)$. It is shown that;

$$R_s = \overline{R_L . \Psi} \qquad (1)$$

where,

$$\Psi = \int_0^{\pi} [\sin\alpha + (\tfrac{\pi}{2} - \alpha) \cos\alpha] f(\alpha) d\alpha \qquad (2)$$

R_s is precisely equal to the expected value of the product $R_L \psi$ in the vertical sections. Equation (1) is a fundamental relationship; it is equally applicable to anisotropic fracture surfaces, where R_L may vary with the vertical sectioning plane orientation (see Figure - 1). Using computer simulations and design based statistical sampling techniques we have shown that the measurements on at the most three vertical sections (mutually at 120°) are sufficient for a reliable estimate of the roughness of any fracture

surface (using equation - (1)). These results are recently reported in two paper in press at Metall. Trans. (papers (3) and (4); copies are enclosed). It is proposed to utilize these results to investigate the following.

(a) We now have a unique opportunity to rigorously investigate the fractal behavior of real 'surfaces'in three-dimensional space, by measuring R_L and ψ as a function of the ruler length; estimation of R_s (using equation (1)) as a function of ruler length should provide the necessary fractal data without involving any assumptions. Note that most of the earlier experimental investigations of fractal behavior were concerned only with 'lines'in a plane.

(b) Equation (1) is equally applicable to a set of discontinuous identifiable segments of fracture surface. Thus, a host of 'local' and 'semi-global' roughness parameters can be defined, and they can be estimated from the corresponding measurements on the fracture profiles without involving any assumptions whatsoever. These parameters may provide new quantitative information on the operative fracture micromechanisms.

(c) Assumption-free estimation of surface roughness will be utilized to develop experimental correlations with toughness, and finally with the fracture toughness.

We have also developed an approximate but simple parametric equation for calculation of R_s of isotropic fracture surface from the measurement of only R_L on a single vertical section (paper no. 1). The procedure is useful for quick estimation of R_s for the

quantitative analysis of the SEM images. In another contribution, we systematically investigated the criteria for the selection of optimum resolution for quantification of the fracture profiles (paper no. 2). The P.I. has recently developed a stereological equation which relates the orientation distribution function (ODF) of the surface elements on fracture surface, and the angular orientation distribution function of the line elements on the fracture profile (PDF); the two distributions are related through an integral equation. This development generalizes the results of Scriven and Williams for equiaxed, monosize, planar grain boundary facets having rotationally symmetric anisotropy; no such assumptions are involved in our equation. We propose to continue this work to develop a practical and efficient procedure for the estimation of fracture surface anisotropy; analytical theoretical work as well as computer simulations will be utilized for this purpose. We propose to correlate the ODF of the fracture surface to the anisotropy of bulk microstructure; such correlations should be useful for understanding the effect of microstructural anisotropy on the fracture behavior.

(II) Development of Design Based Stereology: Assumption-free experimental estimation of microstructural properties of anisotropic microstructures has been quite troublesome: too many measurements on too many sectioning planes are necessary to obtain reliable and unbiased estimates of the microstructural attributes. However, design based stereology is developing rapidly: the test probe shape (for example, cycloid shape test lines), orientation,

and sectioning plane (or foil) orientations are chosen by statistical design such that limited measurements performed on a few sectioning planes lead to representative isotropic sampling of the structure which then yields reliable and unbiased estimates of microstructural attributes, without any assumptions whatsoever. The P.I. has contributed significantly to these developments; copies of three recent contributions sent to Journal of Microscopy (paper no. 5,7,8) are enclosed. The main results are as follows:

(1) Internal surface area of any anisotropic features can be estimated from the design based measurements performed on just three specific sectioning planes (paper no. 7).

(2) Total length of anisotropic lineal features can be efficiently estimated from the design based intercept counts on the projected images (paper no. 5).

(3) Microstructural anisotropy can be efficiently quantified via intercept counts using specific design based test line shapes (paper no. 8).

We propose to continue our research efforts in this area via analytical theoretical work and computer simulations.

(III) Experimental Work: Our recent experimental measurements are on metal matrix composite (MMC) consisting of unidirectional continuous Al_2O_3 fibers in Al-Li alloy matrix. We have studied fatigue, and tensile fracture surfaces as a function of fiber orientation with respect to the stress axis, and in specimens having different fiber volume fractions. The profilometric measurements involved global profile roughness parameter R_L,

separate profile roughness of fibers and matrix, R_L^f and R_L^m, and angular orientation distribution of profile line elements of fibers and matrix. The SEM fractographic measurements involved true area fraction and number densities of the processing defects such as voids, oxide inclusions, overgrown fibers, and broken fibers. The stereological measurements were performed on plane sections through bulk material to estimate the volume fractions of different processing defects and their number densities. Further, nearest neighbor distance distribution of fiber section centers on a plane section perpendicular to fibers was measured from digitized centroid coordinates; the radial distribution function of these fiber section centers was also calculated from the centroid coordinates data.

Monte Carlo simulations of the spatial distribution of fiber sections was carried out with nonoverlaping circles constraint. We have developed software to generate vertical sections of anisotropic ruled surfaces at different orientations. The profile roughness and profile element angular orientation distribution can be calculated for any vertical section orientation. Computer simulation sectioning of anisotropic internal boundaries in microstructure by vertical sectioning planes is also carried out.

The nearest neighbor distance distribution of fiber section centers and Monte Carlo simulations have led to objective measures of clustering/ordering tendency of fibers in MMC. The data should be useful for developing stochastic models of deformation and fracture processes in MMC. Computer simulations of sectioning of

fracture surfaces and anisotropic internal boundaries in microstructure have resulted in very efficient stereological sampling procedures (paper no. 2,7). Quantitative measurements of area fractions and number densities of processing defects in the fracture surface and their values on a sectioning plane through the microstructure have led to important information concerning the role of processing defects in the deformation and fracture of MMC (see paper no. 9).

THESIS ACKNOWLEDGING NSF SUPPORT

Name	degree	year
K. Banerji	Ph.D.	June 1986
K. Ringel	M.S.	July 1988
W.J. Drury	M.S.	November 1988

PUBLICATIONS ACKNOWLEDGING NSF SUPPORT

1. A.M. Gokhale and E.E. Underwood; "A New Parametric Roughness Equation for Quantitative Fractography", Acta Stereologica, 1989, vol. 8, pp. 43-52.

2. A.M. Gokhale and K. Banerji; "Criteria for Selecting Optimum Resolution for Quantitative Analysis of Fracture Surfaces", Microstructural Science, 1989, vol. 17, pp. 67-79.

3. A.M. Gokhale and E.E. Underwood; "A General Method for Measurement of Fracture Surface Roughness-I; Theoretical Aspects", Metall. Trans.-A, in press.

4. A.M. Gokhale and W.J. Drury; "A General Method for Measurement of Fracture Surface Roughness-II; Practical Considerations", Metall. Trans.-A, in press.

5. A.M. Gokhale; "Unbiased Estimation of Curve Length in 3D Using Vertical Slices", Journal of Microscopy, in press.

6. S.D. Antolovich, A.M. Gokhale, and C. Bathias; "Application of Quantitative Fractography and Computed Tomography to Fracture Processes in Materials", ASTM Special Tech. Pub., No. 1085, in press.

7. A.M. Gokhale and W.J. Drury; "Efficient Vertical Sections: The Trisector", Journal of Microscopy, submitted.

8. A.M. Gokhale; "Design Based Test Lines for Efficient Measurement of Anisotropy", Journal of Microscopy, submitted.

9. W.J. Drury; "Involvement of Processing Defects in Failure of FP/Al-Li", Metall. Trans-A, 1989, vol. 20A, pp 2175-2179.

10. E.E. Underwood; "Recent Advances in Quantitative Fractography", in Fracture Mechanics: Microstructures and Mechanisms, ed. by S.V. Nair, et al., ASM International, 1989, 87-109.

11. E.E. Underwood; "The Current Status of Modern Quantitative Fractography", Proc. Seventh Int. Conf. on Fracture (ed. by K. Salama, et al.), Advances in Fracture Research, Pergamon Press, Vol. 5, 1989, 3391-3409.

12. E.E. Underwood; "Evaluation of Overlaps in Fracture Surfaces", MiCon 90: Advances in Video Technology for Microstructural Control, ASTM STP 1094, ed. by G.F. Vander Voort, American Society for Testing and Materials, Philadelphia, 1990. Submitted.

13. E.E. Underwood; "Treatment of Reversed Sigmoidal Curves for Fractal Analysis", ibid. Submitted.

14. E.E. Underwood and K. Banerji; "Quantitative Fractography", In Vol. 12 Fractography, ASM Handbook Series, 9th Ed., 1987, 193-210.

15. E.E. Underwood and K. Banerji; "Fractal Analysis of Fracture Surfaces", ibid., 211-215.

16. W.J. Drury, K. Banerji and E.E. Underwood, ; "Metallographic and Fractographic Analyses of MMC Microstructures. **Leadoff paper**, Proc. Advanced Materials Conference, TMS, Denver, CO, 1987, 279-287.

17. E.E. Underwood; "Stereological Analysis of Fracture Roughness Parameters", 25th Memorial Volume of the Int. Soc. for Stereology, ed. by M. Kalisnik, Ljubljana, Yugoslavia, 1987, 169-178.

18. E.E. Underwood and W.J. Drury; "Quantitative Fractographic Analysis of Oriented Fracture Surfaces". Proc. 7th Int. Congr. for Stereology, Caen, France, ed. by M. Kalisnik, Ljubljana, Yugoslavia, 1987, 549-554.

19. E.E. Underwood; "The Analysis of Nonplanar Surfaces by Stereological and Other Methods", **Keynote Lecture** in Session on Nonplanar Surfaces, ibid., 855-876.

20. E.E. Underwood and K. Banerji; "On Estimating the Fracture Surface Area of Al-%Cu Alloys". Microstructural Science, Vol. 13, ed. by S.A. Shiels, et al., Philadelphia, PA, 1986, 537-551.

21. E.E. Underwood; "Estimating Feature Characteristics by Quantitative Fractography", Jnl. Metals, Vol. 38, No. 4, 1986, 30-32.

22. E.E. Underwood and K.Banerji; "Fractals in Fractography", **Invited Review**, Mats. Sci. and Eng., Vol. 80, 1986, 1-14.

CURRENT AND PENDING SUPPORT

A.M. Gokhale

Source of Support	Project title	Award	Funding Period	Effort	Location
NSF	1	$332,300	8/85-7/90	2 months (summer)	Ga. Tech

E.E. Underwood

Source of Support	Project title	Award	Funding Period	Effort	Location
NSF	1	$332,300	8/85-7/90	2 months (cal.)	Ga. Tech

project titles

1. Quantitative Analysis of Fracture Surfaces Using Stereological Methods.

PROJECT DESCRIPTION

(1) INTRODUCTION:

The end point of deformation and fracture processes is the generation of fracture surface. The local and global geometry of fracture surface and its microstructural features are dictated by the material chemistry, bulk microstructure, and the processes that lead to fracture. The materials science literature abounds with a number of contributions where the observations on the fracture surfaces are related to the processes responsible for fracture[1-10]. With the developments of quantitative theories and models for the fracture processes which incorporate microstructural and fractographic parameters[11-25], it is important to develop rigorous quantitative techniques for the characterization of fracture surface geometry and the geometry of bulk microstructure. In this way, the predictive capabilities of the theories can be fully exploited, and the objective experimental quantitative correlations between the microstructure and the fracture behavior can be developed. The basic objective of the proposed research is to develop the required general stereological procedures which are statistically exact, unambiguous, unbiased, and efficient. There has been a significant progress in stereology[26-46] during the past five years or so; the Georgia Tech group has contributed significantly to these developments, particularly because of the results that have emerged from this project work. A solid foundation has been developed in the areas of analytical theoretical concepts,[32-34,38,39,41] computer simulations,[33,42] and the

experimental techniques,[35,36,46] due to the work done in this project, which provides the necessary frame work for the proposed research.

During the next three years, we propose to direct our research efforts in the following areas.

(1) 3D Nearest Neighbor Distributions: Development of stereological procedures for the estimation of the nearest neighbor distance distribution of the features in the three dimensional microstructure from the measurements performed on the plane sections or projected images needs significant attention. We propose to develop a general procedure applicable to features of any size or size distributions, and for any locational distribution (not necessarily random). The related statistics background does exist for such development[44,52]. However, considerable amount of analytical theoretical work, computer simulations and experimental measurements are necessary,and we propose to put our efforts in this direction. The nearest neighbor distance distribution and average nearest neighbor distance are very important parameters in dimpled fracture by microvoid coalescence[11,21,22] creep fracture by intergranular cavitation[19-20], effect of inclusions on fracture process[13], etc. These parameters are also important in the theories of particle coarsening[47-49], and microstructural evolution during recrystallization, where the nucleation sites are inclusions or second-phase particles[50], etc. It is important to emphasize that at present such stereological procedures are not available, either for microstructural features on fracture surface or in

three-dimensional structures, except for the case of randomly distributed point particles[52].

(2) Anisotropy: Development of efficient general stereological techniques for the measurement of anisotropy of fracture surfaces (angular orientation distribution function of the surface elements) from the measurements performed on the fracture profiles require lot of attention. This topic is of prime importance, especially for composite materials. We have already made a beginning in this direction. However, significant additional work is necessary; the details are given in the next section. Development of design based stereological procedures for efficient estimation of microstructural and fractographic properties from limited measurements performed on a few sectioning planes need more attention. We have made significant contributions to these developments recently[32-34] (copies of three papers are enclosed). We propose to continue analytical theoretical work, computer simulations, and experimental measurements for further development of this important area. A part of our efforts would be to develop the computer software, so that the design based measurements can be performed automatically by our recently acquired Zeiss VIDAS image analysis system.

(3) Surface Roughness and Fractals: A general method for measurement of surface area of any nonplanar surface is now available[41,42] (copies of appropriate papers are enclosed). This is a major development in the field. We propose to define a number of 'local' and 'semiglobal' roughness parameters and estimate these

parameters experimentally from the corresponding measurements on the fracture profiles. These measurements should provide additional information on the fracture micromechanisms. Our general relationship for measurement of fracture surface roughness[41-42] provides us a unique opportunity to study the fractal behavior of nonplanar fracture '<u>surfaces</u>' in three-dimensional space, from the measurements performed on the vertical section fracture profiles, without any assumptions whatsoever. We propose to carry out the required experimental measurements to examine this fractal behavior. The experimental work will be complemented by computer simulations of the fractal behavior. Note that most of the previous investigations were on profiles or 'lines' in a plane. The fractal characteristics of fracture profiles have been utilized to detect temper embrittlement[53], and correlations with fracture toughness[54], and with crack propagation rate[55] are claimed. The true fractal characteristics of fracture 'surfaces' are expected to be even more useful, as the sectioning bias is eliminated. From an abstract point of view, these data should be of importance in the development of the fractal geometry of 'surfaces' in three-dimensional space.

(4) <u>Experimental Work</u>: While the above proposed research topics will involve extensive experimental measurements, our major thrust is on the development of stereological techniques rather than generation of mechanical and fracture properties data. With this consideration, we propose to carry out experimental work on the fracture surfaces of tensile, impact, and fracture toughness

conditions samples of 4340 steel with different microstructures and initial deformation. It is proposed to continue our work on unidirectional continuous Al_2O_3 fibers - (Al-Li) alloy matrix composites. We will investigate the effects of initial damage (introduced by high and/or low temperature thermal cycling)[72,73] on the mechanical and fracture behavior of this composite, and the evolution of damage during tensile tests. We have already initiated the fabrication of the set up for thermal cycling. We also propose to study the evolution of intergranular creep cavities during high temperature creep in copper, with the major emphasis on the quantification of the nearest neighbor distance distribution of the cavities on the grain boundaries. This input should extremely useful for modelling the microstructural evolution of cavities[20].

The above discussion gives the brief account of the proposed research, its relation to our previous work, and its relevance to the modern research efforts in areas of mechanical and fracture behavior of materials, microstructural evolution during solid state transformation and materials processing, etc. Our research efforts are also expected to provide useful input in other sciences as well. Freeze fracture surfaces are often utilized to study biological structures[56]; our results on nonplanar fracture surfaces are equally applicable to such surfaces. The stereological techniques are also utilized for research in the areas of pathology[57], anatomy[58], neuroscience[59], histopathology[60], botany[61], geology[62], petrography[63], characterization of

concretes[64], etc. Thus, stereology research is relevant to many disciplines across the board where internal microscopic structure is of interest; our general results will be of relevance in such disciplines.

(2) PROPOSED RESEARCH:

The basic objective of the proposed research is the development of general procedures for the geometric quantification of the fracture surfaces and microstructures using stereological principles. The different aspects of the research are interlinked; the basic components are analytical theoretical work, computer simulations and calculations, specialized software development for digital image analysis, experimental measurements, and correlations of the measured attributes with the deformation and fracture process descriptors, to demonstrate the utility of the new stereological procedures.

There has been significant progress in stereology during last five years. The general stereological equations are now available for unbiased estimation of the number of particles (features) per unit volume using the 'disector' and related test probes[26,29]. The first, second and third moments of the volume distribution of particles of <u>arbitrary</u> shapes ($\bar{V}$, $\bar{V}^2$, and $\bar{V}^3$) are accessible via plane section measurements or limited serial sectioning[31]. The global properties such as volume fraction, total surface area, integral mean curvature, etc. can be, estimated of course, from the measurements on random plane sections[70,71]. However, little attention has been given to the following aspects of the

microstructure characterization; these attributes are of significant importance in the deformation and fracture behavior of materials, and microstructural evolution processes.

(i) spatial distribution of microstructural features in three-dimensional microstructure, in terms of nearest neighbor distance distributions.

(ii) Stereology of anisotropic microstructures, particularly, the development of efficient procedures for the quantification of anisotropy and global properties from the limited number of measurements performed on a few sectioning planes.

There have been significant advances which concern the stereology of fracture surfaces. A major development[41,42], which has emerged from the research efforts in this project, concerns assumption-free estimation of fracture surface roughness from the measurements performed on the vertical section fracture profiles. This progress provides the necessary vital input for the following:

(i) Fractal analysis of nonplanar, rough fracture surfaces in three-dimensional space from the measurements performed on just three vertical section fracture profiles.

(ii) Development of the stereological procedures for the estimation of the 'local' and 'semiglobal' roughness parameters, without any assumptions; such parameters should provide information on fracture micromechanisms.

(iii) Development of objective and unbiased quantitative correlations of surface roughness with the fracture process parameters such as toughness and fracture toughness. Assumption-

free estimation of surface roughness will ensure that the observed correlations are real, and that real correlations are observed.

Development of stereological procedures for the estimation of the following attributes of the fracture surfaces need significant attention:

(i) Angular orientation distribution of the anisotropic fracture surfaces, and

(ii) Spatial distribution of the microstructural features in the fracture surfaces.

Taking the above considerations into account, it is proposed to focus our research efforts on the following topics:

(1) Estimation of nearest neighbor distance distributions in three-dimensional microstructures and fracture surfaces.

(2) Efficient procedures for stereological characterization of anisotropy of fracture surfaces and microstructures, and for the estimation of the global properties of the anisotropic microstructures.

(3) Surface roughness and fractal behavior of nonplanar fracture surfaces.

(4) Experimental work to demonstrate the feasibility and applications of the new stereological techniques.

The following subsections describe the proposed research on the above topics and the proposed experimental research program.

(2.1) 3D Nearest Neighbor Distributions: Consider an ensemble of particles in a three-dimensional microstructure. It is desired to measure average or expected distribution of the center to center nearest neighbor distances between these particles, $G(x)$. Thus, $G(x)dx$ is the average probability that there is no other particle

center in a sphere of radius x drawn around the center of an arbitrary particle and there is at least one particle center in a spherical shell of radii x and (x + dx). Recently, the P.I. has shown that the nearest neighbor distribution function G(x) is related to the radial distribution function of the particle centers in three dimensional space $\bar{\phi}_v$ (x) as follows.

$$G(x) = 4\pi x^2 . \bar{N}_v . \bar{\phi}_v(x) . \; Exp\{-\int_o^x 4\pi x^2 \bar{N}_v \phi_v(x) dx\} \qquad (3)$$

where, $\bar{N}_v$ is the average number of particle centers per unit volume. For randomly distributed point particles (zero size) equation (3) reduces to the classical result given by Chandrasekhar[51], because for this special case $\bar{\phi}_v(x)$ is equal to one. However, equation (3) is also applicable to the finite size particles of any arbitrary size distribution, and not necessarily random locations. The average nearest neighbor distance $\bar{x}$ is simply given by;

$$\bar{x} = \int_o^\infty x \; . \; G(x) dx \qquad (4)$$

The radial distribution function $\bar{\phi}_v(x)$ in three dimensional space is related to the measurable radial distribution function of the particle section centers in a random two dimensional sectioning plane through microstructure $\bar{\phi}_A(x)$, as follows[44,52].

$$\bar{\phi}_A(x) = \frac{1}{4(\bar{R})^2} \; . \; \int_o^\infty \gamma(u) \; . \; \bar{\phi}_v \; [(x^2 + u^2)^{\frac{1}{2}}] \; . \; du \qquad (5)$$

where,

$$\gamma(u) = 2 \int_o^\infty [1 - F\{\frac{|u-v|}{2}\}] \; [1 - F\{\frac{u + v}{2}\}] \; dv \qquad (6)$$

$\bar{R}$ is the average particle size, and F is the cumulative frequency function of the particle sizes. Note that equation (5) is applicable to the spherical particles of any arbitrary size distribution, and volume fraction; the locations of the particle centers need not be random. According to Hanish, Konig and Stoyan[44], equation (5) is an excellent approximation for nonspherical but equiaxed particles. The radial distribution function of the particle section centers in the metallographic plane of polish, $\bar{\phi}_A(x)$, can be experimentally measured; we have developed the software to extract $\bar{\phi}_A(x)$ from the digital image analysis data. Figure - 2 shows the experimentally measured $\bar{\phi}_A(x)$ for the fiber section centers in a metal matrix composite containing unidirectional continuous Al_2O_3 fibers in Al-Li alloy matrix. Thus, equations (3) to (6) provide the necessary frame work for the estimation of the average nearest neighbor distance distribution and the average nearest neighbor distance between the particles (voids, inclusions, etc.) in three dimensional microstructure from the measurements performed on the metallographic sections. It is proposed to utilize this background for the following

(i) Development of efficient computer code to obtain numerical solution to equation (5) so that $\bar{\phi}_V(x)$ can be calculated from measured $\Phi_A(x)$.

(ii) Verification of the accuracy of the numerical solution by computer simulations.

(iii) Experimental measurements of the nearest neighbor distribution of inclusions in 4340 steel specimens.

(iv) Modification of equations (3) to (6) for the estimation of nearest neighbor distribution of intergranular creep cavities on the grain boundary facets. This is possible because the statistics of sectioning of spheres in three dimensional microstructure by a sectioning plane, and circles (areas of grain boundary occupied by cavities) in a plane (grain boundary facets) by straight lines are very similar[74]. Thus, equations (3) to (6) can be modified. One can observe the cavity sections on the grain boundary traces (which can be regarded as test lines on the grain boundary facets) in a metallographic sectioning plane, and the 'linear' radial distribution of the cavity sections along the grain boundary traces can be experimentally measured. These input data can be utilized to estimate the nearest neighbor distribution of the cavities on the grain boundary facets. We propose to carry out these measurements on interrupted creep test samples of copper.

(v) It is proposed to utilize equations (3) to (6), and their appropriate modifications to experimentally measure the nearest neighbor distance distribution of inclusions near the fracture surfaces of tensile, impact, and fracture toughness test specimens of 4340 steel specimens.

(vi) It is proposed to extend the concepts contained in equations (3) to (6) to develop the stereological procedures to quantify the spatial distribution of surface elements and lineal features in microstructures; some theoretical results for the

lineal features are available in the literature[44].

[2.2] Anisotropy: The basic input data required for the quantitative estimation of the anisotropy of the internal boundaries in three microstructure consist of the measurements of the number of intersections of straight test lines with the internal boundaries in three dimensional microstructure, as a function of test line orientation in three dimensional space. Let $I_L(\theta,\phi)$ be the average number of intersections of a straight test line of unit length having orientation (θ,ϕ) (see Figure - 3) with the internal boundaries of interest. Hilliard[65] has given a general procedure for the estimation of the angular orientation distribution function (ODF) of the internal boundaries from the experimentally measured $I_L(\theta,\phi)$. In practice, it is necessary perform the intersection counts on straight test lines of different orientations (typically, eighteen equally spaced orientations in the range 0° to 180°, with respect to a reference direction) in a sectioning plane of known orientation; the measurements are then repeated on different sectioning planes of different known angular orientations. Translated in simple terms, this implies measurements on too many straight test lines of different orientations. This is perhaps the reason for very small number of assumption free experimental measurements of anisotropy, although the required stereological relationships are available for more than twenty years[65].

It is thus of interest to devise the sampling procedure such that the intersection counts on few test lines of specific shapes

(not straight test lines) yield the required information, $I_L(\theta,\phi)$. In a recent contribution[34] (a copy is enclosed), the P.I. has shown that this is indeed possible: intersection counts pertaining to few test lines of specific shapes, yield the necessary information on the variation of intersection counts of straight test lines as a function of orientation in the sectioning plane. It is shown that intersection counts of test lines of specific shapes directly yield the coefficients of the Fourier series which describes variation of intersection counts of straight test line as a function of orientation. As few terms of the Fourier series are usually sufficient, the intersection counts on few design based test lines can yield the required information in a very efficient manner. It is proposed to continue this work and focus our efforts in the following areas.

(i) Direct estimation of the coefficients of spherical harmonics of the orientation distribution function of the internal boundaries in three dimensional microstructure from the intersection counts pertaining to few design based test lines on few sectioning planes. We propose to analyze this problem via analytical theoretical work as well as computer simulations.

(ii) Development of automatic image analysis software to count the intersections with the test lines of design based shapes automatically. Preliminary work has been initiated in this direction: we have programed our VIDAS image analyzer to count the intersections of internal boundary traces with cycloid shape test lines (see Figure - 4).

(iii) Experimental measurements of the angular orientation distribution function of the internal boundaries in deformed 4340 steel specimens, grain boundary facets containing creep cavities (in copper), and anisotropy of microstructural damage in metal-matrix composite specimens.

Quantification of anisotropy of fracture surfaces is a related problem, but it requires an entirely different approach. This is because the sampling with test lines (of any shape) is <u>not</u> practically feasible in the case of fracture surfaces (see enclosed paper on surface roughness for related discussion). In this case, the basic input data are the angular orientation distribution function of the <u>line</u> elements on the fracture profiles, which can be obtained via digital image analysis[35,36]; we have the necessary computer code to calculate the orientation distribution of the fracture profiles from the digitized co-ordinates data. To develop the basic ideas, let the direction normal to average fracture surface plane be the reference direction or vertical axis, and Z-axis of the frame of reference. Any metallographic plane containing the vertical axis (Z-axis) is called vertical sectioning plane, and the resulting fracture profile is called vertical section fracture profile (see Figure - 5). Thus, vertical axis (Z-axis) can be identified in any vertical section and the angle between the vertical axis and a line element on the fracture profile, α, can be measured. The frequency function of the occurrence of the α values along the various line elements of the fracture profile is the angular orientation distribution of the fracture profile (PDF),

which can be experimentally measured (see Figure - 1). In general PDF depends on the nature of the anisotropy of the fracture surface and the orientation of the vertical sectioning plane ϕ_p (see Figure - 5). Let $f(\alpha,\phi_p)$ be the PDF of vertical section fracture profile generated from the vertical sectioning plane of orientation ϕ_p. Let $g(\theta,\phi)$ be the angular orientation distribution function (ODF) of the surface elements on the fracture surface; θ is angle between normal to a surface element and vertical axis (Z-axis), and ϕ is the angle between the projection of this surface normal on xy plane, and x-axis (see Figure - 3). Note that $g(\theta,\phi)$ is the quantitative measure of fracture surface anisotropy: $g(\theta,\phi)\sin\theta d\theta\, d\phi/2\pi$ is equal to the fraction of fracture surface area having the orientation in the range θ to $(\theta+d\theta)$ and ϕ to $(\phi + d\phi)$. One can experimentally measure $f(\alpha,\phi_p)$ and $g(\theta,\phi)$ is to be estimated from this information. The P.I. has recently derived the following relationship which connects these two distribution functions.

$$f(\alpha,\phi_p) = \frac{R_s}{R_L(\phi_p)} \cdot \frac{1}{\xi^2} \int_{-\xi}^{+\xi} \frac{\eta^2 g(\theta,\phi)\, d\eta}{[\xi^2-\eta^2]^{\frac{1}{2}}} \qquad (7)$$

where, $\eta=\cos\theta$, $\xi = \sin\alpha$, R_s is the surface roughness parameter[68] (true fracture surface area divided by projected area on plane normal to vertical axis), and $R_L(\phi_p)$ is the profile roughness parameter[69] (true profile length divided by projected length on line perpendicular to the vertical axis and in the sectioning plane). The integral in equation (7) is similar to path integral; ϕ values that appear in $g(\theta,\phi)$ must be along the following path.

$$\sin(\phi - \phi_p) = \cot\theta \cot\alpha \qquad (8)$$

Equation (7) generalizes the result given by Scriven and Williams() for equiaxed monosize grain boundary facets having rotationally symmetric orientation distribution function; there are no assumptions involved in equation (7). For rotationally symmetric fracture surface anisotropy, $g(\theta,\phi)$ does not depend on ϕ, and hence all vertical section fracture profiles are statistically similar, thus $f(\alpha,\phi_p)$ does not depend on vertical section orientation ϕ_p and it is symmetric around vertical axis. In such a case equation (7) reduces to the following form.

$$f(\alpha) = \frac{R_s}{R_L} \cdot \frac{1}{\xi^2} \int_0^{\xi} \frac{\eta^2 g(\theta)\, d\eta}{[\xi^2-\eta^2]^{\frac{1}{2}}} \qquad (9)$$

For rotationally symmetric ODF, one can estimate $g(\theta)$ from measurement of $f(\alpha)$ in just one vertical section fracture profile, we have the computer program for these calculations. However, estimation of ODF which is rotationally <u>asymmetric</u> (for example, fracture surfaces of anisotropic material such as composites) is still problematic although equation (7) provides the required stereological relationship. The following efforts are proposed to obtain practically feasible solution to this knotty problem.

(i) An average ODF $\bar{g}(\theta)$ can be defined by averaging $g(\theta,\phi)$ over all ϕ values. This average ODF $\bar{g}(\theta)$ can be calculated from measured average $\bar{f}(\alpha)$ obtained from few fracture profiles of different orientations ϕ_p. This average $\bar{g}(\theta)$ can give the basis for modelling the functional form of $g(\theta,\phi)$ with unknown but adjustable parameters.

(ii) Once $g(\theta,\phi)$ is modelled, $f(\alpha,\phi_p)$ can be calculated using equation (7) and it can be compared with the experimentally measured profile distributions; the values of the adjustable model parameters which yield calculated PDF's matching the experimental distributions can then yield the information on the ODF $g(\theta,\phi)$.

(iii) The computer simulated surfaces of known ODF $g(\theta,\phi)$ will be utilized to cross check the applicability of the procedures in (i) and (ii).

(iv) An effort will be made to obtain a direct solution to equation (7) by expanding both $g(\theta,\phi)$ and $f(\alpha,\phi_p)$ in terms of a series of spherical harmonics of unknown coefficients; the unknown spherical harmonics coefficients of $g(\theta,\phi)$ should be then accessible from known coefficients of $f(\alpha,\phi_p)$ obtained from the experimental data.

(v) Once a suitable procedure is developed, it is proposed to estimate the ODF of the fracture surfaces of deformed 4340 steel specimens and the metal matrix composites, and to correlate the anisotropy of the fracture surface to the anisotropy of the bulk microstructure. The results should be useful to understand the effect of microstructural anisotropy on the deformation and fracture behavior.

The microstructural anisotropy affects the deformation and fracture behavior of materials. The advance materials such as composites usually have anisotropic microstructures, which lead to fracture surfaces that are also anisotropic. The stress distribution, operative deformation and fracture processes, and the

microstructural anisotropy determine the anisotropy of fracture surface. Thus, the measurements of fracture surface anisotropy and microstructural anisotropy are useful for understanding the deformation and fracture behavior of anisotropic materials. The measurement of the angular orientation distribution function of fracture surfaces should provide important input for the interpretation of the Mode - III fracture toughness data[12,17,18]; these data should be also useful for understanding the fatigue crack growth behavior[16].

Another aspect of the stereology of anisotropic microstructures which needs further attention, is the design based sampling procedures for the estimation of the global properties of anisotropic microstructures (surface area, integral mean curvature, total line length, etc.) from the limited number of measurements performed on a <u>few</u> sectioning planes. The P.I. has contributed to the recent developments in this area[32-34] (copies of three recent papers are enclosed). It is now possible to reliably estimate the total area of the internal boundaries in microstructure having any arbitrary anisotropy from the measurements on just three sectioning planes mutually at an angle of 120°, and having a common direction[33] (vertical axis); the intersection counts must be performed using cycloid test lines having a specific orientation[30] (see Figure - 3). The total line length of anisotropic lineal features (for example, dislocation lines) can be estimated via similar measurements on <u>projected</u> images[32] (for example, TEM images). It is proposed to continue these efforts via analytical

theoretical work and computer calculations/simulations. The experimental measurements will involve estimation of total area of intergranular creep cavities, and microstructural damage in MMC. These developments should be important for the quantification of partially anisotropic and anisotropic microstructures.

[2.3] Surface Roughness and Fractal Behavior: We have developed assumption free stereological equation for the estimation of surface roughness of any nonplanar, rough fracture surface from the measurements performed on the vertical section fracture profiles; the procedure is very efficient as the measurements on at the most three vertical sections (mutually at 120°) yield a reliable estimate of the surface roughness parameter R_s, without any assumptions whatsoever[41,42] (copies of two related papers are enclosed). It is proposed to apply this technique to fracture surfaces of tensile, impact and the fracture toughness specimens of 4340 steel having different microstructures, and initial deformation. The results will be utilized to correlate the microstructurally induced variations in the and fracture toughness to the surface roughness. The assumption-free estimation of surface roughness is imperative to detect the true correlations.

The surface roughness is a fundamental attribute of the fracture surfaces; the value of the surface roughness parameter R_s is required for quantitative measurements on SEM images of fracture surfaces which involve normalization by the area of the fracture surface (for example, number of microstrucural features per unit fracture surface area), because the area of the field of view n the

SEM image is the projected area (and not true area) of the fracture surface[35,36]. The tortuosity of the fracture surface quantified by surface roughness is important for understanding the role of microstructure in the deformation and fracture processes. The surface roughness is also extremely useful for the interpretation of mode - III fracture toughness data[12,17,18] and fatigue crack growth behavior[16]. Recently Garrison[67] has observed an interesting correlation trend between profile roughness and fracture initiation toughness in some high strength steels; the assumption-free measurements of surface roughness should be extremely useful in detecting quantitative correlations, as the sectioning bias is eliminated.

Our general method for the estimation of the surface roughness parameter R_s provides us with a unique opportunity to investigate the fractal behavior of the 'surfaces' in three dimensional space from the measurements performed on fracture profiles; R_s can be now estimated as function of ruler length η to generate the required fractal data. These measurements will be performed on the fracture surfaces of tensile, impact and fracture toughness test specimens of 4340 steel having different microstructures. It is likely that R_s will approach a finite saturation value R_s^o at small values of η. The fractal dimension pertaining to such 'semifractal' behavior may correlate to the parameters such as fracture toughness. An attempt will also be made to correlate the surface roughness and fractal dimension values of the tensile fracture surfaces of metal matrix composite having different initial microstructural damage (induced

by thermal cycling) to the area under the stress strain curves.

Till now two different approaches have been utilized to quantify the roughness or tortuosity of the fracture surfaces; one involves roughness parameters (usually profile roughness), and the second involves fractal dimension of fracture profiles. However, if the roughness is basically due to fractal characteristics or vice versa, then the saturation value of the surface roughness parameter R_s^o may be related to the fractal dimension pertaining to the semifractal characteristics. Our experimental data will give us an opportunity to detect the correlation between R_s^o and the fractal dimension pertaining to the 'semifractal' behavior of the fracture surfaces. Such correlations will unify the two different approaches to quantify surface roughness. On the other hand, lack of correlation would indicate that <u>both</u> R_s^o and fractal dimension may be necessary to explore the quantitative correlations with the fracture process descriptors.

The general stereological procedure for the estimation of the surface roughness parameter R_s is equally applicable to a set of identifiable discontinuous regions of the fracture surface. For example, average 'local' roughness around the second phase particles (or fibers etc.) can be estimated from the similar measurements on the fracture profiles. Roughness of transgranular and intergranular regions of fracture surface can be separately measured as well, such 'semiglobal' roughness values should provide useful input on the micromechanisms of fracture. It is proposed to rigorously define such 'local' and 'semiglobal roughness

parameters and measure their values in the fracture surfaces under investigation.

[2.4] Experimental Work: It is proposed to do the experiments on three materials: 4340 steel, pure copper, and metal matrix composites containing continuous unidirectional Al_2O_3 fibers in (Al-Li) alloy matrix. Different mechanical tests will be performed on these materials to generate the fracture surfaces.

[2.4.1] Experiments on 4340 Steel: Appropriate hardening and tempering heat treatments will be utilized to generate a series of specimens having different microstructures, strength and toughness values. Tensile, impact, and fracture toughness tests will be performed on these samples. Further, a few interrupted tensile test specimens will be utilized to investigate evolution of microvoids in few samples. A few samples of 4340 steel will be given initial deformation by rolling; the tensile test specimens made from these samples will be utilized to investigate the correlation between the microstructural anisotropy and the anisotropy manifested on the fracture surfaces. The stereological measurements involve nearest neighbor distance distribution of inclusions in the bulk material, detailed characterization of microstructures using design based and classical stereological techniques, characterization of anisotropy of microvoids, and grain boundaries, etc. The fractographic measurements will consist of measurement of surface roughness parameters, fractal characteristics, nearest neighbor distribution and average nearest neighbor distance near the fracture surface, and the fracture

surface anisotropy.

[2.4.2] Experiments on Copper: It is proposed to perform a few isothermal interrupted creep tests on specimens of copper at constant uniaxial load. The stereological measurements will involve nearest neighbor distribution of intergranular cavities on the grain boundary facets, anisotropy of cavities and cavitating grain boundary facets, and global microstructural properties using design based stereology.

[2.4.3.] Experiments on Metal Matrix Composite: The mechanical properties of metal matrix composites are sensitive to the presence of processing defects such as reaction zones, processing voids, etc., which essentially constitute microstructural damage. One way to systematically investigate the effect of initial microstructural damage on the mechanical behavior of these composites is to introduce controlled amounts of microstructural damage by combination of high and low temperature thermal cycling[72,73]. The experimental set up required for thermal cycling is being assembled in our laboratory. We propose to generate a series of samples with different extents of microstructural damage and quantify the damage (which is expected to be anisotropic) using the design based stereological procedures. The tensile tests will be performed on these specimens to generate fracture surface. We propose to quantify the damage observed in the fracture surfaces of tensile specimens. The quantitative measurements in the fracture surface, bulk microstructure, and mechanical tensile test properties will be correlated.

(3) **PLAN OF WORK:**

The analytical theoretical work will continue over the three periods of the proposed research; the theoretical research has yielded significant results during the past two years and it is expected to lead to important developments in the future. During the first year of the funding period, we propose to develop the necessary computer programs for the measurement of nearest neighbor distributions and anisotropy. Simultaneously, the experimental work on 4340 steel will be carried out. It is also proposed to begin the experimental work on the MMC during the first year. The experimental work on the creep tests and the quantification of the creep cavities will be carried out during the second year and a part of the third year of the funding period; the measurements and data-analysis of 4340 steel specimens and MMC will continue during this period. The computer calculations and simulations will aid the data analysis. The third year of the funding period will be devoted to the completion of the creep cavitation work, data analysis, and the development of quantitative correlations of the measured stereological attributes to the parameters of the deformation and fracture process; in this context, additional experimental work will be carried out, if required.

The results of the research work will be reported in scientific journals and in progress reports to NSF; the results will be also presented at important conferences. The publication activities will be, ofcourse, spread over the major portion of the project period.

(4) PROJECT ORGANIZATION

The overall responsibility of the project will rest with the proposed Principal Investigator, Dr. A.M. Gokhale. He will also be the contact person for the administrative matters related to the research project. The proposed P.I. has more than ten years of research experience in the areas of stereology, modelling of global microstructural evolution, and the applications of these disciplines to the materials processes. Dr. Gokhale has been actively involved in the present NSF sponsored project on "Quantitative Evaluation of Fracture Surfaces Using Stereological Methods" over the last two years, and has been the P.I. from July 1989. Dr. Gokhale has contributed significantly to this project and he has authored/coauthored eight papers resulting from his contribution to the project. Dr. Gokhale's expertise will be utilized for analytical theoretical work, computer simulations, and the design and the overall supervision of the experimental program.

Dr. Underwood (proposed Co. P.I.) has more than thirty years of experience in the area of stereology. He has done pioneering work in the area of quantitative fractography. Dr. Underwood was the P.I. of the NSF sponsored project "Quantitative Evaluation of Fracture Surfaces Using Stereological Methods" for the major portion of the funding period. Dr. Underwood is the author of the present classical book "Quantitative Stereology" which is frequently referred to by researchers in stereology all over the world. Dr. Underwood is now Professor Emeritus at Georgia Tech. His rich experience and expertise will provide important inputs to

the proposed research; Dr. Underwood's principal contribution will be as advisor to the overall research program.

IMPACT ON EDUCATION AND HUMAN RESOURCE DEVELOPMENT

Impact on Education

One of the most significant and pervasive trends in modern educational processes is toward quantification, as opposed to qualitative descriptions, in science programs at all levels. This is especially so in courses on microstructural structure in biology, anatomy and materials.

The techniques employed in this research program are completely general. The methods for geometrical quantification apply to any microstructure observed under a microscope. Thus the life sciences and the materials sciences can both profit freely from these powerful, simple and general methods. As Lord Kelvin said many years ago, "...when you can measure what you are speaking about and express it in numbers, you know something about it; but when you cannot express it in numbers, your knowledge is of a meager and unsatisfactory kind; it may be the beginning of knowledge, but you have scarcely in your thoughts advanced to the state of science, whatever the matter may be."

Insofar as these quantitative geometrical methods are appropriate (e.g., in science, research, and teaching), only improvement in the general scientific level is to be expected. This applies equally to both teachers and students. As these new capabilities become better known, and used, it is inevitable that the learning process is accelerated. Ideas become sharper; appreciation for subtle differences in structure, form and texture are revealed; and new application of these powerful techniques suggest themselves readily to the inquiring, receptive mind.

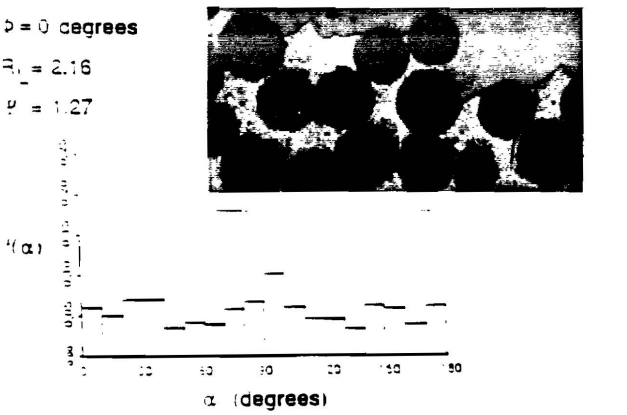

Figure - 1 The Profile roughness parameter R_L of anisotropic fracture surface of metals matrix composite depends on the sectioning plane orientation; the angular distribution of line elements on fracture profile also varies with the sectioning plane orientations.

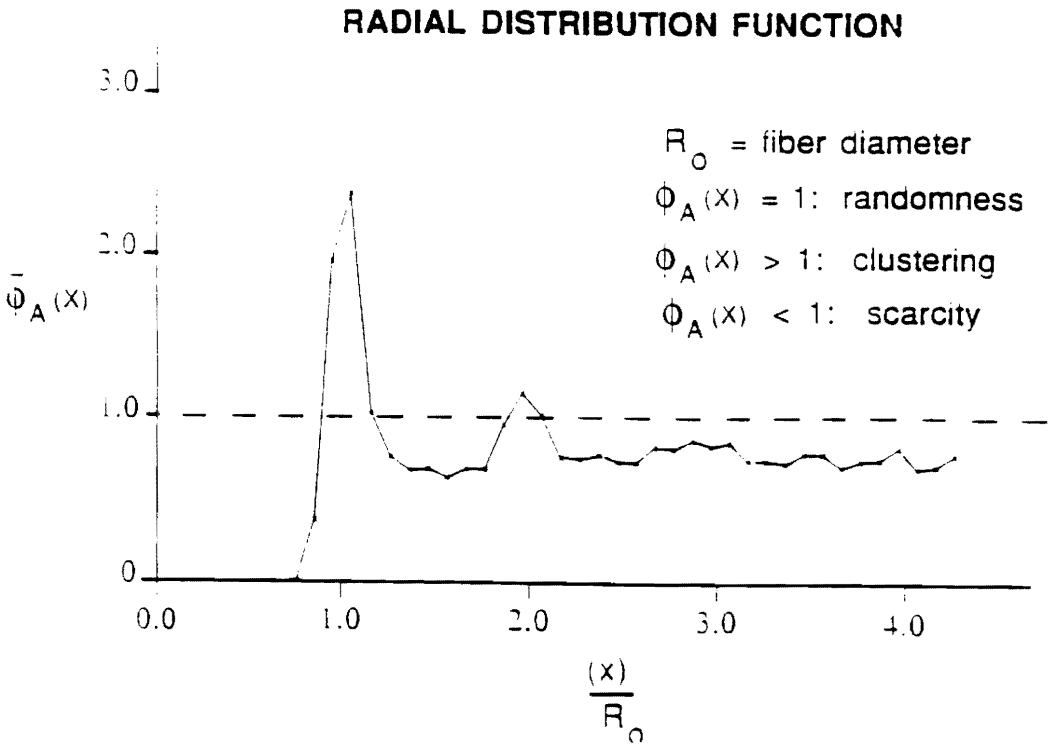

Figure - 2 Experimentally measured radial distribution function $\bar{\phi}_A(x)$ of the fiber section centers in MMC in the sectioning plane perpendicular to the fibers.

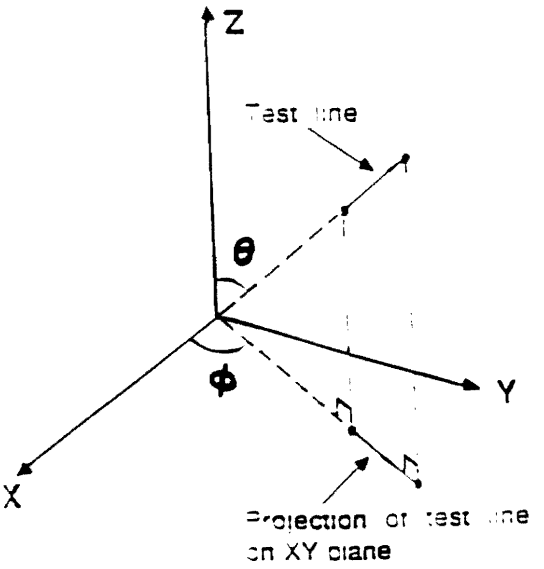

(a)

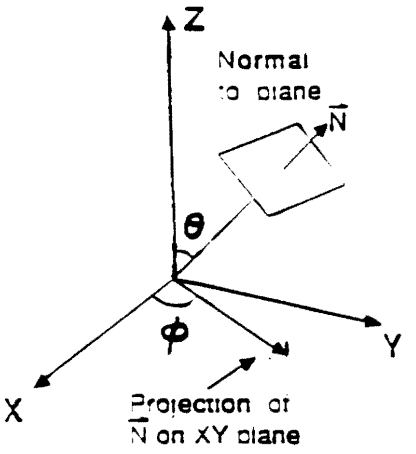

(b)

Figure - 3 (a) Specification of test line orientation by angles θ and ϕ. (b) Specification of the orientation of a surface element.

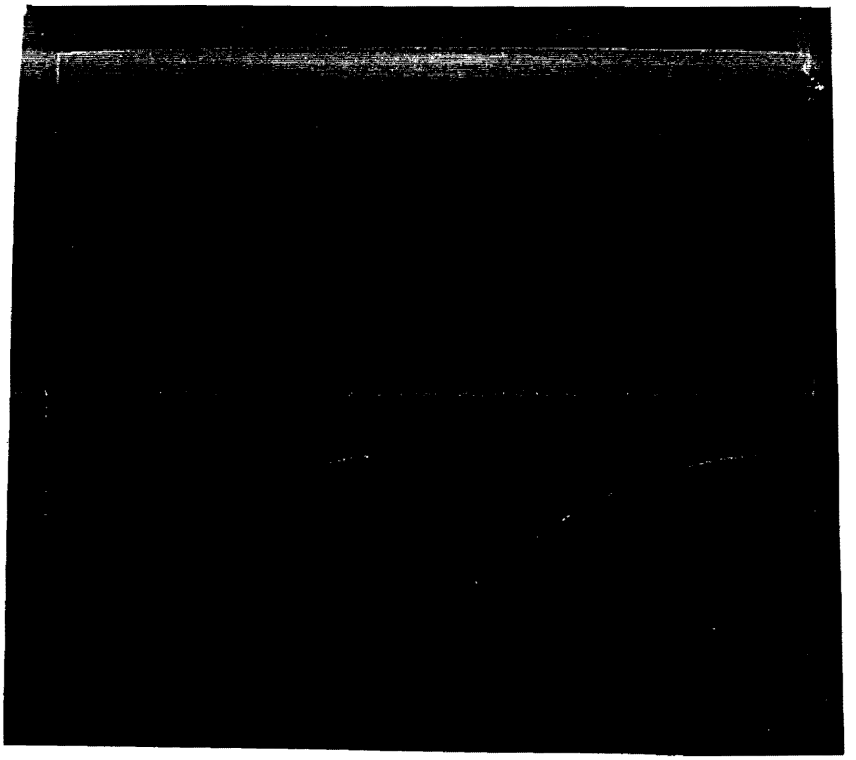

(a)

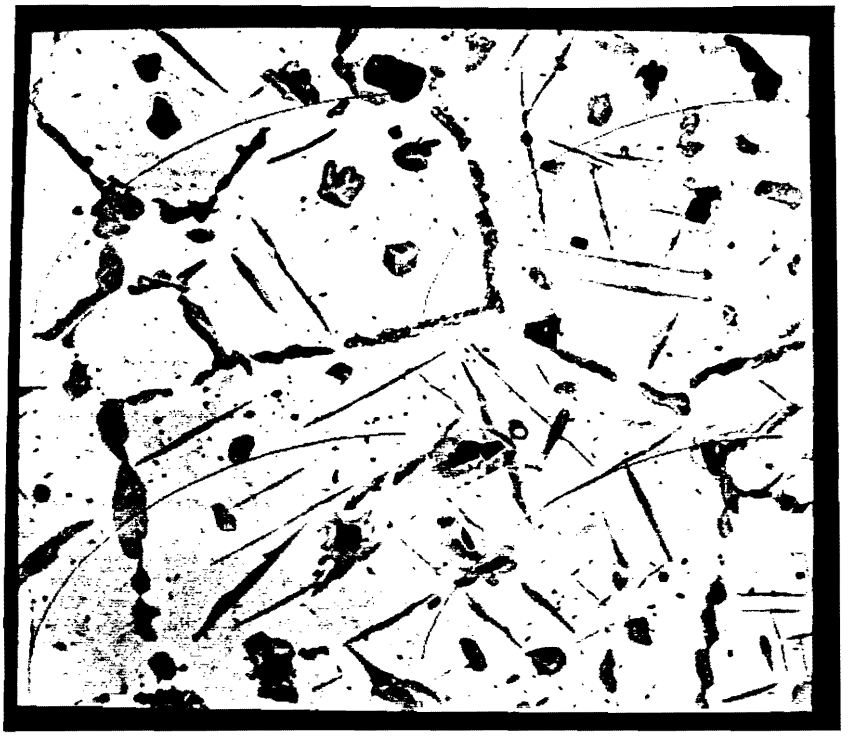

(b)

Figure - 4 (a) Cycloid test lines generated by VIDAS image analyzer. (b) Test lines in (a) overlayed on the microstructure; intersection counts can be performed automatically.

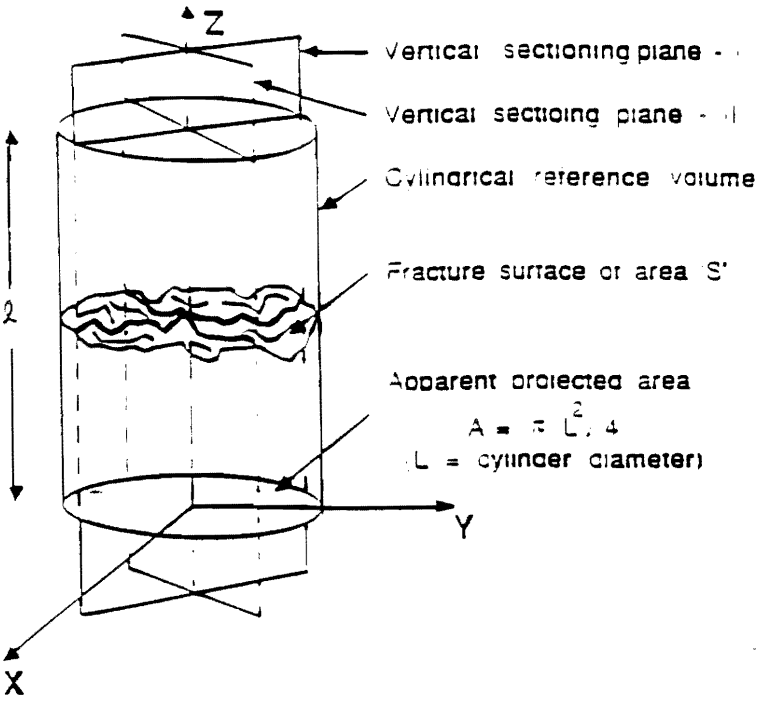

(a)

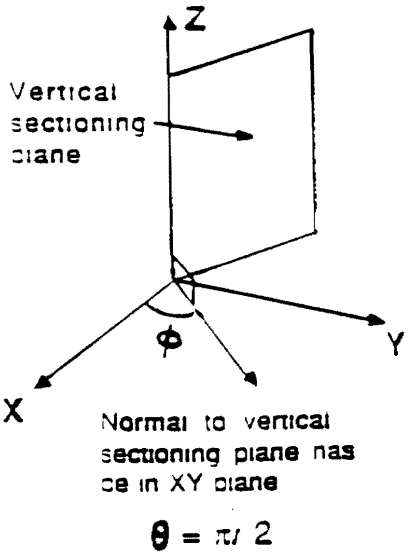

(b)

Figure - 5 (a) Definition of vertical axis, and vertical sectioning plane. (b) Orientation of the vertical sectioning plane.

REFERENCES:

(1) R.H. Van Stone, T.B. Cox, J.R. Low, Jr., and J.A. Psioda, Int. Met. Rev., 1985, Vol.30, pp. 157-179

(2) C.A. Hippsley and S.G. Druce, Acta Met., 1983, vol. 31, pp 1861-1872

(3) A.W. Thompson and J.C. Chestnut, Metall. Trans., 1979, vol. 10A, pp 1193-1196

(4) I.W. Hall, G.R. Brewer, and A. Magata, J. Mat. Sc. Letters, 1989, vol. 8, pp 343-345

(5) H.E. Exner and L.S. Sigl, Metall. Trans. -A, 1987, vol. 18A, pp. 1299-1308

(6) R.H. Van Stone and T.B. Cox,, Fractography - Microscopic Cracking Processes. (ed. by C.D. Beacham and W.R. Warke), 1976, ASTM Spec. Tech. Pub. 600, ASTM Philadelphia, pp 5-29

(7) W.W. Gerberich, S.H. Chen, C.S. Lee, and T. Livne, Metall. Trans. - A, 1987, vol. 18A, pp. 1861-1875.

(8) G.R. Irwin, X.J. Zhang, and R.W. Armstrong, J. Mat. Sc. Letters, 1989, Vol. 8, pp 844-848

(9) X.J. Zhang, R.W. Armstrong, and G.R. Irwin, Metall. Trans.-A, 1989, Vol. 20A, pp. 2862-2866

(10) R. Gurbuz, M. Doruk, and W. Schutz, Advances in Fracture Research, Proc. Int. Conf. on Fracture (eds. K. Salama et al.), Pergamon press, Vol. 5, 3429-3426

(11) R.H. Jones, C.A. Lavender, and M.T. Smith, Scripta Met. 1987, Vol. 21, pp 1565-70

(12) T.S. Gross and D.A. Mendelsohn, Metall. Trans. - A, 1989, Vol. 20A, pp 1988-1999

(13) J.C. Lautridou and A. Pineau, Engg. Fracture Mech, 1981, Vol. 15, pp 55-71.

(14) W.R. Tyson, Metall. Trans. - A, 1989, Vol 20A, pp 2680-2862

(15) K.S.Zhang, L.S. Hua, C.Q. Zheng, and J.C. Radon, Engg. Fracture Mechanics, 1989, Vol. 33, pp 671-677

(16) S. Suresh, Metall. Trans. - A, 1985, Vol. 16A, pp 249-255

(17) E.K. Tschegg and S. Suresh, Metall. Trans.-A, 1988, Vol. 19A, pp 3035-3044

(18) E.K. Tschegg. Acta. Met., 1983, Vol. 31, pp 1323-30

(19) D.S. Wilkinson, Acta Met., 1988, Vol. 36, pp 2055-2063

(20) H. Riedel, Fracture at High Temperature, Materials Science and Engineering Series (eds. B. Ischner and N.J. Grant), Springer-Verlag, New York, 1986.

(21) R. Becker, J. Mech. Phy. Solids, 1987, Vol 35, pp 577-582

(22) W.A. Spitzig, R.E. Smelser, and O. Richmond, Acta Met., 1988, Vol. 36, pp 1201-1211

(23) J. Gurland, Int. Met. Rev., 1988, Vol. 33, pp 151-166

(24) B. Roebuk and E.A. Almond, Int. Met. Rev., 1988, Vol. 33, pp 90-110

(25) J.H. Steele, Jr., Advances in Fracture Research, Proc. Int. Conf. on Fracture (eds. K. Salama, et al.), Pergamon Press, 1989, vol. 5 pp 3449-3456

(26) D.C. Sterio, J. Microscopy, 1987, Vol. 145, pp 127-136

(27) L.M. Cruz-Orive, J. Microscopy, 1987, Vol. 145. pp 121-142

(28) V. Howard, S. Reid, A.J. Baddeley, and A. Boyd, J. Microscopy, 1985, Vol. 138, pp 203-212

(29) H.J.G. Gundersen, J. Microscopy, 1987, Vol. 147, pp. 229-263

(30) A.J. Baddely, H.J.G. Gundersen, and L.M. Cruz-Orive, J. Microscopy, 1985, vol. 138, pp 203-212

(31) H.J.G. Gundersen and E.B. Jenson, J. Microscopy, 1985, Vol. 138, pp 127-142

(32) A.M. Gokhale, Unbiased Estimation of Curve Length in 3D Using Vertical Slices, J. Microscopy, in press (a copy of the paper is enclosed)

(33) A.M. Gokhale and W.J. Drury, Efficient Vertical Sections: The Trisector, J. Microscopy, submitted (a copy of the paper is enclosed)

(34) A.M. Gokhale, Design Based Test Lines for Efficient Measurement of Anisotropy, J. Microscopy, submitted (a copy of the paper is enclosed)

(35) K. Banerji, Metall. Trans. a A, 1988, Vol. 19A, pp 961-971

(36) E.E. Underwood and K. Banerji, ASM Metals Handbook, 1987, 9th ed., Vol. 12, pp. 193-210, ASM International, Metals Park, Ohio.

(37) J.L. Chermant and M. Coster, Precis d'Analyse d'Images, CNRS, Paris, 1985

(38) A.M. Gokhale and E.E. Underwood, Acta Stereologica, 1989, Vol. 8, pp 43-52

(39) A.M. Gokhale, Metallography, 1988, Vol 21, pp. 241-250

(40) R.T. DeHoff, J. Microscopy, 1985, Vol. 138, pp. 143-151

(41) A.M. Gokhale and E.E. Underwood, "A General Method For Measurement of Fracture Surface Roughness - I; Theoretical Aspects", Metall. Trans. - A, in press (a copy of this paper is enclosed).

(42) A.M. Gokhale and W.J. Drury, "A General Method For Measurement of Fracture Surface Roughness - II; Practical Considerations", Metall. Trans.- A, in press (a copy is enclosed).

(43) J.C. Russ, J. Comp. Assisted Microsc., 1989, Vol. 1, pp. 39-77

(44) K.H. Hanish, D. Konig, and D. Stoyan, J. Microscopy, 1985, Vol. 140, pp 361-370

(45) H.E. Exner and M. Fripan, J. Microscopy, 1985, Vol. 138, pp 161-178

(46) G.F. Vander Voort, ASTM Spec. Tech. Pub. No. 987, 1988, pp 226-249

(47) P.W. Voorhees and M.E. Glickman, Acta Met., 1984, Vol. 32, pp 2001-2011

(48) R.T. DeHoff, A Geometrically General Theory of Particle Coarsening, Acta Met., Submitted

(49) P.W. Voorhees, Acta Met., 1988, Vol, 36, pp 207-216

(50) E. Nes and J.K. Solberg, Mater. Sci. Tech., 1986, Vol. 2, pp 19-25

(51) S. Chandrasekhar, Rev. Mod. Phy., 1943, Vol. 15, p. 86

(52) K.H. Hanish and D. Stoyan, J. Microscopy, 1981, Vol. 122, pp. 131-144

(53) K. Banerji and E.E. Underwood, Advances in Fracture Research, Proc. 6th Int. Conf. on Fracture, Pergamon, London, 1984, Vol. 2, pp 371-378

(54) B.B. Manderbolt, D.E. Passoja and A.J. Paullay, Nature, 1984, Vol. 308, pp. 721-722

(55) J.L. Chermant, Chermant, and M. Coster, Advances in Fracture Research, Proc. 7th Int. Conf. on Fracture (ed. K. Salma et. al.), Pergamon press, 1989, Vol. 5, pp 3413-3420

(56) E.R. Weibel, G.A. Losa, and R.P. Bolender; Proc. 4ICS NBS STP 431 (ed. E.E. Underwood, et al.), 1976, pp. 277-280.

(57) A. Brungger and L.M. Cruz-Orive, Arch. Dermatol. Res., 1987, Vol. 279, pp 412-414

(58) E.R. Weibel, Stereological Methods: Practical Methods for Biological Morphometry, Vol. 1., Academic Press, New York, 1980

(59) H. Brandegaard, J. Neurosci. Methods, 1986, Vol. 18, pp 39-78

(60) T. Takahashi and N. Iwama, J. Experi. Med., 1984, Vol. 143, pp. 451-465

(61) R.E. Shanks, Ecology, 1954, Vol. 35 pp. 237-244

(62) S. Gentier and J. Riss, Acta Stereologica, 1987, Vol. 6, pp 223-228

(63) R. Ehrlich, S.K. Kennedy, and R.L. Cannon, J. Sedimentary Petrography, 1984, Vol. 54, pp. 1365-1378

(64) P. Stroeven, Acta Stereologica, 1987, Vol. 6, suppl. 11, pp. 147-156

(65) J.E. Hillard, Trans. Met. Soc. AIME, 1967, Vol. 224, pp. 1201-1211

(66) R.A. Scriven and H.D. Williams, Trans. Met. Soc. AIME, 1965, Vol. 233, pp 1593-1602

(67) W. Garrison, Metall. Trans., in press.

(68) S.M. El-Soudani, Metallography, 1978, Vol. 11, pp 127-130

(69) J.R. Pickens and J. Gurland, Proc. 4th Int. Congr. for Stereology (eds. E.E. Underwood, R. deWit, and G.A. Moore), NBS Special Pub. 431, 1976, pp. 269-272

(70) E.E. Underwood, Quantitative Stereology, Addison-Wesley Pub. Co., Reading, Mass., 1970

(71) R.T. DeHoff and F.N. Rhines (eds.), Quantitative Microscopy, McGraw-Hill, New York, 1968

(72) C.S. Less and K.K. Chawla, Proc. Industry-University Adv. Mat. Conf. (ed. J.G. Morse), T.M.S. Pub., 1987, pp. 289-293.

(73) G.B. Cook and K.K. Chawla, ibid, pp. 297-302

(74) A.M. Gokhale and A.K. Jena, Metallography, 1980, vol. 13, pp. 307-317

PUBLICATIONS FOR MERRIT REVIEW

(I) Five Publications Most Relevant to the Proposed Research

1. A.M. Gokhale and E.E. Underwood; "A General Method for Measurement of Fracture Surface Roughness-I; Theoretical Aspects", Metall. Trans. -A, in press. (copy is enclosed)

2. A.M. Gokhale and W.J. Drury; "A General Method for Measurement of Fracture Surface Roughness-II; Practical considerations", Metall. Trans. -A, in press. (copy is enclosed)

3. A.M. Gokhale; "Unbiased Estimation of Curve Length in 3D Using Vertical Slice", Journal of Microscopy, in press. (copy is enclosed)

4. A.M. Gokhale and W.J. Drury; "Efficient vertical section: The Trisector", Journal of Microscopy, submitted. (copy is enclosed)

5. A.M. Gokhale; "Design Based Test Lines for Efficient Measurement of Anisotropy", Journal of Microscopy, submitted. (copy is enclosed)

As (4) and (5) have been recently submitted (although most relevant), the following two equally important papers are also listed.

6. A.M. Gokhale and E.E. Underwood; "A New Parametric Roughness Equation for Quantiative Fractography", Acta Stereologica, 1989, vol. 8, pp. 43-52.

7. A.M. Gokhale and K. Banerji; "Criteria for Selecting Optimum Resolution for Quantiative Analysis of Fracture Surfaces", Microstructural Science, 1989, vol. 17, pp. 67-79.

(II) Five Other Significant Publications:

1. A.M. Gokhale, C.V. Iswaran and R.T. DeHoff, "Use of the Stereological Counting Measurements in Testing Theories of Growth Rates", Metall. Trans.-A, 1979, vol. 10A, pp. 1329-1245.

2. A.M. Gokhale and R.T. DeHoff, "Estimation of Nucleation Rate and Growth Rate From Time Dependence of Global Microstructural Properties During Phase Transformations", Metall. Trans.-A, 1985, vol. 16A, pp. 559-564.

3. A.M. Gokhale, M. Basavaiah, and G.S. Upadyayaya, "Kinetics of Neck Growth During Loose Stack Sintering", Metall. Trans. -A, 1988, vol. 19A, pp. 2153-2161.

4. A.M. Gokhale, "Calculation of Product Phase Grain Boundary Area During Solid State Transformations", Metall. Trans.-A, 1988, vol. 19A, pp. 2123-2131.

5. A.M. Gokhale, "Calculation of Grain Edge Length and Quadruple Points Per Unit Volume During Solid State Transformations", Metall. Trans.-A 1989, vol. 20A, pp. 349-355.

ASSOCIATION WITH GRADUATE STUDENTS AND OTHER SCIENTISTS

(1) Names of Graduate Students: The P.I. has been the thesis advisor of the following students (1985 onwards)

M. Basavaiah
M.H. Hazari
Ashok Kumar
M.N. Mungole

The P.I. is at present the thesis advisor of the following students.

W.J. Drury
W. Whited
S. Mishra

(2) Long Term Association With Other Scientists:

Prof. G.S. Upadhyaya
Prof. R.T. DeHoff (P.I.'s thesis advisor)
Dr. K. Banerji
Prof. E.E. Underwood

RESUMES OF THE INVESTIGATORS

NAME AND TITLE

A. M. Gokhale, Associate Professor
School of Materials Engineering
Georgia Institute of Technology
Atlanta, Georgia 30332-0245

SPECIALIZED EXPERTISE

Stereology, quantitative fractography, modelling of global microstructural evolution and its applications in materials processes.

EDUCATION

Received B.Tech and M.Tech. degress in metallurgical Engineering from the Indian Instuitute of Technology, Kanpur, India in 1970 and 1972, respectively. Received Ph.D. in Materials Science and Engineering from the University of Florida in 1977.

EXPERIENCE

Dr. Gokhale has twelve years of teaching and research experience.

July 1977-August 1980	Lecturer Department of Metallurgical Engineering Indian Institute of Technology Kanpur, India.
September 1980-February 1985	Senior Assistant Manager R&D Centre Hindustan Brown Boveri Ltd., India
March 1985-November 1987	Assistant Professor Department of Metallurgical Engineering Indian Institute of Technology Kanpur, India
December 1987-February 1989	Visiting Associate Professor School of Materials Engineering Georgia Institute of Technology Atlanta, Georgia
February 1989- to present	Associate Professor School of Materials Engineering Georgia Institute of Technology Atlanta, Georgia

AWARDS

Received Kamani Gold Medal for best paper in Trans. I.I.M. in 1984

Received certificate of appreciation for teaching activities from ASM

LIST OF PUBLICATIONS

1. "Use of the Stereological Counting Measurements in Testing Theories of Growth Rates" by A.M. Gokhale, C.V. Iswaran and R.T. DeHoff, Met. Trans. - A, 1979, Vol. 10A, p. 1239.

2. "Continuity Equation for Evolving Particle Size Distribution" by A.M. Gokhale and R.T. DeHoff, Met. Trans.-A. 1979, Vol. 10A, p. 1952.

3. "Estimation of Nucleation Rate" by A.M. Gokhale, Met. Tans. A. 1979, Vol. 10A, p. 1947.

4. "Time Dependence of Average Particle Size during Coarsening" by A.M Gokhale, Met. Trans.-A. 1980 Vol. 11A, p. 1972.

5. "Spheroidization of Pearlite" by A.K. Gogia and A.M. Gokhale, Met. Trans.-A. 1980, Vol. 11A, p. 1077.

6. "Application of Microstructure Modelling to the Kinetics of Recrystallization" by A.M. Gokhale, C.V. Iswaran and R.T. DeHoff, Met. Trans-A. 1980, Vol. 11A, p. 1377.

7. "Austenitization Kinetics of Pearlite and Ferrite Aggregates in a low Carbon Steel Containing 0.15 wt%C" by D.P. Datta and A.M. Gokhale, Met. Trans-A. 1981, Vol. 12A, p.443.

8. "A Test for Randomness of Spatial Distribution of Particles" by A.M. Gokhale, Met. Trans.-A. 1984, Vol. 15A, p. 243.

9. "Estimation of Parabolic Growth Rate from Sterological Counting Measurements" by A.M. Gokhale, Met. Trans.-A. 1984, Vol. 15A, p.391.

10. "Estimation of Grain Boundary Diffusion Controlled Growth Rate from Stereological Measurements" by A.M. Gokhale, Met. Trans.-A. 1985, Vol. 16A, p. 432.

11. "Estimation of Nucleation Rate and Growth Rate from Time Dependence of Global Microstructural Properties During Phase Transformations" by A.M. Gokhale and R.T. DeHoff, Met. Trans.A. 1985, Vol. 16A, p. 559.

12. "Estimation of Average Size of Convex Particles" by A.M. Gokhale, Met. Trans.-A. 1986, Vol. 17A, p. 742.

13. "Application of Microstructure Modelling to the Kinetics of Proeutectoid Ferrite Transformation in Hot-Rolled Microalloyed Steels" by A.M. Gokhale, Met. Trans.-A. 1986, Vol. 17A, p.1625.

14. "Kinetics of Neck Growth During Loose Stack Sintering" by A.M. Gokhale, M. Basavaiah, and G.S. Upadhyaya, Met. Trans.-A. 1988, vol. 19A, p. 2153.

15. "Calculation of Product Phase Grain Boundary Area During Solid State Transformations" by A.M. Gokhale, Met. Trans.-A, 1988, vol. 19A, p. 2123.

16. "Calculation of Grain Edge Length and Quadruple Points Per Unit Volume During Solid State Transformations" by A.M. Gokhale, Met. Trans. A, 1989, Vol 20A, p. 349.

17. A.M. Gokhale and E.E. Underwood; "A General Method for Measurement of Fracture Surface Roughness-I; Theoretical Aspects", Metall. Trans.-A, in press.

18. A.M. Gokhale and W.J. Drury; "A General Method for Measurement of Fracture Surface Roughness-II; Practical considerations", Metall. Trans.-A, in press.

19. A.M. Gokhale and E.E. Underwood; "A New Parametric Roughness Equation for Quantitative Fractography", Acta Stereologica, 1989, vol. 8, pp. 43-52.

20. A.M. Gokhale and K. Banerji; "Criteria for Selecting Optimum Resolution for Quantitative Analysis of Fracture Surfaces", Microstructural Science, 1989, vol. 17, pp. 67-79.

21. S.D. Antolovich, A.M. Gokhale, and C. Bathias; "Application of Quantitative Fractography and Computed Tomography to Fracture Processes in Materials", ASTM Special Tech. Pub., No. 1085, in press.

22. A.M. Gokhale; "Unbiased Estimation of Curve Length in 3D Using Vertical Slices", Journal of Microscopy, in press.

23. A.M. Gokhale and W.J. Drury; "Efficient Vertical Sections: The Trisector", Journal of Microscopy, submitted.

24. A.M. Gokhale; "Design Based Test Lines for Efficient Measurement of Anisotropy", Journal of Microscopy, submitted.

25. "Estimation of Creep Strain Due to Integranular Cavitation" by A.M. Gokhale, Scripta Met., 1989, Vol. 23, p. 1269.

26. "Quantitative Analysis of Cast Microstructures" by P.N. Crep-au, A.M.Gokhale, and C.W. Meyers, Journal of Metals, 1989, February, p. 16.

27. "Size Distribution of Grain Boundary Precipitates" by A.M. Gokhale and A.K. Jena, Metallography, 1980, Vol. 13, p. 307.

28. "Stereology of Grain Boundary Precipitates" by A.M. Gokhale, C.V. Iswaran and R.T. DeHoff, Metallography, 1981, Vol. 14, p. 151.

29. "Estimation of Parabolic Growth Rate from Section Size Distribution" by A.M. Gokhale, Metallography, 1985, vol. 18, p. 427.

30. "Stereology of Plane Convex Loops Distributed in Three Dimensional Microstructure" by A.M. Gokhale, Metallography, 1988, vol. 21, p. 241.

31. "Estimation of Average Size of Plane Convex Loops" by A.M. Gokhale, Metallography, 1989, vol. 22, p.69.

32. "Coarsening of Cementite in a Commercial Eutectoid Steel" by A.M. Gokhale, A.K. Jena and T.R. Ramachandran, Trans. IIM., 1973, Vol. 34, p.22.24."Characterization of Microstructures" by A.M. Gokhale, Trans. I.I.M., 1981, Vol. 34, p. 71.

33. "Interpretation of Grain Size Descriptors" by A.M. Gokhale Trans. I.I.M., 1982, Vol. 35, p.595.

34. "Analysis of Microstructural Dynamics During Precipitate Dissolution" by A.M. Gokhale, Trans.I.I.M., 1983, Vol. 36, p.431.

35. "Kinematics of Global Microstructural Evolution" by A.M. Gokhale, Trans. I.I.M., 1984, Vol. 37, p.193.

36. "Use of Linear Intercept Distributions for the Study of Paraboloic Growth Rate" by A.M. Gokhale, Trans.I.I.M., 1984, Vol. 37, p. 243.

37. "A Stereological Method for Estimation of Average Interfacial Energy Ratio of Grain Boundary Precipitates" by A.M. Gokhale, Trans. I.I.M., 1985, Vol. 38, p.309.

38. "Analysis of Particle Coarsening Kinetics in an Al-Pb Alloy" by Ashok Kumar and A.M. Gokhale, Trans. I.I.M., in press.

39. "A Critical Assessment of Abrasion Resistance Test for Synthetic Enamelled Copper Wires" by A.L. Vadhiya, B.H. Narayana and A.M. Gokhale, IEMA Journal, 1985, Vol. V., No. 9, p.27

40. "Quantitative Stereology" by A.M. Gokhale, Proceedings of Symposium on "Structure-Property Correlations and Instrumental Techniques in Materials Research", October, 1977 organized by Department of Atomic Energy, Rourkela, India, 1977, (Invited paper).

41. "Principles of Quantitative Microstructural Analysis" by A.M. Gokhale, Proceedings of Workshop on "Quantitative Metallography", July 1982, organized by Steel Authority of India Ltd., Ranchi; India (Invited Paper).

42. "Factors in Selection of Materials" by A.M. Gokhale, Proceedings of Workshop on "Engineering Materials and Properties" organized by Gujarat Engineering Research and Development Association, Vadodara, India, October 1983, (Invited paper).

43. "Geometry of Microstructures" by A.M. Gokhale, Proceedings of National Workshop on "Modern Experimental Techniques in Materials Research", organized by I.I.T., Kanpur, March 1985, p. 26 (invited paper).

44. "Induction Hardening" by A.M. Gokhale, Intensive Course on "Surface Hardening of Steel," organized by ASM, India Chapter, Bombay, November 1984 (Invited paper).

45. "Quantitative Image Analysis" by A.M. Gokhale, intensive course on Laboratory Automation, organized by Steel Authority of India Ltd., Ranchi, India, October, 1986 (Invited paper).

46. "Computer Applications in Quantitative Microscopy" by A.M. Gokhale, Intensive course on "Computer Applications in Metallurgical Processes", by Department of Metallurgical Engineering, I.I.T., Kanpur, India, June, 1987 (Invited paper).

RESUME

GEORGIA INSTITUTE OF TECHNOLOGY
School of Materials Engineering

UNDERWOOD, Ervin E. - Professor of Metallurgy Emeritus

SPECIALIZED EXPERTISE

Quantitative stereology, quantitative fractography, quantitative characterization of damage by fracture and fatigue.

EDUCATION

Sc.D. Physical Metallurgy, 1954; Massachusetts Institute of Technology, Thesis: "Precipitation in Gold-Nickel Alloys", Advisors Professors B. L. Averbach and Morris Cohen.

S.M. Physical Metallurgy, 1951; Massachusetts Institute of Technology, Thesis: "Thermodynamic Activities of Zinc in Silver-Zinc Alloys and Their Powders", Advisors: B. L. Averbach and Carl Wagner.

B.S. Metallurgical Engineering, 1949; Purdue University.

PATENT

U.S. No. 3,337,334, issued 22 August, 1967 "Beryllium-Aluminum Alloy" (Lockalloy, Be-38%Al). First alloy patent based on quantitative microstructural parameters.

SELECTED LISTINGS

Who's Who in Engineering (1959, 1977, 1982)
Leaders in American Science (1965)
American Men of Science (1967)
American Men and Women of Science, Physical and Biological Sciences, (12th, 15th Edition)
Who's Who in Technology Today

PROFESSIONAL SOCIETIES

American Institute of Mining, Metallurgical, and Petroleum Engineers (AIME); later TMS
American Society for Metals (ASM) - Fellow
Institute of Metals (British)
International Society for Stereology (President) 1972-1975
American Institute for Aeronautics and Astronautics (AIAA)
Society of Aerospace Material and Process Engineers (SAMPE)
Royal Microscopical Society (RMS) - Fellow
American Society for Testing and Materials (ASTM)
International Metallographic Society (IMS)

EMPLOYMENT HISTORY

Georgia Institute of Technology 1975 - 1988
Professor of Metallurgy, School of Materials Engineering

Max-Planck-Institute for Metal Research, Stuttgart, 1974 - 1975
Germany, Visiting Scientist; on leave of absence.

Georgia Institute of Technology 1971 - 1974
Alcoa Professor, joint appointment to Schools of Mechanical Engineering and Chemical Engineering, teaching graduate and undergraduate courses in materials, processing, and technology.

The Lockheed-Georgia Company 1965 - 1971
Associate Director, Materials Research and Development Laboratories. Responsible for research and development programs on materials. Directed the efforts of 100 scientific and technical personnel until laboratory was closed.

The Lockheed Missiles and Space Company 1962 - 1965
Staff Scientist and Assistant to Manager of Materials Research Laboratory. Performed research on the physical metallurgy of beryllium and its alloys, also co-inventor of the Be-38%Al ductile beryllium alloy (Lockalloy). Investigated superplasticity in alloys, the "memory effect" in TiNi alloys, and deformation in unidirectionally solidified lamellar eutectics.

Battelle Memorial Institute 1954 - 1962
Research Metallurgist and Assistant Division Consultant. Engaged primarily in metallurgical research on creep in alloy single crystals, effects of stress on transformation, deformation twinning, liquid metal embrittlement, and particle strengthening in alloys. Some investigations were performed in cooperation with Drs. Edgar Bain, Egon Orowan, and in Geneva with Walter Bollmann.

Massachusetts Institute of Technology 1949 - 1954
Graduate Student and Research Assistant. Performed research work, wrote progress reports and supervised technicians.

Military Service 1941 - 1948
Major, Artillery, U.S. Army, 66th Infantry Division. Instructor in Gunnery at Field Artillery School, Ft. Sill, Oklahoma. Investigator for Office of Military Government, U.S. Zone, German Iron and Steel Section, after hostilities ended.

U. S. Steel Corporation, Gary Works 1940 - 1941
Open Hearth Metallurgical Observer, responsible for proper shop practice and technical records.

U. S. Steel Corporation, Sheet and Tin Mills 1936 - 1937
Laborer in Annealing Department and Cold-roll Department.

EXPERIENCE

Dr. Underwood has held industrial positions at Battelle Columbus Lab, U. S. Steel Corporation, Lockheed Missiles and Space Company, and Lockheed-Georgia Company, where as Associate Director, he headed the Materials Research and Development Labs and directed the efforts of 100 scientific and engineering personnel.

When the Lockheed Laboratory closed in 1971, he came to Georgia Tech as Alcoa Professor with a joint appointment in the Schools of Mechanical and Chemical Engineering. In 1974-1975, he spent 12 months as Guest Scientist at the Max-Planck-Institut for Metal Research in Stuttgart, Germany.

Upon returning to Georgia Tech, he joined the new Fracture and Fatigue Research Lab, doing research and teaching, directing graduate studies, and engaging in scientific and industrial consulting. In recent years, he has been funded by NSF in the stereological study of fracture and fatigue, which has led to the development of a new, quantitative treatment of fracture geometry and fractals. He was selected to receive a 2-year extension to his NSF grant for creativity in his research.

Currently, he is writing a companion volume to his 1970 book Quantitative Stereology, which concerns methods for the quantitative characterization of microstructure.

On October 18, 1970, Dr. Underwood was elected Fellow of the American Society for Metals, and was the first Georgian to receive this honor. He received the International Metallographic Society's Ninth Sorby Award "in recognition of outstanding contributions to the field of metallography" in 1984, and the American Society for Testing and Materials' J. R. Villela Award "in recognition of a paper of outstanding significance to the science of metallography" in 1986. He was also awarded Honorary Membership in the International Society for Stereology "in recognition of scientific contributions in the field of stereology". Starting in October 1987, Dr. Underwood spent one year with NSF in Washington, DC as Program Director, Metallurgy Division of Materials Research.

PUBLICATIONS

Book:

Quantitative Stereology, Addison-Wesley Publishing Company, Reading, Mass. (1970) pp. 274.

Chapters in Books:

R.W. Fenn, D.D. Crooks, W.C. Coons, and E.E. Underwood, "Properties and Behavior of Beryllium-Aluminum Alloys, in Beryllium Technology, Vol. 1, Gordon and Breach, NY (1966) p. 103.

E.E. Underwood, "Microstructures and Properties," in An Atomistic Approach to the Nature and Properties of Materials, John Wiley and Sons, Inc. NY (1967) p. 432.

E.E. Underwood, "Surface Area and Length in Volume" (Ch. 4), and "Particle Size Distribution" (Ch. 6) in Quantitative Microscopy (R.T. DeHoff and

F.N. Rhines, Ed.), McGraw-Hill Book Co., NY (1968) p. 77 and 149.

E.E. Underwood, A.R. Colcord and R.C. Waugh, "Quantitative Relationships for Random Microstructures," in Ceramic Microstructures--Their Analysis, Significance, and Production, (R.M. Fulrath and J.A. Pask, Ed.) John Wiley and Sons, Inc. (1968) p. 25.

T.J. Headley, D. Kalish, and E.E. Underwood, "The Current Status of Applied Superplasticity," (Ch. 14) in Ultrafine-Grain Metals (J.J. Burke and V. Weiss, Ed.), Syracause Univ. Press, NY (1969) p. 325.

E.E. Underwood, "Application of Quantitative Metallography," in Metals Handbook, Vol. 8, Metallography, Structures and phase Diagrams, 8th Ed., Amer. Soc. for Metals, Ohio (1973) p. 37.

E.E. Underwood, "Superplasticity," in Encyclopedia of Science and Technology, (D.N. Lapedes, Ed. in Chief), McGraw-Hill Book Co., NY, Vol. 13 (1977) p. 321. "Superplasticity in Aluminum Alloys" (1982).

E.E. Underwood, "Stereological Analysis of Particle Characteristics," Chap. 5 in Testing and Characterization of Powders and Fine Particles, (J.K. Beddow and T.P. Meloy, Eds.), Heyden and Son, Inc., Philadelphia (1980) p. 77.

Journal Articles:

E.E. Underwood and B.L. Averbach, "Vapor Pressures of Zinc Over AgZn Alloys," Trans. AIME, 191 (1951) p. 1198.

E.E. Underwood and L.L. Marsh, "Effects of Alloying Elements on Plastic Deformation in Aluminum Single Crystals," Trans. AIME 206 (1956) p. 477.

E.E. Underwood, "Creep of Al-Cu Alloys During the Age Hardening," Trans. AIME 209 (1957) p. 1182.

E.E. Underwood, "Creep Properties from Short Time Tests," Materials & Methods 45 (April 1957) p. 127.

E.E. Underwood, E.M. Stein and G.K. Manning, "Strengthening of Iron-Base Alloys Containing Columbium," Trans. AIME 221 (1961) p. 676.

E.E. Underwood, "Quantitative Metallography," Metals Engr'g Qtrly; Part 1, 1 No. 3 (1961) p. 70; Pt. 2, ibid., No. 4, p. 62.

E.E. Underwood, "A Review of Superplasticity and Related Phenomena," Journal of Metals (Dec. 1962) p. 914.

R.W. Fenn, Jr., D.D. Crooks, and E.E. Underwood, "Beryllium-Aluminum Alloys - Promising New Structural Metals," Materials in Design Engineering (September 1964), p. 103.

E. U Lee and E.E. Underwood, "Defect Structures and Interactions in Al-Zn Eutectoid Alloys," Met. Trans. 1 (1970) p. 1399.

E.E. Underwood and V. Nagpal, "Analysis of Axisymmetric Flow Through Curved Dies Using a Generalized Upper Bound Approach," in Proceedings, 2d Amer. Metalworking Res. Conf., Madison, Wisc. (1974), p. 225. Soc. Manufacturing Engrs., Mich.

E.E. Underwood, "Three-Dimensional Shape Parameters from Planar Sections," in National Bureau of Standard Spec. Publ. 431 (E.E. Underwoood et al., Eds.) (1976) p. 91. Proceedings, Fourth Int. Cong. for Stereology, N.B.S., Gaithersburg, Md. (Sept. 1975).

E.E. Underwood, and E.A. Starke, Jr., "Quantitative Stereological Methods for Analyzing Important Microstructural Features in Fatigue of Metals and Alloys," in Fatigue Mechanisms, (J.T. Fong, Ed.) ASTM STP 675, (1979) 633. Proceedings of Intern. Conf. on Fatigue Mechanisms, Kansas City, May 1978.

C.E.S. Ueng, E.E. Underwood, and T.L. Liu, "Shear Modulus of Superplastically Formed Sandwich Cores," in Proceedings of Symp. on Future Trends in Computerized Struct. Analysis and Synthesis, (a.K. Noor and H.G. McComb, Jr., Eds.), Washington, DC, Pergamon Press (1978) p. 393.

E.E. Underwood, T.H. Sanders, and J.W. Johnson, "Microstructural Analysis of Wrought RSP Al-Fe-Ni-Co Alloys" in Rapid Solidification Processing: Principles and Technologies II, ed. by R. Mehrabian, B.H. Kear and M. Cohen, Claitor's Publ. Div., La. (1980) 141.

E.E. Underwood and J.T. Berry, "Quantitative Measurements of Cast Iron Microstructures," AFS Trans. (1981) 755-766.

Articles in Foreign Journals:

E.E. Underwood, "Strength, Stability, and the Equicohesive Point," J. Inst. Metals, 88 (1959-60) p. 266.

E.E. Underwood, A.E. Austin and G.K. Manning, "The Mechanisms of Hardening in 17-7 Ni-Cr Precipitation-Hardening Stainless Steels," J. Iron Steel Inst. 200 (1962).

E.E. Underwood, "Interrelationships Among High Temperature Strength and Ductility Criteria," in Proceedings, Joint Inter. Conf. on Creep, Vol. 1, NY and London, Publ. by Inst. of Mech. Engrs., London (1963), p. (6)-49.

E.E. Underwood and G.K. Manning, "Effects of Creep stress on Processes Occurring at Elevated Temperatures in Al-Cu Alloys: Particle Dissolution, Grain Growth, and Precipitation," Revue de Metallurgie 60, No. 9 (1963). In French.

E.E. Underwood, "Stereological Analysis of Lockalloy Microstructures," in Beryllium 1977 Proceedings, London, England (1978), Paper No. 11.

C.E.S. Ueng, T.L. Liu, R.E. Crooks and E.E. Underwood, "Fabrication, Testing and Analysis of New Design Cores for Structural Sandwich Panels," in Proceedings 5th Inter-Amer. Conf. on Materials Techn., Sao Paulo, Brazil, (1978) p. 531.

E.E. Underwood, "Shape Parameters in Cast Iron," Acta Statistical Study of Graphite and Pearlite in Nodular Cast Iron," Pract. Metallography (June 1982) p. 346.

Life-Science and Non-Metallic Materials:

E.S. Underwood and E.E. Underwood, "Analysis of Partially-Oriented Linear Elements in a Plane," in Quantitative Analysis of Microstructures in Materials Science, Biology, and Medicine, (J.-L Chermant, Ed.), Dr. Riederer-Verlag GmbH, Stuttgart, Germany, Spec. Vol. No. 8 (1978) p. 116. Second European Symposium, Caen, France, Oct. 1977.

E.E. Underwood, "Vesicle Analysis" (p. 1545) and "Quantification of Microstructures by Stereological Analysis," (p. 1536), in J. Histochem. and Cytochem. 27 No. 11 (1979), from 30th Annual Meeting of the Histochemical Soc., Keystone, Colo., (1979).

E.E. Underwood and C.J. Aloisio, "Microstructural Study of Foamed Rubber," Proc. 5th Int. Cong. for Stereology, Salzburg, Austria (1981) p. 311.

S.B. Reese and E.E. Underwood, "Quantitative Microstructural Analysis of Dental Amalgam," Quint. Intern. 2 (1982) 223.

SELECTED STEREOLOGICAL PUBLICATIONS

H.B. Aaron, R.D. Smith and E.E. Underwood, "Spatial Grain-Size Distribution from Two-Dimensional Measurements" in Proceedings, First Inter. Cong. for Stereology, Vienna, Austria, (H. Haug, Ed.) (April, 1963) Paper 16/1.

E.E. Underwood and W.C. Coons, "The Role of Quantitative Stereology in Deformation Twinning" in Deforation Twinning, (R.E. Reed-Hill, et al., Ed.) Gordon and Breach, NY (1964) p. 405.

E.E. Underwood, "The Mathematical Foundations of Stereology", in Stereology and Quantitative Metallography, ASTM STP 504 (1972) p. 3, Symp. on Stereology and Quant. Met., 74th Annual Meeting of ASTM, Atlantic City, N.J. (July, 1971).

E.E. Underwood, "The Stereology of Projected Images" in Stereology 3, (E.R. Weibel, et al., Eds.), Blackwell Sci. Publs., Oxford (1972) p. 25. Proceedings, Third Inter. Cong. for Stereology, Berne, Switzerland (Aug. 1971).

E.E. Underwood, "Quantitative Shape Indices by Stereological Methods", in Quantitative Analysis of Microstructures in Medicine, Biology and Materials Development, (H.E. Ener, Ed.), Dr. Riederer-Verlag GmbH, Stuttgart, Germany Spec. Vol. No. 5 (1975) p. 223. Proceedings of Symposium, "Quantitative Gefugeanalyse", Leoben, Austria, Oct. 1974.

E.E. Underwood, "Quantitative Analysis of Shape in MIcrostructures", in Proceedings, 3rd Annual Meeting of Microscopical Soc. of Canada, Ottowa, Canada, Imperial Press, Toronto, Canada (1976). Proc. Microscopical Soc. of Canada 3 (1976) 69. Ed. by G.H. Haggis, et al.

E.E. Underwood, "Quantitative Shape Parameters for Microstructural Features", The Microscope, 24 1st Q. (1976) p. 49.

E.E. Underwood, "Shape--A Many Slendored Thing", B and L Omnicon Scan Lines, Vol. 1, No. 2 (Jan, 1978).

E.S. Underwood and E.E. Underwood, "Analysis of Partially-Oriented Linear Elements in a Plane", in Quantitative Analysis of Microstructures in Materials Science, Biology and Medicine, (J.-L. Chermant, Ed.), Dr. Riederer-Verlag GmbH, Stuttgart, Germany, Spec. Vol. No. 8 (1978) p. 116. Second European Symposium, Caen, France, Oct. 1977.

E.E. Underwood, "Stereological Analysis of Lockalloy Microstructures", in Beryllium 1977 Proceedings, London, England (1978), Paper No. 11.

E.E. Underwood and E.A. Starke, Jr., "Quantitative Stereological Methods for Analyzing Important Microstructural Features in Fatigue of Metals and Alloys", in Fatigue Mechanisms, (J.T. Fong, Ed.) ASTM STP 675, (1979) 633. Proceedings of intern. Conf. on Fatigue Mechanisms, Kansas City, May 1978.

E.E. Underwood, "Stereological Analysis of Particle Characteristics," Chap. 5 in Testing and Characterization of Powders and Fine Particles, (J.K. Beddow and T.P. Meloy, Eds.), Heyden and Son, Inc., Philadelphia (1980) p. 77.

E.E. Underwood and C.J. Aloisio, "Microstructural Study of Foamed Rubber", Proc. 5th Int. Cong. forStereology, Salzburg, Austria (1981). Mikroskopie 37 (Suppl.) (1980) 311.

E.E. Underwood and S.B. Chakrabortty, "Quantitative Fractography of a Fatigue Ti-28V Alloy", ASTM STP 733, L.N. Gilbertson and R.D. Zipp, eds. (1981) 377.

E.E. Underwood and J.T. Berry, "Quantitative Measurements of Cast Iron Microstructures", AFS Trans. (1981) 755.

E.E. Underwood, J.C. Grebetz and R. Koos, "Statistical Study of graphite and Pearlite in Nodular Cast Iron", Proc. 3d European Symp. for Stereology, Ljubljana, Yugoslavia, 22-27 June 1981. Pract. Mat. 19 (1982) 347.

E.E. Underwood, "Streological Analysis of Particle Characteristics", Acta Stereologica, Vol. 1 (1982).

E.E. Underwood and E.S. Underwood, "Quantitative Fractography by Computer Simulation", Acta Streologica, 1 (1982) 89.

E.E. Underwood, "Practical Solutions to Stereological Problems", in Practical Applications to Quantitative Metallography, ASTM STP 839, edited by J.L. McCall and J.H. Steele, Jr. (1984) 160-179.

QUANTITATIVE FRACTOGRAPHY & FRACTALS

E.E. Underwood, "Quantitative Fratography: A Prelimary Analysis," Unpublished Report, Georgia Tech, 10 Mar 1979.

E.E. Underwood and E.A. Starke, Jr. "Quantitative Stereological Methods for Analyzing Important Microstructural Features in Fatigue of Metals and Alloys", in Fatigue Mechanisms ASTM STP 675, Ed. by J. Fong, (1979) 633-682.

E.E. Underwood and S.B. Chakrabortty, "Quantitative Fractography of a Fatigued Ti-28V Alloy" in Fractography and Materials Science, ASTM STP 733, Ed. by L.N. Gilbertson and R.D. Zipp, (1981) 337-354.

E.E. Underwood and E.S. Underwood, "Quantitative Fractography by Computer Simulation", Proc. 3rd European Symp. Stereology, 2nd Part, Ljubljana, Yugoslavia, (1982) 89-101.

E.E. Underwood, Discussion in Fatigue Mechanisms: Advances in Quantitative Measurements of Physical Damage, ASTM STP 811, Ed. by J. Lankford, et al., (1983) 490-491; 43; 111; 205; 258; 44.
K. Banerji and E.E. Underwood, "Quantitative Analysis of Fractographic Features in a 4340 Steel," Proc. 6th Int. Congr. Stereology, Gainesville, FL (1983) 65-70.

E.E. Underwood and K. Banerji, "Statistical Analysis of Facet Characteristics in a Computer Simulated Fracture Surface," Proc. 6th Int. Congr. Stereology, Gainesville, FL (1983) 75-80.

K. Banerji and E.E. Underwood, "Fracture Profile Analysis of Fractographic Features in a 4340 Steel," Proc. 6th Int. Conf. on Fracture, New Delhi, India, Vol. 2 (1984) 1371-1378.

E.E. Underwood "Practical Solutions to Stereological Problems," in Practical Applications to Quantitative Metallography, ASTM STP 839, ed. by J.L. McCall and J.H. Steele, Jr. (1984) 160-179.

K. Banerji and E.E. Underwood, "Interpretations of Fracture Mechanisms in a Al-4% Cu Alloy by Quantitative Fractography." Presented at TMS/AIME Annual Meeting, NY, (1985) (abstract only).

E.E. Underwood, "Recent Developments in Quantitative Fractography," Proc. Australian Inst. of Metals (1985) Ballarat, Australia, D7-D11.

E.E. Underwood, "Recent Developments in Quantitative Fractography," Sydney, Australia, meeting of ASSia-85 (1985) Ballarat, Australia, D7-D11.

E.E. Underwood, Fractals in Fractography," Queensland University, Brisbane, Australia (1985) (abstract only).

E.E. Underwood and K. Banerji, "Quantitative Fractographic Analysis of Dimple Size in a 4340 Steel Fractured in Tension," Proc. 4th European Symposium for Stereology, Gothenberg, Sweden (1985). Ed. by M. Kalsvnik,

B. Karlsson, R. Warren and J. Wasin, Ljubljana, Yugoslavia, p. 205-210.

E.E. Underwood and K. Banerji, "Recent Advances in Quantitative Fractography," AIME, New Orleans (1986) in Session on Stochastic Aspects of Fracture (abstract only).

K. Banerji and E.E. Underwood, "Quantitative Analysis of Fracture Surface Morphology During FCP in High-Purity Al-4% Cu Binary Alloys," AIME, New Orleans (1986) in General Abstracts Session (abstract only).

K. Banerji and E.E. Underwood, "On Estimating the Fracture Surface Area of Al-4% Cu Alloys, Proc. Inter. Met. Soc. 17, Philadelphia, PA, 1985. Microstructural Science Vol. 13 (1986) 537-551.

E.E. Underwood, "Quantitative Fractography," Chap. 8 in Applied Metallography, G.F. Vander Voort, Ed., Van Nostrand Reinhold Co. (1986) 101-122.

E.E. Underwood, "Estimating Feature Characteristics by Quantitative Fractography," Jnl. Metals, April (1986) 30-32.

E.E. Underwood and K. Banerji, "Quantitative Fractography," in Vol. 12, series, 9th Ed., ASM Handbook, Fractography, (1987) 193-210.

E.E. Underwood and K. Banerji, "Fractal Analysis of Fracture Surfaces," in Vol. 12, series, 9th Ed., ASM Handbook, Fractography, (1987) 211-215.

E.E. Underwood and K. Banejri, "Fractals in Fractography," presented at TMS/AIME Annual Meeting in Denver (1987).

E.E. Underwood and W.J. Drury, "Stereological Characterization of Fiber-Reinforced MMC" ASM Advanced Materials Conference, Denver (1987) (extended abstract).

W.J. Drury, K. Banerji and E.E. Underwood, "Quantitative Metallographic and Fractographic Analyses of MMC Microstructures," Proceedings Advanced Materials Conference, Denver (1987), 279-287.

E.E. Underwood, "Sterelogical Analysis of Fracture Roughness Parameters." Twenty-Five Years of Stereology (1987), 169-178.

E.E. Underwood and W.J. Drury, "Quantitative Fractographic Analyses of Oriented Fracture Surfaces," 7th Int. Congr. Proceedings for Stereology, Caen, ed. by J.L. Chermant, France (1987), 549-554.

E.E. Underwood, "The Analysis of Nonplanar Surfaces using Stereological and Other Methods", Keynote Lecture in Session on "Nonplanar Surfaces" Proceedings, 7th Int. Congr. for Stereology, Caen, France, ed. by J.L. Chermant, (1987), 855-876.

REFERENCES TO PAPERS PRODUCED WITH NSF SUPPORT

"Recent Advances in Quantitative Fractography", in Fracture Mechanics: Microstructures and Mechanics, ed. by S.V. Nair, et al., ASM

International, 1989 87-109.

"A New Parametric Roughness Equation for Quantitative Fractography", with A.M. Gokhale. Acta Stereologica, Vol. 2, No. 1, 1989, 43-52.

"The Current Status of Modern Quantitative Fractography", Proc. Seventh Int. Conf. on Fracture (ed. K. Salama, et al.), Advances in Fracture Research, Pergamon Press, Vol. 5, (1989), 3391-3409.

"Treatment of Reversed Sigmoidal Curves for Fractal Analysis", ibid.

"Evaluation of Overlaps in Fracture Surfaces", MiCon 90: Advances in Video Technology for Microstructural Control, ASTM STP 1094, ed. by G.F. Vander Voort, American Society for Testing and Materials, Philadelphia, 1990.

"A New Procedure for Quantitative Fractography Based on Directed Measurements", to be submitted to Jnl. of Metals, 1990.

SEMINARS

"Quantitative Stereology," Dept. of Biology, Univ. of Texas, Arlington (Sept., 1977).

"Structural Analysis," College of Veterinary Medicine, Iowa State Univ., Ames (May, 1978).

"Quantitative Characterization of 3-d Microstructural Features,"Ames Bioengr. Seminar, Univ. of Cal./San diego, at La Jolla (Feb., 1979).

"Mathematical Basis for Morphometry," and Vesicle Analysis," Stereology Workshop, 30th Annual Meeting Histochemical Soc., Keystone, Colo. (Apr., 1979).

"On Quantification of Structure," Medical College of Georgia, Augusta, (Jan. 1980). Lecture to Medical and Dental groups.

"Introduction to Stereology and Morphometry," Annual Meeting Neurosciences Soc., (Oct. 1981) Los Angeles.

"Quantitative Description of Materials and Biological Microstructure," Vanderbilt University, School of Anatomy, (Sept. 1981).

PROFESSIONAL ACTIVITIES

Consultant on numerous industrial and legal problems involving corrosion, welds, impact and fatigue failures. Also contributed to the development of new methods and techniques for improved quality control of both metallic and polymeric materials. Companies include large pipeline, chemical, mineral and manufacturing firms, as well as military agencies, insurance and telephone companies.

Member of Mechanical Failures Prevention Group, Design Committee, sponsored by various government agencies and Battele Memorial Institute.

Committee E-4 on Metallography, ASTM.
Chairman, ASTM Task Group E4.802
Committee E-9 on Fatigue, ASTM.
Committee E-24 on Fracture Testing, ASTM.

Member of Industry Advisory Group to the University of Tennessee Space Institute (UTSI), Tullahoma, Tenn. as Lockheed-Georgia Co. representative for three years.

Attended Lockheed-Emory University Management Institute, 1969.

Distinguished Lecturer Series, Air Force Materials Laboratory, WP-AFB, Dayton, Ohio, 1969

Vice-Chairman, Session on "Reliability of NDE - A Regulatory Case Study," in ASME-ASNT-NBS Symp. on NDE: Reliability and Human Factors, October 12, 1981, Atlanta, GA. Invited to attend ASME-PVP-M$F Advisory Board Meeting, Shoreham Hotel, Washington, DC, 1981.

Chairman, Georgia Chapter of AIME, 1968; Membership Chairman of Atlanta Chapter, ASM; Member, ASM National Career Development Committee for three years; Chairman of ASM Materials Characterization Activity, in Materials Testing and Quality Control Committee, for three years. President, International Society for Stereology, from 1972 to 1976.

Member, ASM-Inst. of Metals (British) Joint Committee for International Metals Reviews. (1977-).

Course Director, ASM courses on "Quantitative Metallography" and "Quantitative Metallography in Failure Analysis"; speaker at ASM courses on "Fractography". Course Director for Georgia Tech Continuing Education courses on "Quantitative Microscopy in the Life Scieces, Dentistry, and Medicine", and speaker at course on "Principles of Metal and Alloy Selection and Failure Analysis for Management and Engineers" (1973-1982).

THESIS TOPICS

"Mechanical Properties of Superplastic Al-Zn Alloys Near the Transition Region" by S.A. Hamid Ghazanfar, for M.S. in Mechanical Engineering, Georgia Tech (1973).

"Particle Effects in Superplastic Al-78% Zn Alloys," by O.D. Puche, for M.S. in Mechanical Engineering, Georgia Tech (1974).

"A Lower Upper-Bound Approach to Some Metal Forming Problems," by V. Nagapal, for Ph.D. in Mechanical Engineering, Georgia Tech (1974).

"Design and Construction of New Honeycomb Sandwich Panels Using Superplastic Forming and Vacuum Forming Technique," by A.J. Gomez Fermin, for Ph.D. in Mechanical Engineering, Georgia Tech (1976).

"Development, Production and Testing of Superplastically Formed Zinc-Aluminum Sandwich Cores," by R.E. Crooks, for M.S. in Metallurgy, Georgia Tech (1979).

RESEARCH GRANTS

"The Effect of Alloying Elements on Plastic Deformation in Metals," NACA (1954). (Aluminum alloy single crystals.)

"Creep of Aluminum-Cooper During Age Hardening," NACA (1955).

"Effects of Creep Stress on Particulate Aluminum-Copper Alloys," NACA (1957).

"The Effects of Solute Elements on the Strength Properties of Iron- and Cobalt-Base Alloys," ARL, WADC (1958).

"The Mechanism of Hardening in 17-7 PH Stainless Steel," ARL, WADC (1959).

"A Literature Survey of Theories and Methods of Predicting Characteristics of Materials", AF Missle Dev. Center (1959).

"Mechanism of Superplasticity in Al-78%Zn Alloys," ONR (1967), 4 years.

"Superplastically Formed Cores for Structural Sandwich Panels," with Dr. C.E.S. Ueng, ESM, Georgia Tech, NSF (1976), 2 years.

"Quantitative Evaluation of Bone Ingrowth into Dental Implants," Biomed. Res. Support Grant Comm., Georgia Tech (1982).

"Quantitative Evaluation of Fracture Surfaces by Stereological Analysis," NSF (1982).

FACILITIES AND EQUIPMENT

The Mechanical Properties Research Laboratory (MPRL) is the nucleus of all fracture, fatigue and deformation behavior research at the Georgia Institute of Technology. It is equipped for a variety of investigations involving mechanical testing and structural characterization. A wide range of x-ray, electron and chemical characterization apparatus are available to MPRL researchers in the School of Materials Engineering, the School of Physics and in the Micro Electronics Research Center. In addition, several facilities of the nearby Oak Ridge National Laboratories (ORNL) are also available to Georgia Tech researchers through the Oak Ridge Associated Universities (ORAU) program. These include the Small Angle Neutron Scattering Center, the Melting and Processing Laboratory and the High Voltage Electron Microscopy Laboratory.

In the following sections the capabilities currently available at Georgia Tech. that are pertinent to the proposed research are described.

Mechanical Testing

Tensile and Fatigue Test Facility

Seven closed-loop servohydraulic test machines are available for monotonic, low cycle/high cycle fatigue testing, and fatigue crack propagation studies. Each machine has a capacity of 10 tons. Load or strain of the specimen or crosshead motion can be electronically controlled to follow a prescribed function, at frequencies in the range of 0.0001-100 Hz, by means of closed-loop electronics. Computer interfacing currently is available on three of the systems. One 10-ton screw driven Instron machine is available for performing monotonic and low cycle fatigue testing. It can also be fitted with a 1/2-ton load cell for accurate mechanical property measurements of small samples. For even more accurate measurements there is a 50 Kg screw driven table top MTS machine.

Crack length can be measured during the test by optical, electric potential or unloading compliance methods. An assortment of high precision diametral and longitudinal strain extensometers including a ZYGO laser extensometer capable of resolving 10^{-6} in displacement are available for use over a wide range of temperatures and frequencies.

The laboratory is currently conducting tensile, cyclic stress-strain, plane strain fracture toughness, K_{IC}, J_R-Resistance Curve, fatigue crack growth testing, low and high cycle fatigue tests over a wide range of temperatures on metallic and non-metallic materials on a routine basis.

A facility to conduct multi-axial loading tests for deformation and fracture studies at elevated temperature has also been developed within the MPRL.

High Temperature High Vacuum Test Facility

A high temperature and high vacuum (10^{-10} torr) mechanical testing facility is available within the MPRL. The project to build this facility was sponsored by the U.S. Air Force.. The test chamber is large enough to hold an IT compact type fracture toughness and crack growth specimen. A residual gas analyzer is also attached to the system. The system is capable of conducting fatigue tests from essentially static load levels to 10 Hz with a load capacity of 10 metric tons.

Creep Testing Facility

One 20 KIP capacity and six 12 KIP capacity dead weight load type creep machines are available for conducting creep deformation and rupture as well as creep crack growth testing. One of these machines is also equipped with a cyclic module to conduct tests at very low frequencies (on the order of one cycle per twenty four hours). In addition, two stress relaxation machines (10 KIP capacity) are available with tension compression cyclic load capabilities. These machines are being used for conducting creep deformation, rupture and crack

growth testing on Electric Power Research Institute (EPRI) and Department of Energy (DOE) sponsored programs.

Hardness Testing

Facilities for various types of hardness measurements are available in the MPRL. These include the Knoop hardness, Vicker's hardness and the Rockwell and the Brinell hardness.

Structural Analysis

Transmission Electron Microscopy (TEM)

Several electron microscopes are available at Georgia Tech. A JEOL 100C microscope provides flexible specimen examination. It is fitted with attachments for both scanning transmission (STEM) and scanning electron microscopy (SEM) and an energy dispersive x-ray spectrometer. This instrument is capable of 3.4A lattice resolution in the TEM mode. Various attachments for the JEOL are used to obtain additional information. These include secondary and backscattered electron (scanning) imaging for fractographic and microstructural analysis, chemical analysis of microconstituents (200A resolution for thin foils), microelectron diffraction for orientation and phase analysis from areas of a thin foil (300A resolution). The microscope is also equipped with a specimen rotating holder. The holder is designed to rotate the specimen 360° in the plane of the specimen, and tilt +60° about the rotation axis. The attachment is crucial in carrying out detailed quantitative analyses of microstructural features.

Sample preparation facilities for TEM include two Streuers Tenupols equipped with a cooling unit to perform dual jet polishing at controlled temperatures as low as -80°C, an ISI sputter/coater, and Commonwealth Scientific ion-milling equipment. Also, spark machining capabilities are available for machining delicate specimens such as single crystals.

Scanning Electron Microscope (SEM)

Several SEM's are available at Georgia Tech. A Coates and Welter QWIK Scan #104 SEM located in the School of Materials Engineering permits a TV scan rate operation to a magnification of 80,000X with a resolution of 90A. The unit is equipped with a Kevex model 7500 energy dispersive x-ray analyzer that provides standard quantitative elemental analysis. For insulator material observations, conducting film deposition is also available via Au/Pd sputter coater or a carbon coater using heated carbon thread. A Cambridge S-4 scanning electron microscope is located within the MPRL. This microscope permits direct viewing of samples at magnifications from 20 to 40,000X with extreme depths of field. The instrument is equipped with an image enhancement module and wobbler focus. Samples can be tilted 0-90° and rotated 360°.

Image Analysis Equipment

This laboratory facility includes both automatic and semi-automatic image analysis equipment. A Zeiss Vidas automatic image analysis system is available for automatic measurements; an interactive semiautomatic mode is also available. Image editing can be carried out by dilation, erosion, Laplacian, etc. It is a flexible software based system; it can be programmed for design based mesurements. A separate Zeiss Videoplan System, coupled with a Zeiss ICM 405 inverted light microscope, handles all functions of quantitative microscopy on a semi-automated basis. The Videoplan performs routine data acquisition, storage and manipulations. There is also an interface to our main-frame Cyber computer which allows more sophisticated data manipulation. Measurements of area, diameter, angle, length, centroid, and form factor can be made, as well as the digitizing of irregular curves such as fracture profiles. This instrument significantly reduces the level of effort necessary to quantitatively analyze micrographs or curves, and plays a central role in our analyses for quantitative

fractography.

Computing Facilities

The Schools of Chemical Engineering and Materials Engineering operate a dedicated computer center for their own computer needs. This center is located on the floor above the MPRL and consists of a VAX 11/780 and a PDP 11/34 DEC computer. The VAX 11/780 is a 32 bit super mini computer with 1 megabyt of MOS memory and 456 megabytes of storage on a single fixed disk. A nine-track tape drive and a cassette tape drive serve as load devices. Several ports are available for terminal connection. The VMS operating system, FORTRAN 77, and interactive graphics are available, as well as an interface with the institutes CYBER system.

The PDP 11/34 is a 16-bit minicomputer with 256 kilobytes of MOS memory and 20.4 megabytes of storage on two cartridge disk drives. Eight ports are available for terminal connection. The PDP 11/34 runs the RSX11M operating system and has FORTRAN 77 and graphics capabilities. The LPA11 subsystem provides realtime capabilities. The microprocessor-based system includes A/D and D/A conversion, digital 1/0 and realtime clock. The VAX and PDP 11/34 are interfaced via a DECnet link, allowing each machine to access the peripherals of the other.

The computer center is housed in a three-room complex consisting of a machine room with raised floor and independent temperature and humidity control, a system manager's office, and a terminal room. At present, the terminal room is equipped with 16 VT101 terminals, a Tektronix graphics terminal with a hardcopy unit, and various other terminals. In all, 22 work stations distributed among the VAX PDP 11/34, and CYBER systems are available in the terminal room. In addition, most faculty offices and some graduate student offices and labs have hard-wired connections to the machine room. Expansions are already underway

which will increase the number of ports on the VAX from 16 to 48, and on the PDP 11/34 from 8 to 16.

Metall. Trans.-A
in press

:A General Method for Estimation of Fracture Surface Roughness-I; Theoretical Aspects:

By

A. M. Gokhale and E. E. Underwood
School of Materials Engineering
Georgia Institute of Technology
Atlanta, Georgia 30332-0245

:ABSTRACT:

An assumption free general method is developed for quantitative estimation of fracture surface roughness from the measurements performed on the fracture profiles generated by sectioning planes which are normal to the average topographic plane of the fracture surface. The input data are the profile roughness parameter R_L and angular orientation distribution of line elements on the fracture profile $f(\alpha)$. It is shown that:

$$R_s = \overline{R_L \cdot \Psi}$$

where, R_s is the fracture surface roughness parameter, and Ψ is the profile structure factor which is completely determined by the profile orientation distribution function $f(\alpha)$. $\overline{R_L \cdot \Psi}$ is the expected value of the product $R_L \cdot \Psi$ on a set of sectioning planes normal to average topographic plane of fracture surface: measurement of R_L and Ψ on few such sectioning planes can give reliable estimate of the fracture surface roughness R_s. The result is geometrically general and it is applicable to fracture surfaces of any arbitrary complexity and anisotropy.

:A General Method for Estimation of Fracture Surface Roughness - I; Theoretical Aspects:

INTRODUCTION: The deformation and fracture processes generate fracture surface. The geometric attributes of fracture surface and the associated microstructural features may contain quantitative information concerning the processes that lead to fracture. It is essential to establish such correlations by using the characterization techniques which are assumption free and unbiased. An important geometric characteristic of fracture surface is the quantitative measure of its roughness. It is the propose of this paper to develop an assumption free and unbiased method for the estimation of the fracture surface roughness from the measurements performed on the fracture profiles observed in the metallographic sections through fracture surface.

The quantitative descriptor of the surface roughness is the fracture surface roughness parameter R_s defined as follows[1].

$$R_s = \frac{S}{A} \tag{1}$$

S is the true fracture surface area, and A is the apparent projected area on a plane parallel to mean or average topographic plane of the fracture surface (see Figure 1a). The overlapped segments of the projected area are not added for calculating the apparent projected area A. The surface roughness parameter R_s is equal to true average area of a fracture surface segment having unit apparent projected area. For a flat surface R_s is equal to one. The rougher the fracture surface, higher is the value of R_s. In general, R_s can have any value ranging from one to infinity[2,3].

A fracture profile is a line generated by intersection of fracture surface and a metallographic sectioning plane (see Figure 1b). In general, a fracture profile is an irregular line of complex nature and it may contain overlaps. In practice, it is convenient to generate fracture profiles on sectioning planes which are perpendicular to average topographic plane of fracture surface[2-4]. Analogous to the surface roughness parameter, the profile roughness parameter R_L is defined as follows[1,4] (See Figure 1b).

$$R_L = \frac{\lambda o}{L} \tag{2}$$

λo is the true length of fracture profile, and L is its apparent projected length on mean or average topographic direction of the profile. The overlapped segments of projected length are not added for calculating L. For a straight line, R_L is equal to one. In general, R_L can have any value from one to infinity[2,3]. The sectioning planes of different angular orientations can yield the fracture profiles having significantly different values of R_L (see Figure 2). Thus, in general, the profile roughness parameter R_L depends on the nature of the fracture surface, and the orientation of the sectioning plane.

The profile roughness parameter R_L is relatively easy to measure; the details of the experimental technique are described by Banerji[5]. A large number of parametric equations have been derived[1,3,6-9] to relate the measurable quantity R_L to the desired parameter R_s. The present analysis differs significantly from all the earlier treatments because it is assumption free and it does not involve any approximations. Thus, the present results are applicable to fracture surfaces of any arbitrary complexity and anisotropy.

BACKGROUND: The present analysis is based on the following general results of quantitative microscopy.

(I)The total surface area S of a collection of surfaces or a single surface (such as fracture surface) contained in a reference volume V_o can be estimated by using the following classical result due to Smith and Guttman[10]

$$\frac{S}{V_o} = 2\,\bar{P}_L$$

$\bar{P}_L$ is the average value of the number of intersections of a test line with the surfaces of interest per unit test line length obtained by averaging the measurements over all possible test line orientations. The angular orientation of a test line is specified by two angles θ and ϕ defined with respect to a fixed frame of reference as shown in Figure 3; θ is the angle between the test line and z axis, and ϕ is the angle between the projection of the test line on xy plane and x-axis. Let $P_L(\phi,\theta)$ be the average or representative value of the number of intersections of a test line of orientation (ϕ,θ) with the surfaces of interest per unit test line length. The probability that a uniformly sampled test line has an orientation in the range θ to $(\theta + d\theta)$ and ϕ to $(\phi + d\phi)$ is equal to $\sin\theta d\theta d\phi/4\pi$ hence, $\bar{P}_L$ is given as follows.

$$\bar{P}_L = \frac{1}{4\pi} \int_0^{2\pi}\int_0^{\pi} P_L(\phi,\theta)\cdot\sin\theta\cdot d\theta\cdot d\phi \qquad (4)$$

Equations (3) and (4) are completely general, and they do not involve any assumptions. In practice, $\bar{P}_L$ must be obtained by averaging the measurements over randomly or uniformly sampled test line locations and angular orientations.

However, if the microstructure is homogenous (i.e. no gradients) and isotropic, the measurements performed on a single test line orientation can give a reliable value of $\bar{P}_L$.

(II) In a two dimensional plane section through collection of internal surfaces or fracture surface contained in a reference volume V_o, the intersections of surfaces of interest with a sectioning plane yield line traces (or fracture profile in the case of a single fracture surface). The average value of number of intersections of test lines having orientation ω <u>in the sectioning plane</u> (see Figure 4) with the fracture profile or line traces of surfaces of interest per unit test line length $P_L(\omega)$ is given by the following general equation.[11]

$$P_L(\omega) = \lambda_A\ (\omega + \pi/2) \tag{5}$$

$\lambda_A\ (\omega + \pi/2)$ is the <u>total</u> projected length (all overlaps in projected length added) of the fracture profile or the traces of interest in a direction perpendicular to the test line (i.e. having orientation $(\omega + \pi/2)$ in the sectioning plane) per unit area of the sectioning plane.

(III) Consider a fracture surface of area S contained in a cylindrical reference volume of length ℓ and diameter L as shown in Figure 5. For the present analysis, the direction perpendicular to the average topographic plane of the fracture surface is specified as the reference axis; let this direction be the cylinder axis in Figure 5, and the z axis of the frame of reference. It is sufficient to focus our attention only on the sectioning planes which contain the reference z-axis; such sectioning planes are called vertical sectioning planes,[12] and the resulting fracture profiles are the vertical section fracture profiles (see Figure 5). Vertical sections are used extensively in quantitative

fractography [3,5,8,13]. Recently, Baddeley, Gundersen, and Cruz Orive [12] have discussed a design based intercept counting procedure for estimation of a total area of internal boundaries in anisotropic microstructures from the measurements performed on the vertical sections. The procedure involves $\bar{P}_L$ measurements using oriented 'cycloid' shape test lines; these measurements have to be performed on the vertical sections only. The sampling of fracture surface by vertical sections is also the basis of the present treatment and it draws significantly from the stereological concepts developed by Smith and Guttman,[10] and Baddeley, Gundersen and Cruz Orive.[12] However, use of test lines (either straight test lines or any other design based shape) leads to serious practical difficulties in the characterization of the fracture surfaces. A fracture surface represents a structure having extreme inhomogeneity: all the surface area is restricted to one surface, unlike internal boundaries in microstructure where a large number of interface boundaries are distributed throughout the specimen volume. If the fracture surface is artificially enclosed in a reference volume of magnitude Vo, equation (3) is indeed applicable in principle, but the variance of P_L measurements is expected to be extremely large. In other words extremely large number of measurements are necessary to obtain a reliable estimate of $\bar{P}_L$: this is not practically feasible as it involves sectioning by a large number of planes having different locations and orientations. The use of design based intercept counting proposed by Baddeley, Gundersen, and Cruz Orive[12] does not eliminate this problem. This is because even to obtain a reliable value of average number of intersections of test line with fracture profile in the given vertical section, the test line must be placed at very large number of locations due to intrinsic inhomogeneity of the structure; it is expected to result in a large

large variance of $\bar{P}_L$ measurements, making the results practically meaningless. It must be concluded that use of test lines is of little practical significance for the analysis of fracture surfaces, although the related stereological relationships are applicable, in principle!

There is another practical difficulty associated with the characterization of fracture surfaces. The stereological equations express the global microstructural properties referred to (or normalized by) unit volume of sample or microstructure (for example, surface area per unit volume). The concept of sample volume or reference volume is quite trivial in the case of microstructures. However, for fracture surfaces, the reference volume is <u>not</u> naturally defined. Consequently, sectioning plane area and test line length are also not defined, in practice. It is thus desirable to develope the characterization techniques which do not involve reference volume, sectioning plane area or test line length for the practical applications of the results.

The present analysis utilizes the stereological concepts developed by Smith and Guttman[10], and Baddeley et al.[12], but it eliminates the use of test lines; the measurements are directly performed on what is observed, i.e., fracture profiles. Further, the final result does not involve reference volume or the sectioning plane area either implicitly or explicitly, and hence one need not be concerned with these quantities for practical applications of the results.

A geometrically general and statistically exact relationship is developed for the estimation of surface roughness of a fracture surface of any arbitrary complexity and anisotropy.

THEORETICAL DEVELOPMENT:

Consider a fracture surface of area S contained in the cylindrical reference volume of length ℓ and diameter L as shown in Figure 5.

Focus on vertical sectioning planes (i.e. planes whose zone axis is cylinder axis) through cylinder axis in Figure 5. The area of each such sectioning plane is equal to $(\ell \cdot L)$. The angular orientation of any plane is specified by the angles θ and ϕ pertaining to its normal (see Figure 6a). For all the vertical sectioning planes θ is equal to $\pi/2$. Consider one vertical sectioning plane having the orientation angle ϕ equal to ϕ_p (see Figure 6b). The geometric characteristics of the fracture profile generated by such a vertical sectioning plane depend on the nature of the fracture surface, and the orientation ϕ_p of the vertical sectioning plane. Let $\lambda_o(\phi_p)$ be the total length of the fracture profile. The profile roughness parameter $R_L(\phi_p)$ is given by (see Figure 7);

$$R_L(\phi_p) = \frac{\lambda_o(\phi_p)}{L} \tag{6}$$

Thus, the profile roughness parameter is a function of the orientation of the vertical sectioning plane ϕ_p. Note that $R_L(\phi_p)$ is the average or representative value of the profile roughness parameter on parallel sections having the same angular orientation ϕ_p. Focus on a small line element on the fracture profile. Let α be the angle between the tangent to this line element and z-axis in the sectioning plane (Figure 7). Let $d\lambda(\alpha,\phi_p)$ be the total length of line elements in the fracture profile having orientation in the sectioning plane in the range α to $(\alpha + d\alpha)$. Define the profile orientation distribution function $f(\alpha,\phi_p)$ as follows:

$$d\lambda(\alpha, \phi_p) = \lambda_o(\phi_p) \cdot f(\alpha,\phi_p) \cdot d\alpha \tag{7}$$

where, $o \leq \alpha \leq \pi$

obviously, $$\int_o^\pi f(\alpha,\phi_p)\, d\alpha = 1 \tag{8}$$

In general, the profile orientation distribution function $f(\alpha,\phi_p)$ is expected to depend on the orientation ϕ_p of the vertical sectioning plane. Let us calculate the total projected length of the fracture profile on a line having orientation $(\theta + \pi/2)$ in the sectioning plane; the ϕ orientation angle of this projection line in the three dimensional space is equal to $(\phi_p + \pi/2)$ as shown in Figure 7. Thus, the orientation of the projection line in three dimensional space is $(\theta + \pi/2, \phi_p + \pi/2)$. The projected length of elements $d\lambda(\alpha,\phi_p)$ of fracture profile having orientation in the range α to $(\alpha + d\alpha)$ in the sectioning plane, on the projection line of orientation $(\theta + \pi/2, \phi_p + \pi/2)$ is equal to $\left|\cos(\theta + \pi/2 - \alpha)\right| \cdot d\lambda(\alpha,\phi_p)$. Hence, the total projected length per unit area of section plane $\lambda_A(\theta + \pi/2, \phi_p + \pi/2)$ is given by;

$$\lambda_A(\theta + \pi/2, \phi_p + \pi/2) = \frac{\lambda_o(\phi_p)}{\ell \cdot L} \int_o^\pi \left|\cos(\theta + \pi/2 - \alpha)\right| \cdot f(\alpha,\theta_p)d\alpha \tag{9}$$

where, $(\ell \cdot L)$ is the area of the sectioning plane (see Figure 7). However, using equation(5) (with $w = \theta$);

$$P_L(\theta, \phi_p + \pi/2) = \lambda_A(\theta + \pi/2, \phi_p + \pi/2) \tag{10}$$

where, $P_L(\theta, \phi_p + \pi/2)$ is precisely equal to the number of intersections of a test line having orientation $(\theta, \phi_p + \pi/2)$ with fracture surface per unit test line length. Equations (6), (9) and (10) yield the following result:

$$P_L(\vartheta, \phi_p + \pi/2) = \frac{R_L(\phi_p)}{\ell} \int_0^{\pi} \left| \cos(\theta + \pi/2 - \alpha) \right| \cdot f(\alpha, \phi_p) d\alpha \qquad (11)$$

The advantage of vertical sectioning is now obvious. If $R_L(\phi_p)$ and $f(\alpha, \phi_p)$ are experimentally measured, substituting different values of θ in the integral on the right hand side of equation (11), yields $P_L(\theta, \phi_p + \pi/2)$ for different values of ϑ ranging from o to π for fixed ϕ orientation angle equal to $(\phi_p + \pi/2)$; the point is, ϑ orientation is identified in the sectioning plane. Combining equations (3), (4) and (11) yields;

$$\frac{S}{V_o} = \frac{S}{(\pi L^2/4)} \cdot \frac{1}{\ell} = \frac{1}{\ell} \cdot \frac{1}{2\pi} \int_0^{2\pi} R_L(\phi_p) \int_0^{\pi} \sin\theta \cdot \int_0^{\pi} \left| \cos(\theta + \pi/2 - \alpha) \right| \cdot f(\alpha, \phi_p) d\alpha d\theta d\phi_p \qquad (12)$$

The quantity $S/(\pi L^2/4)$ is the ratio of the true area of the fracture surface S and its projected area on its mean topographic plane $\pi L^2/4$ (because cylinder axis is perpendicular to mean topographic plane of the fracture surface), which is by definition, the fracture surface roughness parameter Rs (see equation (1)). Thus, equation (12) can be written as follows:

$$R_s = \frac{1}{2\pi} \int_0^{2\pi} R_L(\phi_p) \cdot \left\{ \int_0^{\pi} \sin\theta \cdot \int_0^{\pi} \left| \cos(\theta + \pi/2 - \alpha) \right| \cdot f(\alpha, \phi_p) d\alpha d\theta \right\} \cdot d\phi_p \qquad (13)$$

Note that equation (13) is independent of the magnitude of the reference cylindrical volume containing fracture surface and dimensions of the reference volume. Define the profile structure factor $\psi(\phi_p)$ as follows:

$$\psi(\phi_p) \equiv \int_0^{\pi} \sin\theta \int_0^{\pi} \left|\cos(\theta + \pi/2 - \alpha)\right| \cdot f(\alpha,\phi_p)\, d\alpha\, d\theta \qquad (14)$$

Note that the profile structure factor $\psi(\phi_p)$ is completely determined by the profile orientation distribution function $f(\alpha,\phi_p)$. Combine equations (13) and (14) to obtain the following result.

$$R_s = \frac{1}{2\pi} \int_0^{2\pi} R_L(\phi_p) \cdot \psi(\phi_p)\, d\phi_p \qquad (15)$$

or

$$R_s = \int_0^{2\pi} R_L(\phi_p) \cdot \psi(\phi_p)\, d\phi_p \Big/ \int_0^{2\pi} d\phi_p \qquad (16)$$

The right hand side of equation (16) is precisely equal to the average value of the product $R_L(\phi_p)\ \psi(\phi_p)$ obtained by averaging it over all possible vertical sectioning plane orientations ϕ_p. Hence one can write;

$$R_s = \overline{R_L \cdot \psi} \qquad (17)$$

The expected value of the product $R_L\psi$ in a set of vertical sectioning planes is precisely equal to the fracture surface roughness parameter R_s; the zone axis of the vertical sectioning planes must be the direction normal to the average topographic plane of the fracture surface. Thus, the product $\overline{R_L \cdot \psi}$ is an unbiased estimator of the surface roughness parameter R_s. There are no assumptions involved in derivation of equation (17), and hence it is applicable to fracture surface of any arbitrary geometry and anisotropy. The order of integration in equation (14) can be interchanged, and with some algebric manipulations the

double integral can be reduced to single integral. The result is as follows:

$$\psi(\phi_p) \equiv \int_0^{\pi} [\sin\alpha + (\pi/2 - \alpha)\cos\alpha] f(\alpha, \phi_p).d\alpha \qquad (18$$

The quantities R_L and profile orientation distribution function can be experimentally measured via digital image analysis, and a number of measurements of these parameters are published in the literature[13-16] Once $f(\alpha)$ is measured, the profile structure factor ψ can be calculated by utilizing equation (18); these calculations can be easily carried out via numerical integration. In practice R_L and ψ can be estimated on a few randomly oriented (random ϕ_p only) vertical sections; the average value of the product $R_L \cdot \psi$ reports the fracture surface roughness paramter R_s. It is not necessary to know the ϕ_p orientations of the vertical sections. In the special cases where the geometry of fracture surface is symmetric with respect to the vertical reference axis, all the vertical sections should yield statistically similar fracture profiles. Under these conditions, measurements of R_L and ψ on a single vertical section should yield reliable estimate of R_s, without involving any further assumptions.

DISCUSSION: The main results of the present paper are contained in equations (17) and (18), which permit estimation of fracture surface roughness parameter R_S from the measurements performed on the vertical section fracture profiles. It is shown that the statistical expected val f the product of the measurable quantitites profile roughness parameters R_L and profile structure factor ψ is precisely equal to the fracture surface roughness parameter R_s. There are no assumptions involved in the present analysis. Thus, equation (17) constitutes

a fundamental result of quantitative fractography. The present result differs from all the earlier equations for estimation of R_s from measurements performed on fracture profiles because it is assumption free and statistically exact. In practice, the parameters R_L and ψ can be measured on a few vertical sectioning planes. In this context, it is important to emphasize that the measurements must be performed on vertical section fracture profiles only, and orientations of the vertical sectioning planes (i.e. angle ϕ_p) must be random. Preparation of metallographic sections is time consuming and tedious. Very often, time and effort necessary for metallographic preparation of fracture profiles exceeds the time and effort required for the measurements. This raises very important question: on how many vertical section fracture profiles the measurements should be performed to obtain a reliable estimate of R_s? The answer to this question obviously depends on the nature of anisotropy of fracture surface under investigation. A significant portion of the companion paper is devoted to analyze this problem[17]. If the angular orientation distribution of the surface elements on the fracture surface is symmetric with respect to the reference axis, then all the vertical section fracture profiles are statistically similar. In such a case, measurements of R_L and ψ on just <u>one</u> vertical section fracture profile gives a very reliable estimate of $R_L \cdot \psi$, and hence R_s, without involving any further assumptions. As the angular orientation distribution of the surface elements on the fracture surface becomes asymmetric with respect to the reference axis, the different vertical section fracture profiles pertaining to different vertical section orientations differ from one another. An extreme case of an asymmmetric fracture is illustrated in Figure 8, where the angular orientation

distribution of the surface elements on the fracture surface have absolutely no symmetry with respect to the vertical reference axis.

It is usually believed that there is one to one quantitative correlation[1] betweem the fracture surface roughness parameter R_s and the profile roughness parameter R_L; i.e. measurement of R_L on one fracture profile uniquely determines R_S. The present analysis clearly demonstrates that this is certainly not true in general, and it is not true even for symmetric fracture surfaces. For a symmetric fracture surface, all the vertical section fracture profiles are statistically similar; $\overline{R_L \cdot \psi}$ is equal to $R_L \cdot \psi$ on any one vertical section. Thus one can write:

$$R_s = \psi \cdot R_L \tag{19}$$

The parameters ψ and R_L represent different <u>independent</u> properties of the fracture profile. Hence two different fracture profiles originating from two fracture surfaces having different R_s can have the same value of R_L provided the profile structure factor ψ is proportionally different. Thus, even for symmetric fracture surfaces, the profile roughness parameter R_L <u>alone</u> does not uniquely determine R_s, it is the product of R_L and ψ that determines the surface roughness parameter R_s. Thus, the fracture process descriptors (for example, fracture toughness) should not be correlated to profile roughness parameter R_L; such correlations may not be real, or the real correlations may not be observed. The assumption free estimation of surface roughness is necessary to establish true correlations with fracture process parameters.

The present result for estimation of R_s is derived from the classical stereological relationship for estimation of total surface area per unit volume by intercept counting [equation (3)]. It may be argued that why can't this

result be directly utilized for estimation of fracture surface area, and hence the surface roughness parameter R_s? Indeed, the result is applicable, in principle, but serious experimental difficulties are involved in the direct application of intercept counting technique to fracture surfaces; this has been the basic impetus for the development of the model based relationships between R_s and R_L. The angular orientations of the surface elements on the fracture surface are usually not random. Further, a fracture surface contained in a reference volume represents a structure having extreme inhomogeniety: all the surface area belongs to one surface, unlike grain boundaries in a microstructure, where a large number of boundary interfaces are distributed throughout the specimen volume. Due to these reasons, to estimate fracture surface area by intercept counting, it is necessary to measure P_L for a large number of random angular orientations of the test line as well as a large number of different random locations of test line in the reference volume. For this purpose, it would be necessary to section the reference volume with sectioning planes of different angular orientations and at different random locations; some sectioning planes may not intersect the fracture surface at all. Thus, it is not practically feasible to directly use intercept counting for the measurement of fracture surface area. The present analysis eliminates the need for the use of test lines and the measurements need to be performed only on vertical sections, which always intersect fracture surface. Further, all the geometric information available on fracture profile is efficiently utilized for the estimation of R_s.

CONCLUSIONS: A general assumption free method is developed for estimation of fracture surface roughness parameter from the measurements performed on the

vertical section fracture profiles. The input measurements are profile roughness parameter and angular orientation distribution of the line elements on fracture profile; these data are easily accessible via digital image analysis. It is demonstrated that the general notion "rougher the fracture profile, the rougher is the fracture surface" is not quantitatively valid even for relatively simple symmetric fracture surfaces.

ACKNOWLEDGEMENT: This work is a part of NSF sponsored project (DMR-8504167) on "Quantitative Analysis of Fracture Surfaces Using Stereological Methods"; this financial support is gratefully acknowledged.

REFERENCES:

(1) S. M. El-Soudani, Metallography, 1978, Vol. 11, pp. 247-336.

(2) E. E. Underwood, Applied Metallography, G. Vander Voort, ed., Van Nostrand Reinhold Co., 1986, pp. 101-121.

(3) E. E. Underwood and K. Banerji, ASM Metals Handbook, 9th edition, Vol. 12, ASM, Metals Park, Ohio, 1987, pp. 193-210.

(4) J. R. Pickens and J. Gurland, Proceedings of 4th International Congress for Stereology, E. E. Underwood, R. deWit and G. A. Moore, eds., NBS Spec. Pub. 431, Gaithersburg, Maryland, 1976, pp. 269-272.

(5) K. Banerji, Met. Trans.-A, 1988, Vol. 19, pp. 264-271.

(6) M. Coster and J. L. Chermant, Int. Met. Rev., 1983, Vol. 28, pp. 228-250.

(7) K. Wright and B. Karlsson, J. Microscopy, 1983, Vol. 130, pp. 37-51.

(8) A. M. Gokhale and E. E. Underwood, Acta Stereologica, 1989, vol. 8, pp 43-52.

(9) S. Gentier and J. Riss, Acta Stereologica, 1987, Vol. 6, pp. 223-228.

(10) C. S. Smith and L. Guttman, Trans. AIME, 1953, Vol. 197, pp. 81-92.

(11) E. E. Underwood, Quantitative Stereology, Addison-Wesley Publishing Co., Reading, Massachusettes, 1970.

(12) A. J. Baddeley, H. J. G. Gundersen and L. Cruz-Orive, J. Microscopy, 1986, Vol. 142, pp. 259-276.

(13) K. Banerji and E. E. Underwood, Microstructural Science, 1985, Vol. 13, pp. 537-551.

(14) K. Banerji and E. E. Underwood, Acta Stereologica, 1983, Vol. 2, Suppl. 1, pp. 65-70.

(15) A. M. Gokhale and K. Banerji, Microstructural Science, in press.

(16) E. E. Underwood and S. B. Chakrabortty, ASTM Special Technical Publication, No. 733, 1981, pp. 337-354.

(17) A. M. Gokhale and W. J. Drury, Met. Trans.-A, submitted.

LIST OF FIGURE CAPTIONS

Figure 1. (a) Definition of fracture surface roughness parameter R_s, (b) Definition of profile roughness parameter R_L.

Figure 2. Different sectioning plane orientations can yield fracture profiles having different roughness.

Figure 3. Specification of test line orientation in three dimensional space.

Figure 4. Relationship between $P_L(\omega)$ and $\lambda_A(\omega+\pi/2)$: (a) Two dimensional section through microstructure containing internal boundaries, (b) A section through fracture surface.

Figure 5. The concept of vertical sections which contain Z-axis.

Figure 6. (a) Orientation of any plane is specified by angles θ and ϕ, (b) For all vertical sectioning planes $\theta=\pi/2$ and $\phi=\phi p$ can have any value from 0 to 2π.

Figure 7. Geometry involved in calculation of $\lambda_A(\theta+\pi/2, \phi_p+\pi/2)$.

Figure 8. Example of an asymmetric fracture surface.

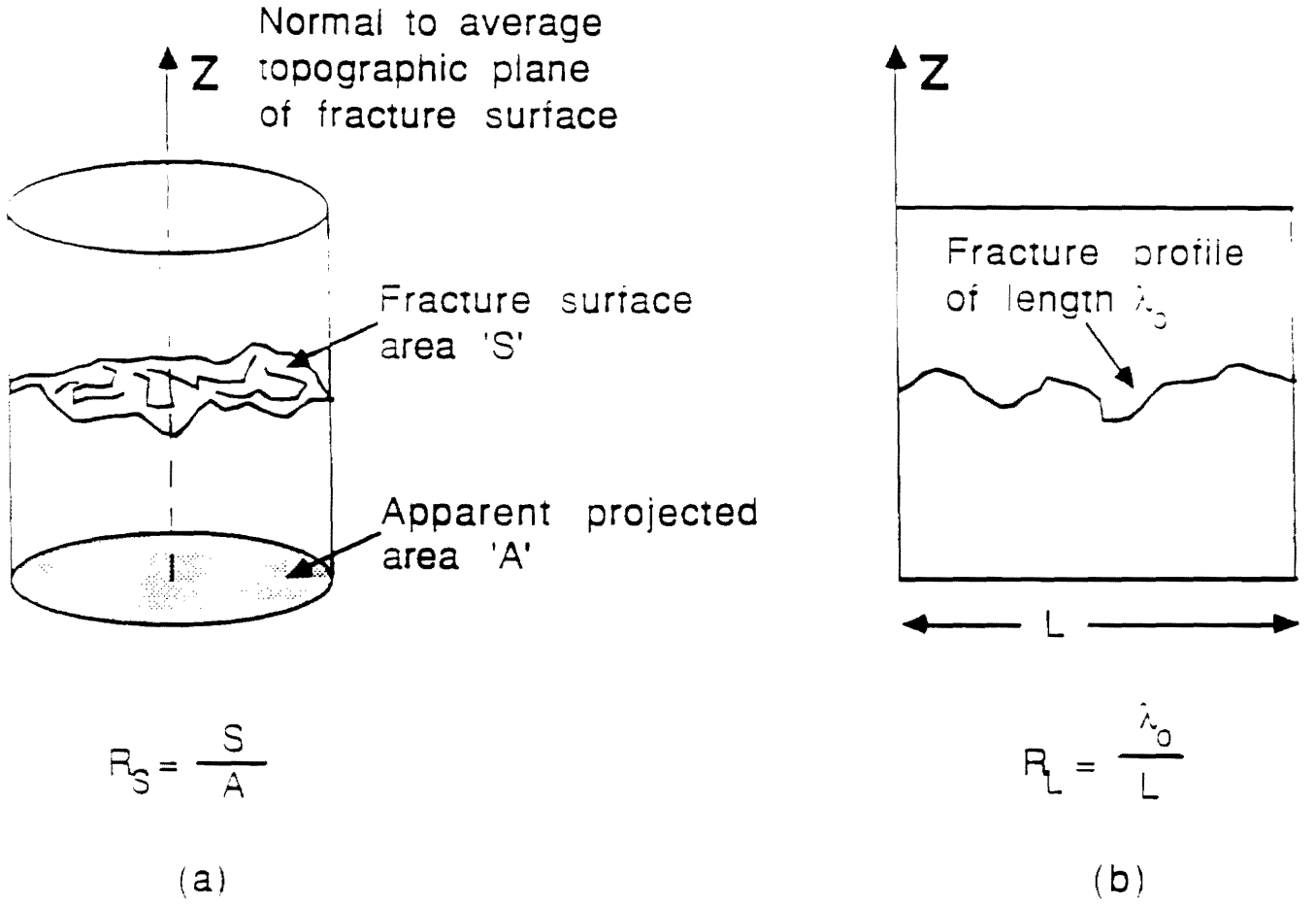

Figure 1. (a) Definition of fracture surface roughness parameter R_s, (b) Definition of profile roughness parameter R_L.

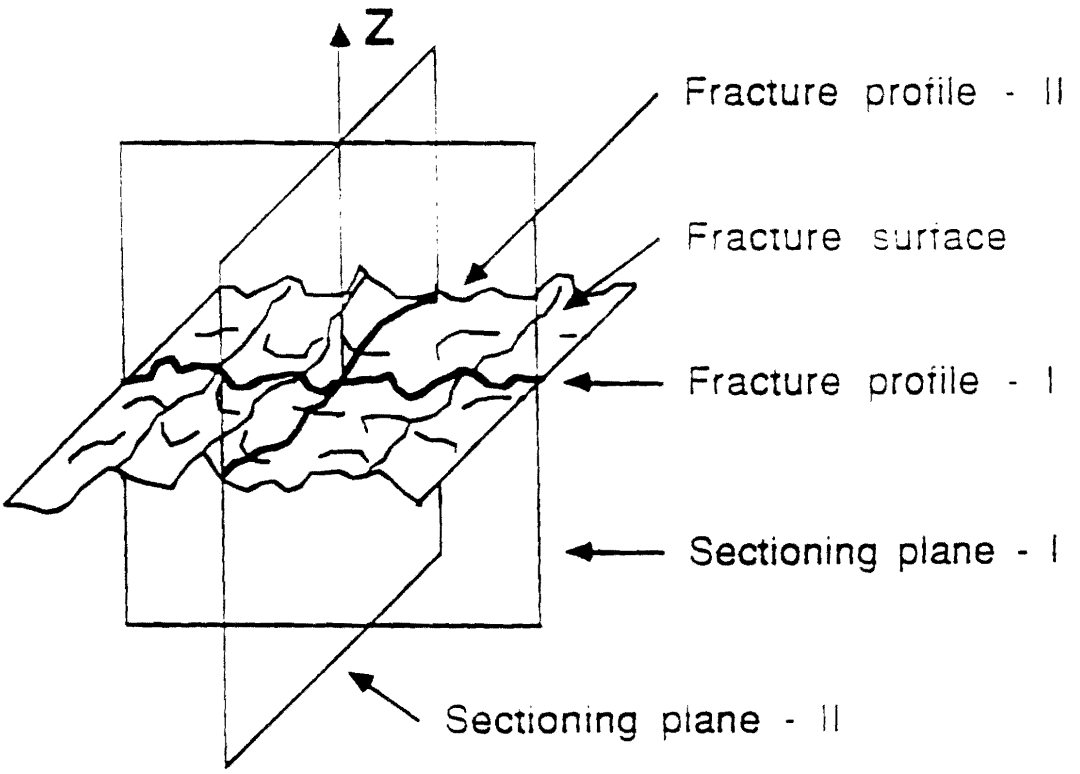

Figure 2. Different sectioning plane orientations can yield fracture profiles having different roughness.

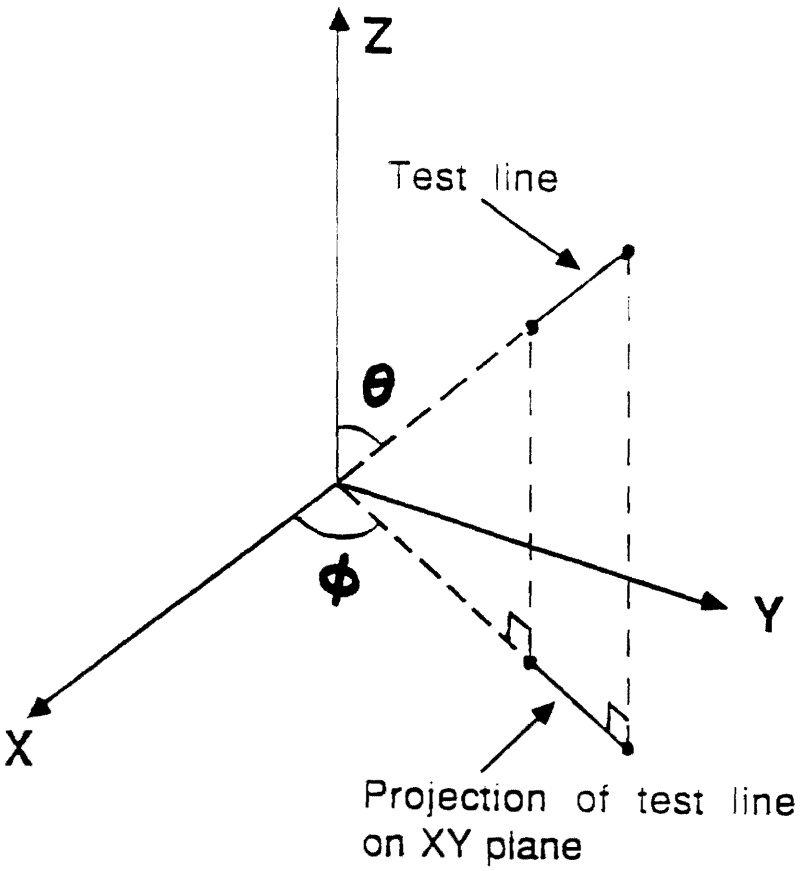

Figure 3. Specification of test line orientation in three dimensional space

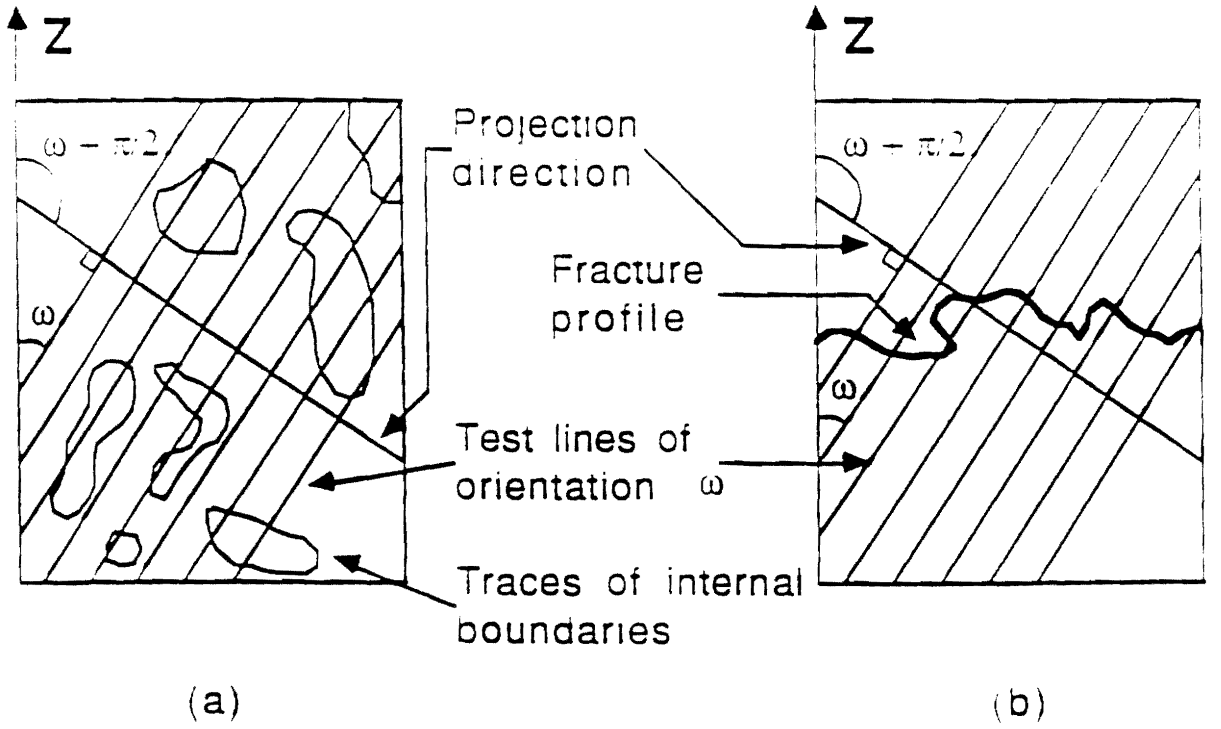

Figure 4. Relationship between $P_L(\omega)$ and $\lambda_A(\omega+\pi/2)$: (a) Two dimensional section through microstructure containing internal boundaries. (b) A section through fracture surface.

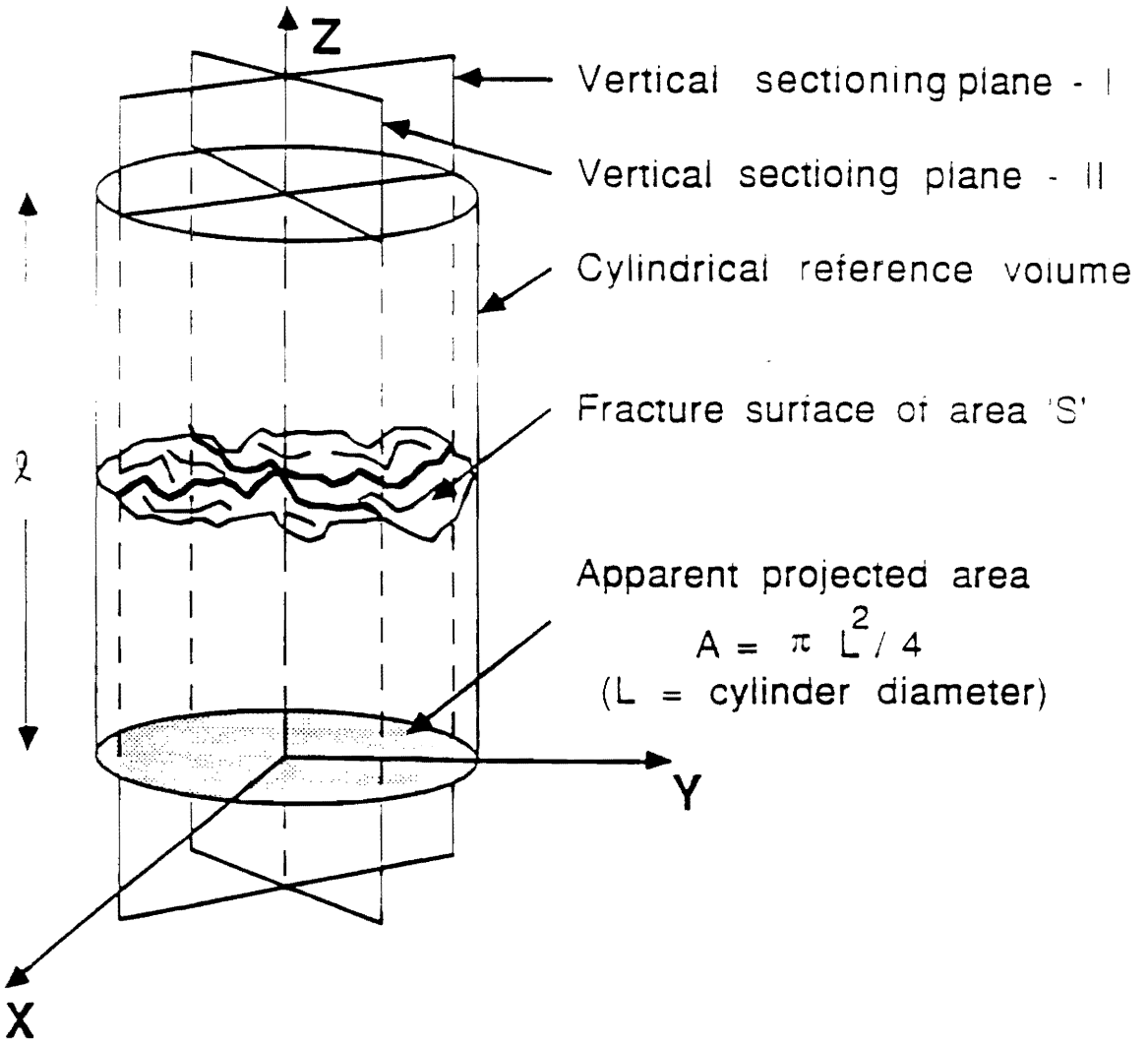

Figure 5. The concept of vertical sections which contain Z-axis.

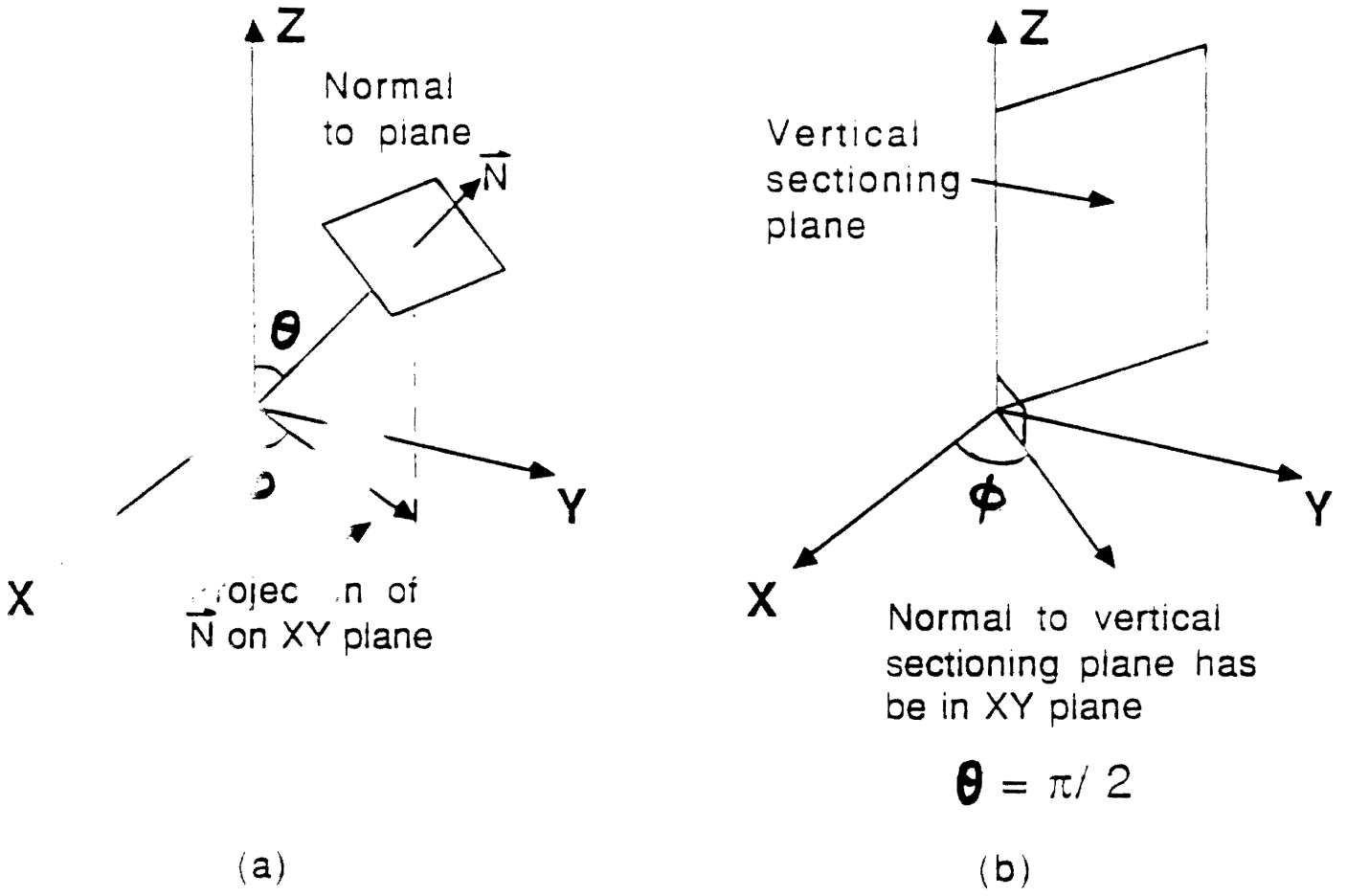

Figure 6. (a) Orientation of any plane is specified by angles θ and ϕ. (b) For all vertical sectioning planes $\theta=\pi/2$ and $\phi=\phi_p$ can have any value from o to 2π.

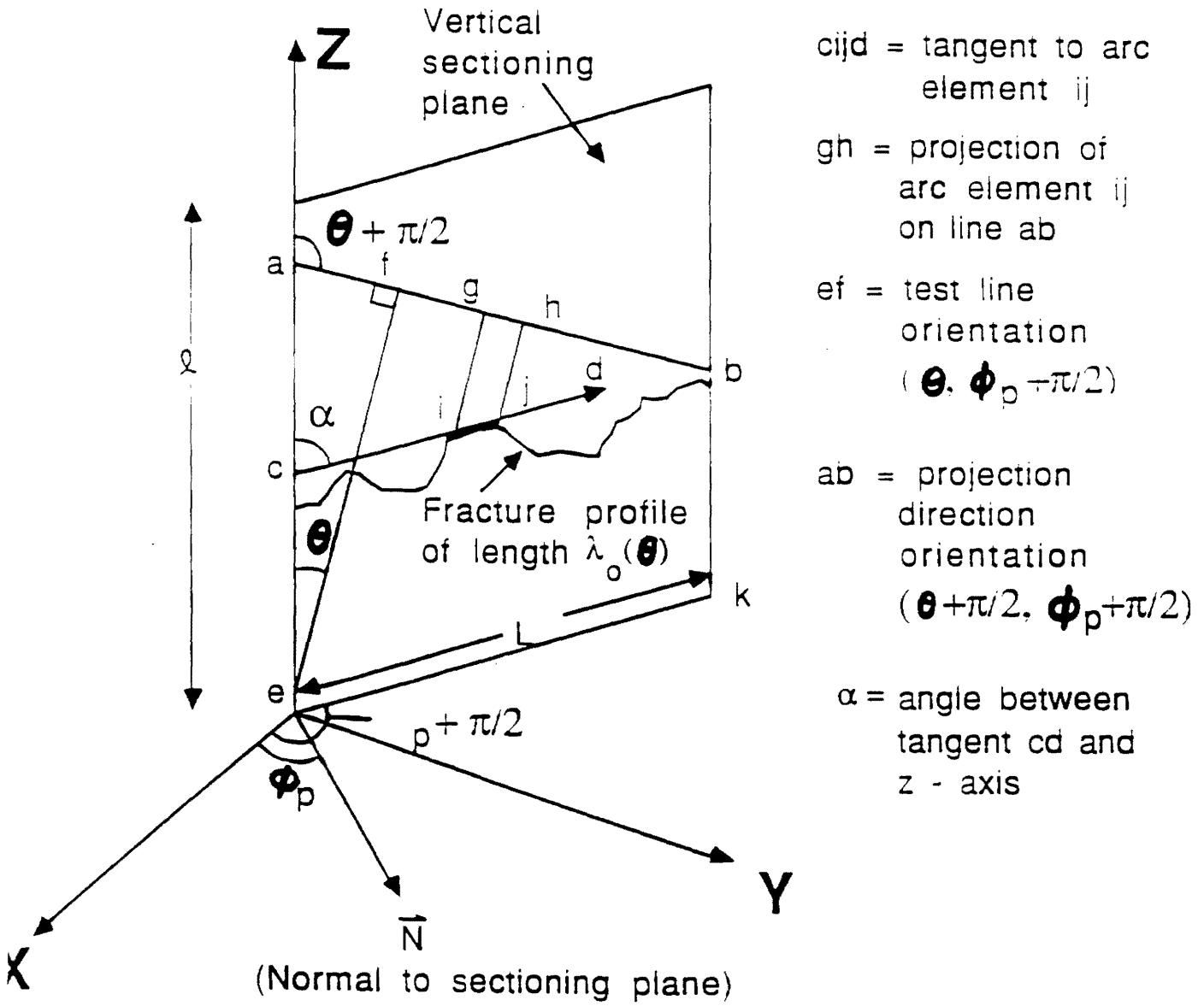

Figure 7. Geometry involved in calculation of $\lambda_A(\phi+\pi/2, \vartheta_p+\pi/2)$.

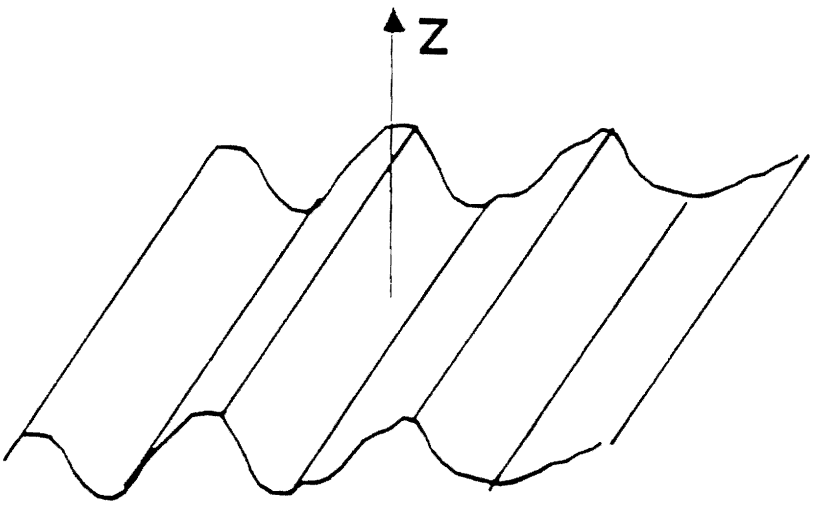

Figure 8. Example of an asymmetric fracture surface

Metall. Trans. - A
(in press)

A General Method for Estimation of Fracture Surface Roughness - II; Practical Considerations

by

A. M. Gokhale and W. J. Drury

School of Materials Engineering
Georgia Institute of Technology
Atlanta, GA. - 30332-0245

ABSTRACT

Surface roughness is an important attribute of fracture surfaces. An assumption free method for estimation of surface roughness presented in the companion paper is analyzed further in this paper. It is shown that three vertical sectioning plane orientations mutually at an angle of 120° contain sufficient information for a reliable estimation of surface roughness; in most of the cases, the sampling error due to measurements on a limited number (three) of vertical section orientations should be less than $\pm$ 6% with the confidence limit of 95%. A simplified procedure is presented for calculation of profile structure factor from the measurements of profile frequency function. A practical example of application of the present analysis involving measurement of fracture surface roughness of metal matrix composite is discussed.

INTRODUCTION: The surface roughness parameter is quantitative index of fracture surface roughness. The nature of fracture surface and its roughness depend on the material chemistry, microstructure, and the deformation and fracture process that lead to fracture. In the companion paper[1], a general theoretical treatment has been presented for the estimation of fracture surface roughness parameter R_s from the measurements performed on the vertical section fracture profiles. Such fracture profiles are lines (usually of irregular shape) generated by intersections of the fracture surface with the metallographic sectioning planes perpendicular to the average topographic plane of the fracture surface. Thus, all the vertical sectioning planes contain the direction normal to the average topographic plane of the fracture surface; this common direction or 'zone axis' is called vertical axis. The estimation of the fracture surface roughness parameter R_s involves the following measurements on the vertical section fracture profiles.

(1) The fracture profile roughness parameter R_p, which is equal to the true length of the fracture profile divided by its apparent projected length (overlaps not counted) on a line perpendicular to the vertical axis and in the corresponding vertical sectioning plane[2] (see Figure - 1).

and,

(2) Profile structure factor ψ, defined as follows[1]

$$\psi \equiv \int_0^{\pi} \sin\theta \int_0^{\pi} \left|\cos(\theta + \pi/2 - \alpha)\right| \cdot f(\alpha)\, d\alpha d\theta \qquad 1)$$

α is the angle between the tangent to an arc element on fracture profile and the vertical axis (see Figure - 1); it specifies the angular orientation of an arc element. In general, different line or arc elements on a fracture profile have different angular orientations: $f(\alpha)$ is the frequency distribution function of arc element orientations in the fracture profile. Thus, $f(\alpha)\,d\alpha$ is equal to the fraction of profile length in the orientation range α to $(\alpha - d\alpha)$. For the present purpose θ is simply a dummy variable of integration in equation (1). Thus, ψ is completely determined by $f(\alpha)$.

The parameters R_L and ψ can be experimentally measured. In general, vertical sectioning planes of different angular orientations may result in fracture profiles having different values of R_L and ψ. It can be shown that[1];

$$R_s = \overline{R_L \cdot \psi} \qquad (2)$$

where $\overline{R_L \cdot \psi}$ is an expected or average value of the product of R_L and ψ on a set of vertical sectioning planes. Note that an average value of the product of R_L and ψ, and <u>not</u> the product of the average values of R_L and ψ, is the quantity equal to R_s. Equation (2) is absolutely general and it does not involve any assumptions concerning the nature of the fracture surface. This result forms the basis for an assumption free and unbiased estimation of the fracture surface roughness parameter R_s, from the measurements of R_L and ψ performed on the vertical section fracture profiles.

It is the purpose of this paper to focus on the practical aspects associated with application of equation (2) for estimation of fracture surface roughness. The estimation of R_s involves measurements of R_ϕ and ϕ on a number of vertical sectioning planes of different angular orientations. This amounts to statistical sampling of R_ϕ values from the population, which raises two questions of significant practical importance:

(A) On how many vertical sectioning plane orientations is it necessary to measure R_ϕ and ϕ to obtain a reliable estimate of $\overline{R_\phi}$ and hence R_s?

(B) How close (or how reliable) is the sample average $(\overline{R_\phi})$ to the population average $\overline{R_\phi}$, i.e. R_s?

This sampling problem is analyzed in the next section with the aid of computer simulations. It is shown that the measurements on three vertical sectioning plane orientations mutually at an angle of 120° are sufficient for a reliable estimation of R_s. In the subsequent section a simple procedure is presented for analytical as well as numerical calculation of the profile structure factor $\ldots$. Finally, a practical example of an estimation of R_s is given for the fracture surface of a metal matrix composite.

EFFICIENT SAMPLING PROCEDURE: Angular orientation of a surface element δS on a fracture surface is given by angles θ_s and ϕ_s pertaining to its normal $\vec{N}_s$ as shown in Figure - 2. Note that Z axis is the vertical axis (direction perpendicular to the average topographic plane of the fracture surface), θ_s is the angle between the normal $\vec{N}_s$ and Z axis, and ϕ_s is the angle between the

projection of $\vec{N}_s$ on XY plane and X-axis. The choice of X-axis is arbitrary in the plane perpendicular to X-axis. In general, different surface elements on a fracture surface may have different angular orientations. Let $g(\phi_s, \theta_s)$ be the angular orientation distribution function (SODF) of the surface elements on a fracture surface, such that $g(\phi_s, \theta_s) \sin \theta_s \, d\phi_s \, d\theta_s$ is equal to the fraction of fracture surface area having angular orientations in the range ϕ_s to $(\phi_s - d\phi_s)$ and θ_s to $(\theta_s - d\theta_s)$. The SODF $g(\phi_s, \theta_s)$ quantifies the fracture surface anisotropy. Intersection of a surface element δS on the fracture surface with a vertical sectioning plane yields an arc element $d\lambda$ on the vertical section fracture profile. The length of such arc element and its angular orientation α in the sectioning plane (see Figure - 1) basically depend on the orientation of the surface element δS given by angles ϕ_s and θ_s, and the orientation of the vertical sectioning plane given by the angle ϕ_p (see Figure -3). It follows that changes in $f(\alpha)$, and hence ψ, with the variations in the vertical sectioning plane orientation ϕ_p are basically determined by the SODF $g(\phi_s, \theta_s)$. Similarly, the SODF also determines variation of R_L as a function of the sectioning plane orientation ϕ_p. In other words, the range of values of the product $R_L\psi$ (or 'spread' around the mean) in a population of vertical section fracture profiles of a given fracture surface is determined by the SODF $g(\phi_s, \theta_s)$. Thus, the average of population of $R_L\psi$ values is always equal to R_s, but the variance is determined by the SODF of the fracture surface under

investigation. Usually, the SODF $g(\phi_s, \theta_s)$ is unknown. For a randomly oriented fracture surface, $g(\phi_s, \theta_s)$ is constant (i.e., all the orientations are equally likely) and hence all the fracture profiles are statistically similar, and measurements on a single vertical section orientation can yield a reliable estimate of R_s. However, real fracture surfaces are unlikely to be randomly oriented due to the basic nature of the fracture processes. If the SODF depends only on θ_s and <u>not</u> on ϕ_s (i.e. $g(\phi_s, \theta_s) = g(\theta_s)$), then the SODF is symmetric with respect to the vertical axis, i.e., for any given interval θ_s and $\theta_s + d\theta_s$ all the ϕ_s angles are equally likely. In such a case, all the vertical section fracture profiles are statistically similar, and variance of R_ϕ values is expected to be very small. Hence, measurement of R_ϕ on a single vertical section orientation should give a reliable estimate of R_s. If the SODF depends on both θ_s and ϕ_s then different vertical section orientations can yield different values of R_ϕ. The range of values of R_ϕ in a population of vertical sections thus depends on how sensitive the SODF $g(\phi_s, \theta_s)$ is to the orientation parameter ϕ_s. The limiting case is a surface where all the surface elements have the same value of ϕ_s (although, they may have different θ_s values), i.e.,

$$g(\Phi_s, \Theta_s) = \delta(\Phi_s^i) \cdot g(\Theta_s) \qquad (3)$$

where, $\delta(\phi_s^i)$ is a delta function around $\phi_s = \phi_s^i$, and $g(\theta_s)$ is a function of θ_s only. The surfaces whose SODF can be represented by equation (3) thus exhibit large variations in R_ϕ values in the vertical section fracture profiles. It follows that such surfaces

would require measurements of R_ψ and ψ on a number of vertical section orientations to obtain a reliable value of $\overline{R_\psi}$, and hence R_v. It follows that, the number of vertical section orientations necessary to obtain a reliable R_v value of such surfaces should be sufficient for a reliable estimation of the fracture surface roughness of <u>any</u> fracture surface. Thus, the problem reduces to determination of the number of vertical sectioning plane orientations necessary for a reliable estimation of R_v of the surfaces whose SODF have functional form given by equation (3), and the development of an efficient sampling scheme to minimize the sampling error. A class of 'ruled surfaces' of geometry[3] have the required form of SODF. Such ruled surfaces can be generated by moving a planar curve in a direction perpendicular to the plane of the curve. Figure - 4 gives three examples of ruled surfaces and the corresponding generating planar curves. A corrugated sheet is an example of a ruled surface. In Figure - 5, the normal vector of any surface element is parallel to the YZ plane, and hence the ϕ_s orientation angle of all the surface elements is equal to $\pi/2$. Thus, the SODF of such ruled surfaces can be represented by equation (3) with ϕ_s equal to $\pi/2$; the function $g(\theta_s)$ is obviously determined by the nature of the generating planar curve. These ruled surfaces have following properties[4].

(1) R_ψ is always equal to 1.0 on the vertical section perpendicular to the planar curve.

(2) R_ψ has a maximum value $(R_\psi)_m$ on the vertical section which contains the planar generating curve, and $(R_\psi)_m$ is precisely

equal to the R_s of the ruled surface.

In the present study a ruled surface having a 'semicircular wave generating curve (Figure - 4a) was simulated on the CYBER 760 mainframe computer at Georgia Tech. It is assumed that the surface is of infinite extent and hence there are no 'edge' effects. The surface was sectioned by vertical sectioning planes of different orientations ϕ_i at intervals of 1° in the range 0° to 180°. The values of R and ψ on resulting vertical section profiles were calculated and stored in the computer memory. Next, three random number integers in the interval 0 to 180 were computer generated independently; each number representing a vertical section orientation. The average of R_ψ values of these three independent random vertical section profiles was calculated. Let this sample average be $(\overline{R_\psi})_s$. The process was repeated one thousand times; each simulation representing vertical section sampling by three planes of independent random orientations. Figure - 6 reports the frequency of occurrence of the sample average $(\overline{R_\psi})_s$ in the one thousand simulations. Inspection of Figure - 6 shows that:

i) The expected value of $(\overline{R_\psi})_s$ is indeed equal to R_s

ii) There is a very large spread in the $(\overline{R_\psi})_s$ values

Increasing the number of sections upto seven did not decrease the spread in $(\overline{R_\psi})_s$ significantly. It must be concluded that the measurements on independent random vertical sections can not yield a reliable estimate of R_s unless the measurements are performed on an extremely large number of vertical section orientations. An alternative to independent random vertical sections is <u>systematic</u>

vertical section sampling[5], where the first vertical section orientation is random but subsequent orientations are chosen with respect to the first one in a systematic manner. This was carried out as follows.

(1) Computer generated a random number integer in the interval 0° to 180° representing the orientation of the first vertical section ϕ_1°.

(2) Orientations of second and third vertical sections were fixed at $(\phi_1^\circ - 120°)$ and $(\phi_1^\circ - 240°)$, respectively. The average value of R_ψ of the corresponding three vertical section profiles $(\overline{R_\psi})_{ss}$ was calculated.

(3) The steps (1) and (2) were repeated one thousand times, representing one thousand experiments consisting of sampling by a randomly rotated triplet of three sectioning planes mutually at an angle of 120°. Figure - 7 reports the frequency of occurrence of $(\overline{R_\psi})_{ss}$ values of the systematic samples generated in the one thousand simulations. It is interesting to note that:

(a) the expected value of $(\overline{R_\psi})_{ss}$ is equal to R_s

and

(b) all the values of $(\overline{R_\psi})_{ss}$ lie in a very narrow range 1.545 to 1.595, i.e. 1.57 ± 0.025

Thus, one experiment involving three vertical section orientations mutually at an angle of 120° yields value of R_s with an error of less than ±2%, for a ruled surface having a 'semi circular wave' generating curve. In order to determine whether these results are

sensitive to the shape of generating planar curve associated with ruled surface (i.e. $g(\theta_i)$ in equation (3)) the following additional ruled surfaces were analyzed.

(i) Ruled surface with sine wave generating curve (see Figure 4b)

(ii) Ruled surface with rectangular wave generating curve (see Figure 4c).

The ruled surface with sine wave generating curve was simulated on computer and systematic vertical section sampling was carried out as discussed earlier, the basic conclusions remain unchanged: a single experiment consisting of three vertical section orientations mutually at 120° gives the value of $(\overline{R_\phi})_{ss}$ with sampling error of less than ±2%. The ruled surface with rectangular generating wave (Figure 4c) can be analyzed in a straight forward manner. Using simple geometric arguments it can be shown that:

$$R_s = 1 + 2m \tag{4}$$

$$R_{s\,\phi} = 1 + \pi\, m\, |\cos\phi_i| \tag{5}$$

Where, R_ϕ is the value pertaining to profile associated with the vertical section having orientation ϕ_i and 2m is equal to ratio of the total length of the vertical line segments of the rectangular generating curve to the total length of its horizontal line segments. If m=1, two third of the surface elements have orientation $\phi_i = \pi/2$, $\theta_i = \pi/2$. The variation of m essentially

reflects a change in the function $g(\theta_s)$ in equation (3). If m=2, 80% of surface area is parallel to the vertical axis (i.e. $\phi_s=\pi/2$, $\theta_s=\pi/2$); an extreme case of anisotropy. For systematic vertical section sampling consisting of three vertical planes mutually at 120°, equation (4) yields the following result.

$$\bar{R}_s = R_s \quad \psi = \left[1 - \frac{\pi m}{3} \left[\left| \cos\phi_1 \right| + \left| \cos\left(\phi_1 + \frac{2\pi}{3}\right) \right| + \left| \cos\left(\phi_1 - \frac{2\pi}{3}\right) \right| \right] \right] \quad (6)$$

Where, ϕ_1 is the orientation of the first vertical section. $(R_\psi)_{ss}$ was calculated for different values of ϕ_1 at an interval of 1° in the range 0° to 120°. It was observed that 95% of the $(R_\psi)_{ss}$ values were within ± 5% of R_s value for ruled surface with m=1, and 95% of the $\overline{(R_\psi)}_{ss}$ values were within ± 6% of R_s value for m=2. Note that the R_s value of a surface with m=2 is 5.0 (see equation (5)), and for this surface 80% of the surface area is parallel to the vertical axis. Real fracture surfaces are not generally expected to have surface roughness higher than 5.0, and they are also not expected to exhibit anisotropy worse than that of a rectangular wave ruled surface with m=2. It is interesting to note that, for a ruled surface with semicircular wave generating curve, $g(\theta_s)$ (see equation (3)) is constant, (i.e., line elements on the generating curve have random orientations in the plane of the curve), whereas for rectangular wave ruled surface $g(\theta_s)$ basically consists of two spikes (one at $\theta_s=0$, and second at $\theta_s=\pi/2$). For a sine wave ruled surface $g(\theta_s)$ has a complicated

form. However, in all three cases at least 95% of $\overline{(R_v \cdot \omega)}_{ss}$ values are within ± 6% of the corresponding R_v value.

The SODF of any arbitrary fracture surface can be written in the following form.

$$g(\theta_s, \phi_s) = g_r(\theta_s) + \sum \delta(\phi_s) \cdot g_s(\theta_s) \qquad (7)$$

where, $\delta(\phi_s)$ are delta functions around different $\phi_s = \phi_{s_i}$ and $g_s(\theta_s)$ are functions of θ_s only. Thus, the SODF of any fracture surface can be represented by a combination of SODFs of randomly oriented surface, rotationally symmetric surface (i.e. $g_s(\theta_s)$), and a number of ruled surfaces. In all these three limiting cases systematic vertical section sampling with three vertical sectioning planes mutually at an angle of 120°, is sufficient to obtain R_v value with an error of less ± 6% with 95% confidence. This sampling should also be sufficient for any arbitrary fracture surface as it can be regarded as the one resulting from superimposition of a number of different ruled surfaces, rotationally symmetric surface, and a random surface (see equation (7)).

The above analysis leads to the following conclusions applicable to any fracture surface.

(1) Systematic vertical section sampling is extremely efficient as compared to sampling by independent random vertical sections.

(2) One experiment consisting of three vertical section orientations mutually at an angle of 120° is sufficient to yield R_s value with sampling error of less than ± 6% with 95% confidence limit for real fracture surfaces.

CALCULATION OF PROFILE STRUCTURE FACTOR: The experimental data on profile element orientation angles α (see Figure - 1) can be conveniently grouped into histogram form. The values of α range from 0° to 180°; this range can be divided into K classes having class interval Δ (where, $\Delta = \pi/K$). Let $h_i\Delta$ be the fraction of profile length having the orientation angle α in the range $(i-1)\Delta$ to $i\Delta$. Thus, h_i is the height of i^{th} histogram bar, and the index i takes integer values from 1 to K. By definition,

$$h_i \Delta = \int_{(i-1)\Delta}^{i\Delta} f(\alpha)\, d\alpha \qquad (8)$$

and,

$$\sum_{i=1}^{K} h_i \Delta = 1 \qquad (9)$$

Equations (1) and (8) lead to the following results

$$v = \int_0^{\pi} \sin\theta \cdot \Delta \cdot \sum_{i=1}^{k} \left| \cos\left[\theta + \frac{\pi}{2} - \left(i - \frac{1}{2}\right)\Delta\right] \right| \cdot h \, d\theta \qquad (10)$$

or,

$$v = \Delta \cdot \sum_{i=1}^{k} a_i h_i \qquad (11)$$

where

$$a_i = \int_0^{\pi} \sin\theta \cdot \left| \cos\left[\theta + \frac{\pi}{2} - (i-1/2)\,\Delta\right] \right| \cdot d\theta \qquad (12)$$

A simple algebraic manipulation of equation (12) gives the following result.

$$a_i = \sin\left[(i - \tfrac{1}{2})\,\Delta\right] + \left[\frac{\pi}{2} - (i - \tfrac{1}{2})\,\Delta\right] \cdot \cos\left[(i - \tfrac{1}{2})\,\Delta\right] \qquad (13)$$

The coefficients a_i depend on i, but they are independent of the nature of the frequency function (i.e. they do not depend on h_i values). Thus, the same set of values of the coefficients a_i can be utilized to calculate the profile structure factor ψ of any fracture profile. Table - I reports numerically calculated values of a_i, in which the data is grouped into 18 histograms of width $\Delta = \pi/18 = 10°$. This table and equation (11) provide a straightforward procedure for calculation of ψ. If it is necessary to group the data into a total number of classes other than 18 (i.e. K = 18,) then equation (12) or (13) can be utilized for calculation of a_i coefficients.

PRACTICAL EXAMPLE: Figure - 8 is an SEM fractograph of the fracture surface of a composite material consisting of continuous unidirectional fibers of alumina in the matrix of Al-Li alloy. The material was fractured by application of uniaxial tensile stress perpendicular to the fibers. The fractures surface is anisotropic because of the material's anisotropic microstructure. The profile structure factor ψ, and the profile roughness parameter R_a are expected to depend on the orientation of the vertical sectioning

plane. The steps involved in the estimation of R_s are as follows.

(1) Thick plating of fracture surface ($\geq 25\mu m$) to avoid distortion during sectioning and metallographic polishing. In the present case, the specimen was electroplated with a thick layer of copper

(2) Metallographic sectioning along three vertical sectioning planes mutually at an angle of 120° and subsequent metallographic polishing using standard techniques to clearly reveal the fracture profiles. Figures - 9 to 11 show the fracture profiles obtained in this manner.

(3) Digitization of fracture profiles via semiautomatic or automatic digital image analysis. In the present case, the profiles were digitized using a Zeiss digitizing tablet attached to a Video-Plan semiautomatic image analyzer. The process involves manual tracing of fracture profile using an electronic cursor. The instrument records the co-ordinates of points on fracture profile at preselected fixed intervals; the intervel length is called 'ruler length'. The profile is thus represented by a series of line segments (Figure - 12); the total profile length λo is equal to the sum of the lengths of all the line segments. The instrument also measures the angle α between each digitized line segment and the vertical axis. The frequency of these α values is the profile frequency function $f(\alpha)$. The values of R_s and $f(\alpha)$ were obtained in this manner and are reported in Figures 9 to - 11.

(4) The profile structure factor ϕ is calculated by substituting histogram bar heights h_i, and a_i values from Table -

I in equation (11).

(5) The fracture surface roughness parameter R_s is equal to the average value of the product $R_l\phi$ on the three vertical sections. In the present case, R_s is estimated to be equal to 2.47

DISCUSSION: It is shown that [1] the fracture surface roughness parameter R_s can be estimated from the measurements of profile roughness parameter R_l and the profile structure factor ϕ on the vertical section fracture profiles; measurements on three vertical section angular orientations mutually at an angle of 120° can yield a reliable estimate of R_s. It is often observed that R_l varies systematically with the resolution or the 'ruler length' utilized for profile digitization. Careful experimental work of Banerji and Underwood[6] demonstrated that although R_l increases with the decrease in the ruler length η, it approaches a finite value $(R_l)_0$ as $\eta \to 0$. In other words, R_l does not approach ∞ as $\eta \to 0$, and hence fracture profiles do not exhibit classical fractal characteristics proposed by Richardson and Manderbolt[7]. The present analysis is applicable to R_l value measured at any length of the ruler η; the estimated R_s value reflects surface roughness at similar level of resolution. The analysis is equally applicable to extrapolated 'true' profile roughness value $(R_l)_0$ as $\eta \to 0$, the estimated value of R_s then represents the surface roughness corresponding to $\eta \to 0$.

The metallographic sectioning of fracture surface by vertical sectioning planes is proposed in the present work. However, actual

physical sectioning of fracture surfaces is not necessary for application of the present analysis. For example, stereo pair images [9] can be utilized to generate the co-ordinates of points on fracture surface along different directions using SEM, and the present procedure can then be utilized for estimation of R_s; this is expected to be more efficient as compared to generation of 'carpet plot' of fracture surface, because it involves sampling of surface along lines rather than 'areas'

It is likely that the surface roughness parameter R_s may correlate to the fracture toughness of materials. However, to develop such correlations it is necessary to estimate R_s without invoking any assumptions concerning the nature of the fracture surface (which can be done using the present procedure). On the other hand, the profile roughness parameter R_l may not correlate to fracture toughness or any other fracture process descriptors for the simple reason that two or more surfaces with different R_s values can yield fracture profiles having the same value of R_l! Finally, it must be pointed out that surface roughness is only one geometric attribute of a given fracture surface. Thus, two fracture surfaces having the same value of R_s need not be similar. A detailed characterization of fracture surface geometry should be possible via estimation of the orientation distribution function $g(\phi_s, \theta_s)$ and R_s. Unfortunately, at present, there is no general, practically feasible procedure for estimation of the orientation distribution function from measurements performed on fracture profiles.

CONCLUSIONS. An efficient sampling procedure is proposed for estimation of fracture surface roughness from the measurements performed on the vertical section fracture profiles. It is shown that appropriate measurements performed on three vertical section orientations mutually at 120° yield reliable estimates of the surface roughness parameter R_s.

ACKNOWLEDGEMENT. This research work is part of NSF sponsored project (DMR-8504167) on "Quantitative Analysis of Fracture Surfaces Using Stereological Methods"; this financial support is gratefully acknowledged.

RENCES:

A. M. Gokhale and E. E. Underwood: Met. Trans-A, submitted

J. P. Pickens and J. Gurland: Proceedings of Fourth International Congress for Stereology, E. E. Underwood, R. deWit, and G. A. Moore, eds., NBS special Pub. 431, Gaithersburg, Maryland, 1976, PP 269-272

D. J. Struik: Classical differential Geometry, 2nd ed., Addison-Wesley Publising Co., Reading, Mass., 1961, pp

E. E. Underwood and K. Banerji: ASM Metals Handbook, 9th edition, Vol.12, ASM, Metals Park, Ohio, 1987, pp. 189 192-210

H. J. G. Gundersen and E. B. Jensen: J Microscopy, 1987 vol. 147 pp. 229-263

E. E. Underwood and K. Banerji: ASM Metals Handbook, 9th edition, vol. 12, ASM Metals Park, Ohio, 1987, pp 211-215

B. B. Manderbolt: The Fractal Geometry of Nature, W. H. Freeman, 1982

L. S. Sigl and H. E. Exner: Metall. Trans, A, 1987, vol. 18A, pp 1299-1308

LIST OF TABLES:

LIST OF FIGURE CAPTIONS·

Figure 1 Definition of R_α and profile element orientation angle α

Figure 2 Angular orientation of a surface element

Figure 3 Orientation of a vertical sectioning plane

Figure 4 Examples of ruled surfaces: (a) Ruled surface with semicircular wave generating curve (b) Ruled surface having sine wave generating curve (c) Ruled surface having rectangular wave generating curve

Figure 5 Orientations of surface elements on a ruled surface

Figure 6 Frequency of $\overline{(R_\alpha)_\phi}$ values values for three independent random vertical sections; the population average

$$\overline{(R_\alpha)_\phi} = R_\phi = \pi/2$$

Figure 7 Frequency of $\overline{(R_\alpha)_{ss}}$ values for systematic sampling by three vertical sections mutually at 120°; Population average

$$\overline{(R_\alpha)_\phi} = R_\phi = \pi/2$$

Figure 8 SEM fractograph of fracture surface of a metal-matrix composite

Figure 9 Vertical section fracture profile ($\phi = 0°$) and corresponding profile frequency function $f(\alpha)$

Figure 10 Vertical section fracture profile ($\phi = 120°$) and corresponding profile frequency function $f(\alpha)$

Figure 11 Vertical section fracture profile ($\phi_1 = 240°$) and corresponding profile frequency function $f(\alpha)$

Figure 12 Digitization of fracture profile

Table - I

Calculated Values of a_i Coefficients

i	a_i*	i
1	1.565	18
2	1.5232	17
3	1.4508	16
4	1.3599	15
5	1.2625	14
6	1.1694	13
7	1.0906	12
8	1.0336	11
9	1.0037	10

* The values are symmetric with respect to $\alpha = \pi/2$.

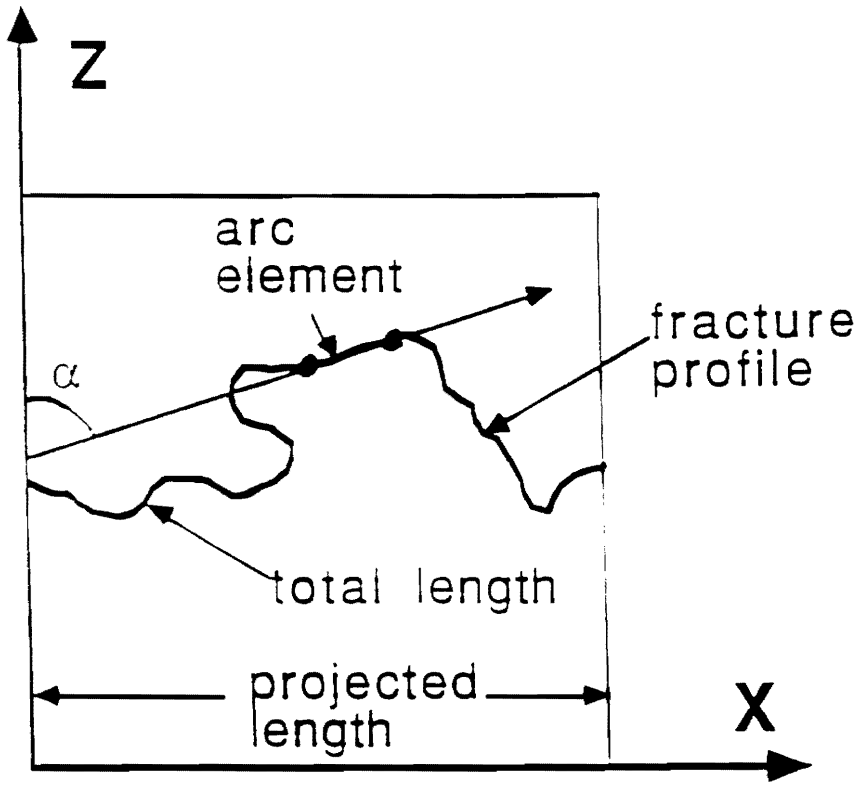

$$R_L = \frac{\text{profile length}}{\text{projected length}}$$

Figure 1 Definition of R_L and profile element orientation angle α

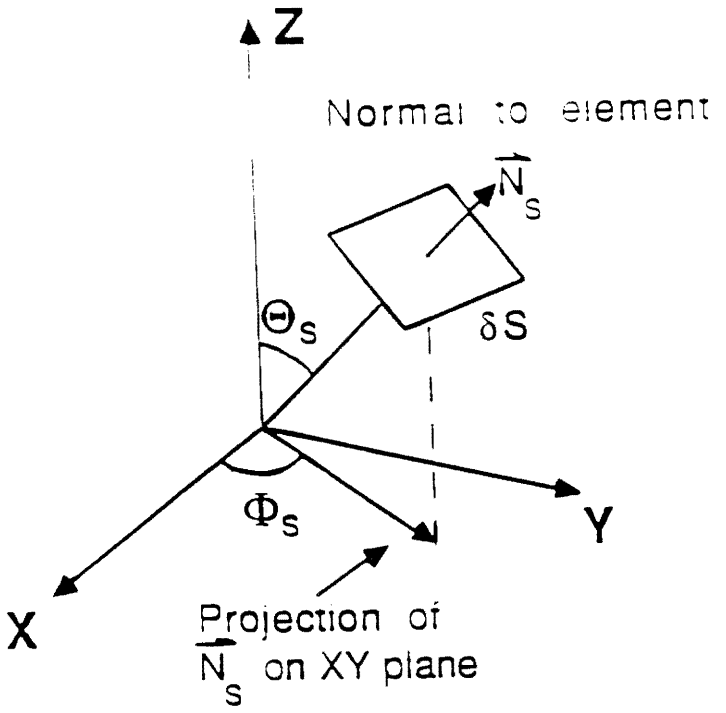

Figure 2 Angular orientation of a surface element

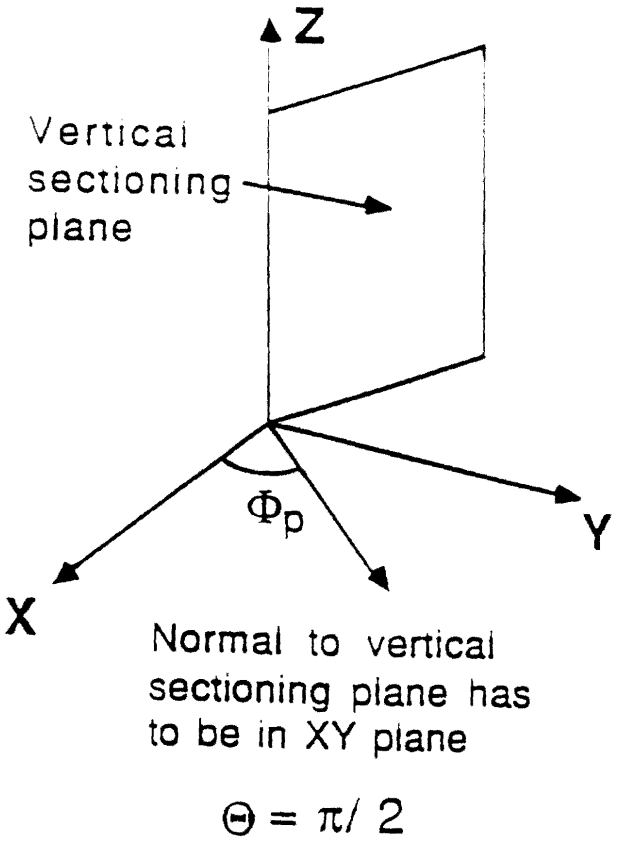

Figure 3 Orientation of a vertical sectioning plane.

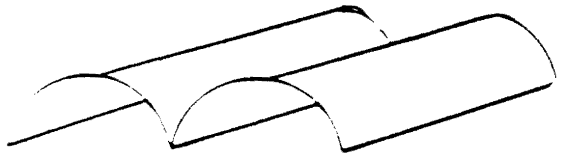

(a)

semi-circular wave
generating curve

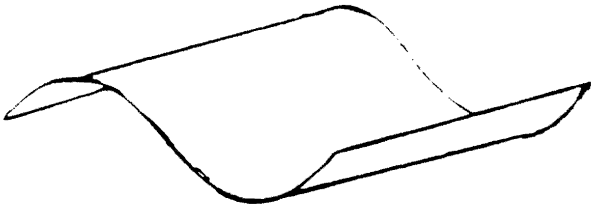

(b)

sine wave
generating curve

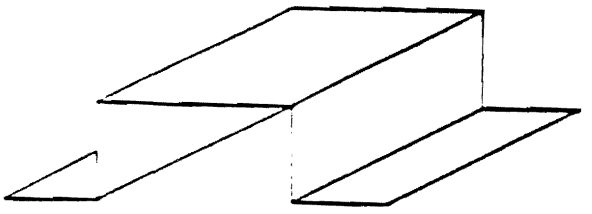

(c)

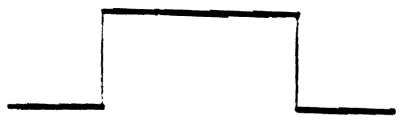

rectangular wave
generating curve
(2m = 0.5)

Figure 4 Examples of ruled surfaces: (a) Ruled surface with semicircular wave generating curve (b) Ruled surface having sine wave generating curve (c) Ruled surface having rectangular wave generating curve

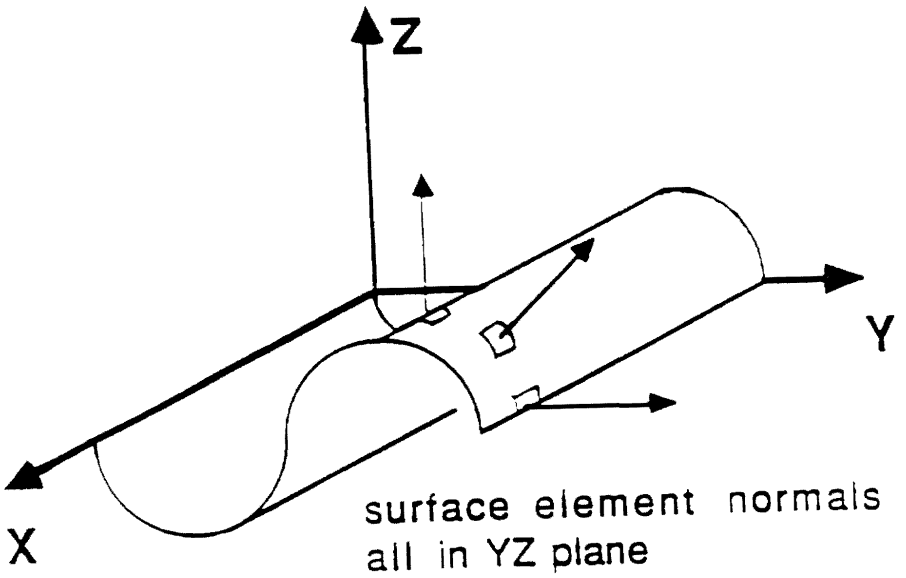

Figure 5 Orientations of surface elements on a ruled surface

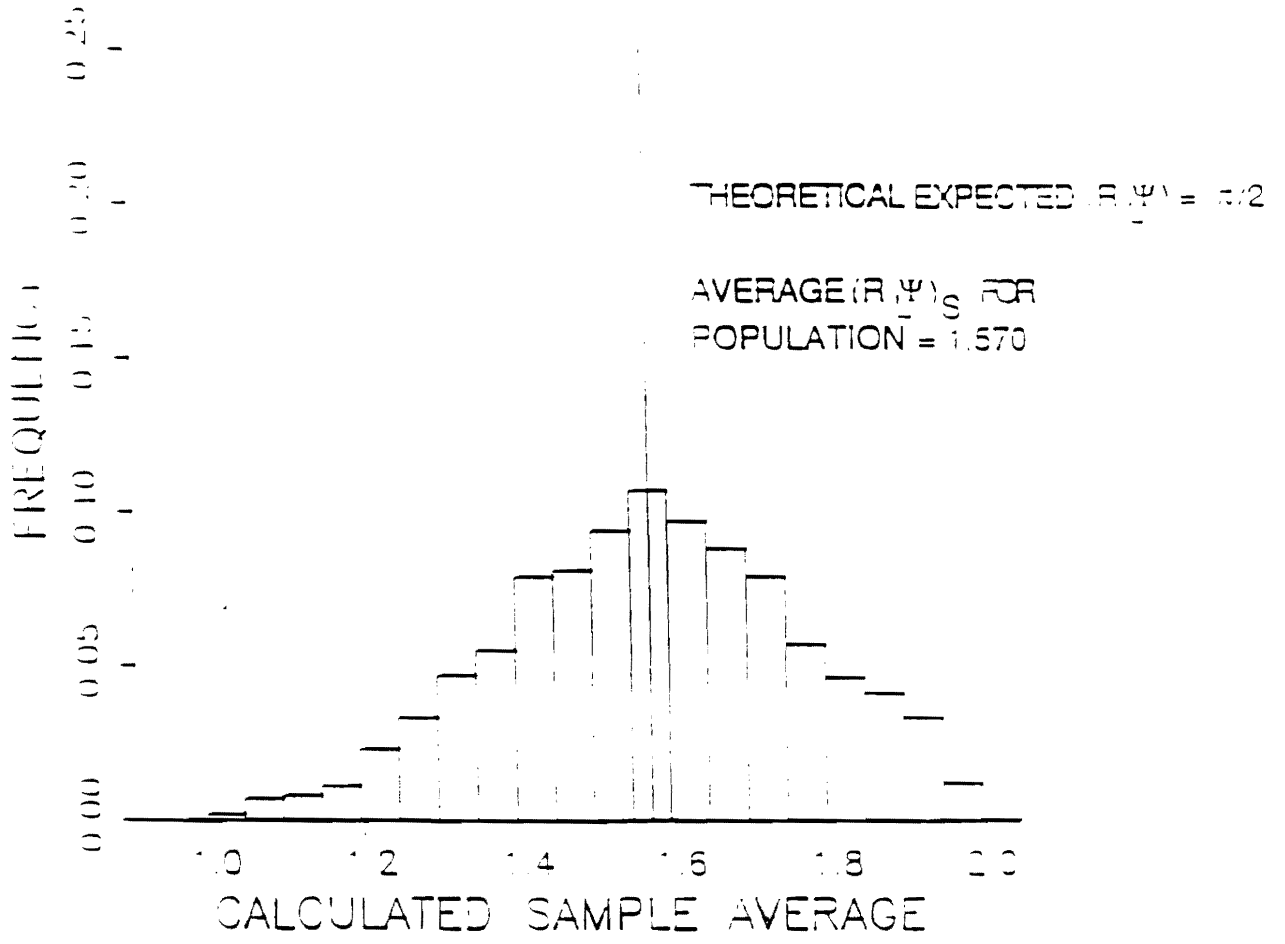

Figure 6 Frequency of $(\overline{R,\psi})_s$ values values for three independen random vertical sections; the population average

$(\overline{R,\psi})_s = R_s = \pi/2$

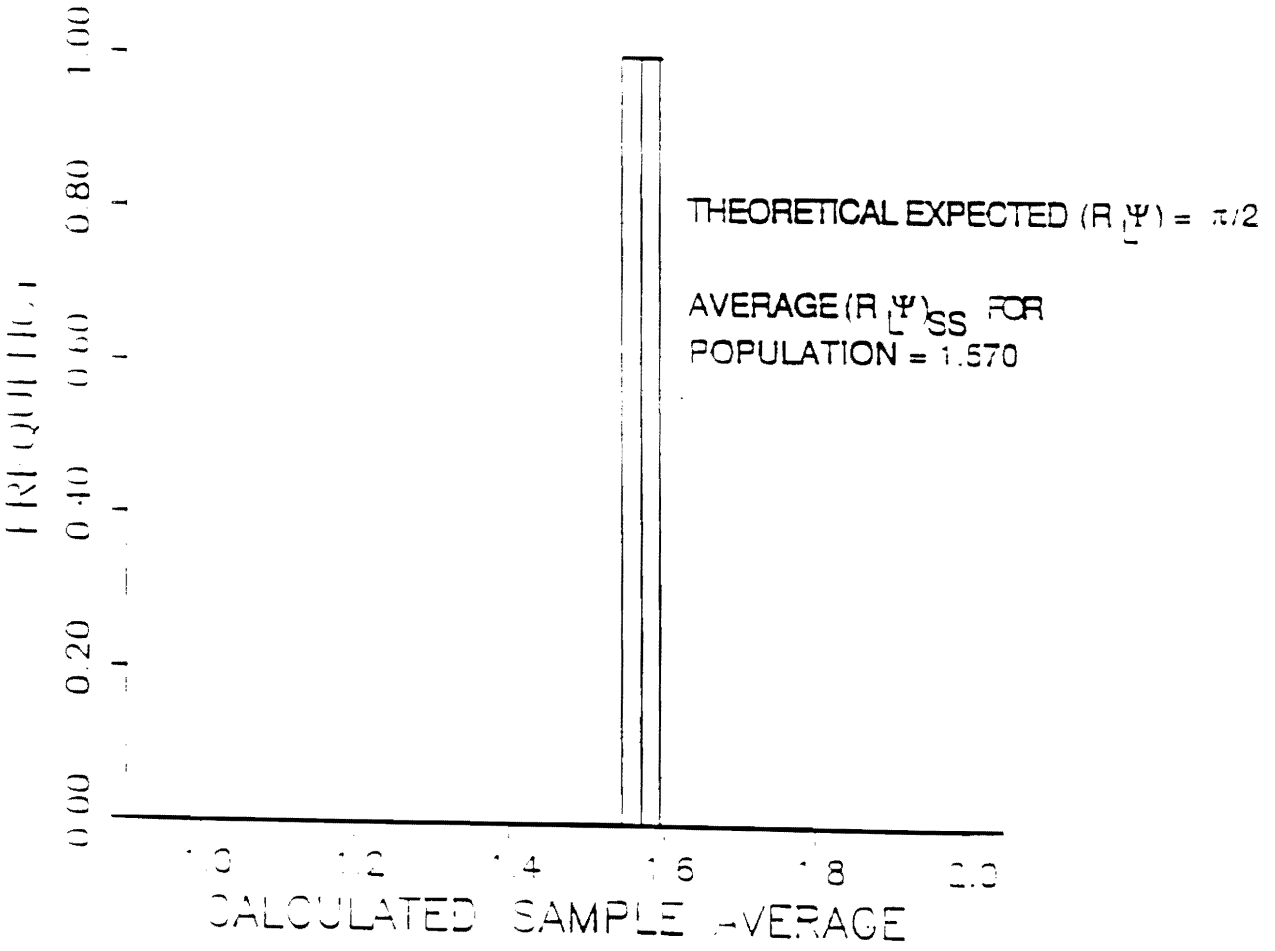

Figure 7 Frequency of $\overline{(R_{\psi})_{ss}}$ values for systematic sampling by three vertical sections mutually at 120°; Population average

$$\overline{(R_{\psi})_s} = R_s = \pi/2$$

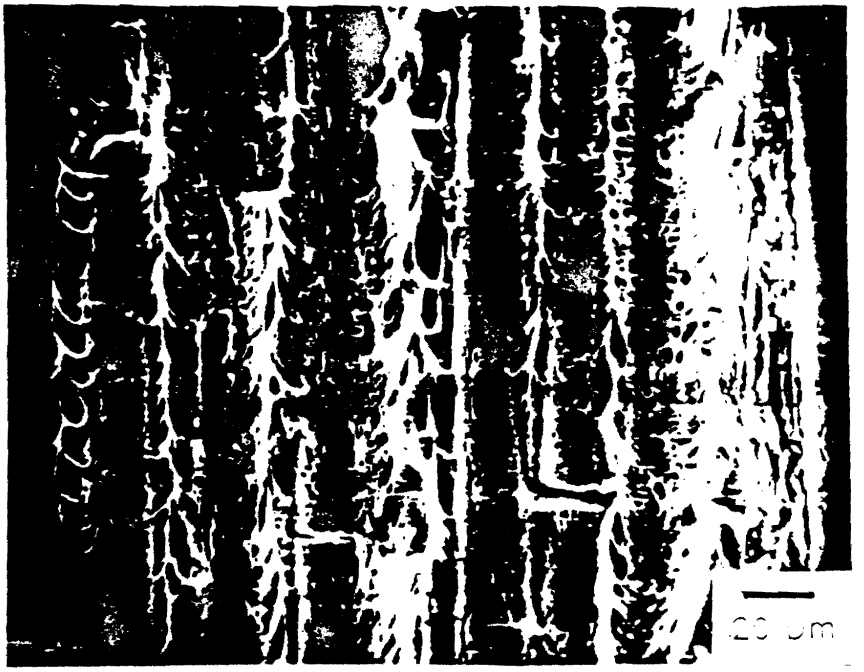

Figure 8 SEM fractograph of fracture surface of a metal-matrix composite

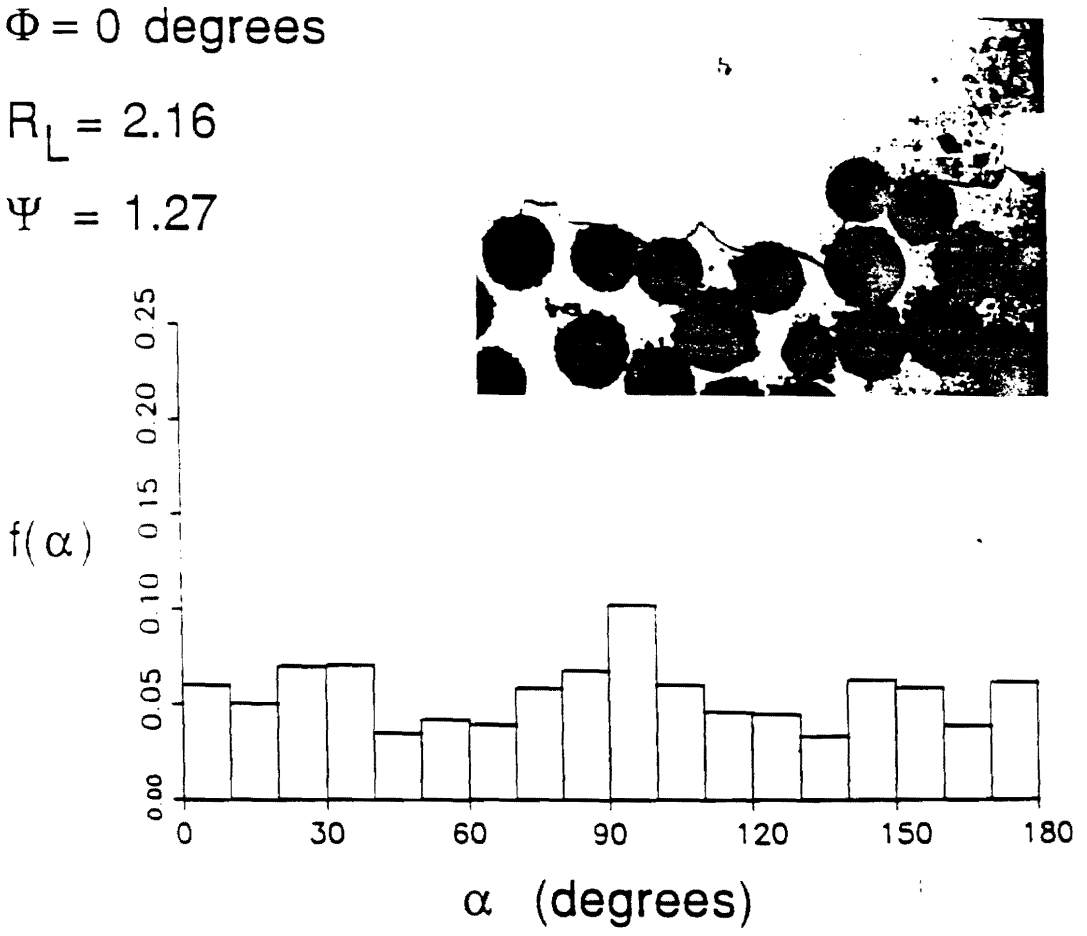

Figure 9 Vertical section fracture profile (ϕ_z = 0°) and corresponding profile frequency function f(α)

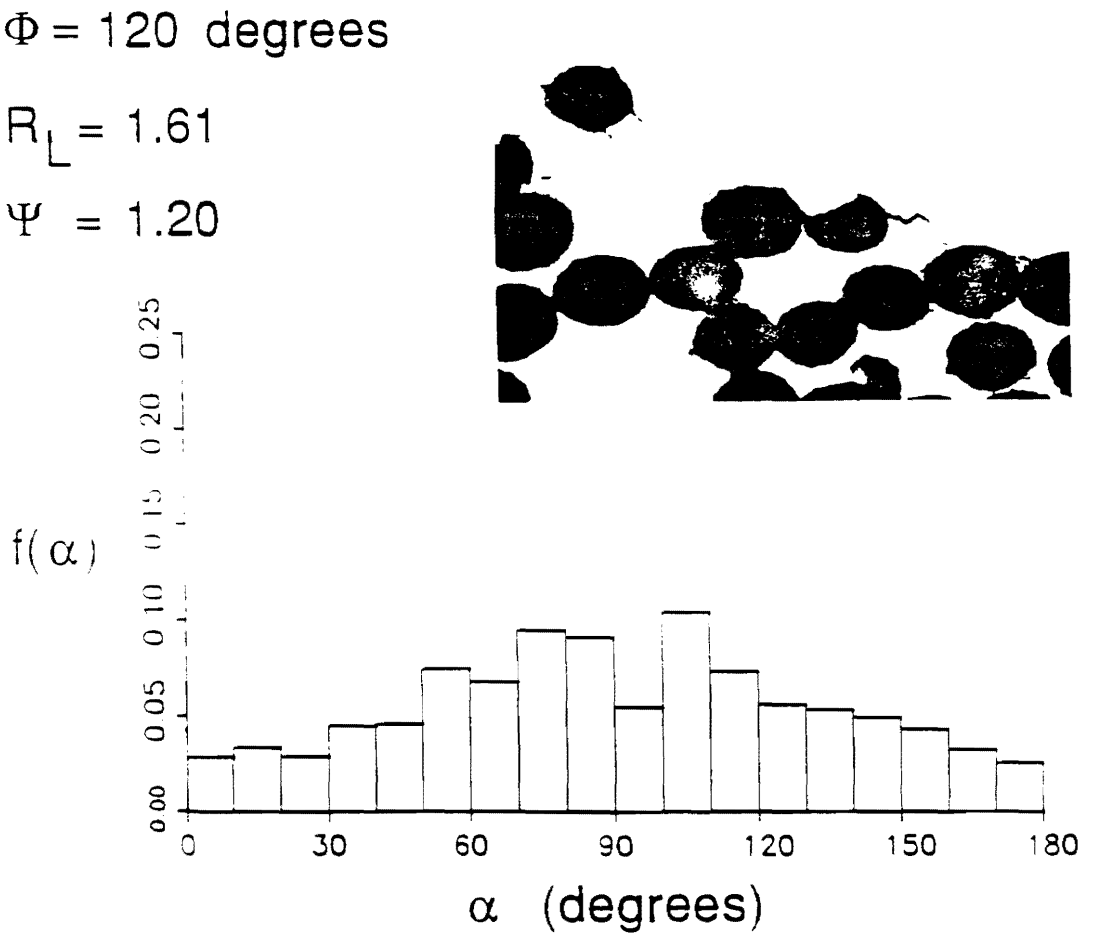

Figure 13 Vertical section fracture profile (ϕ_n = 120°) and corresponding profile frequency function f(α)

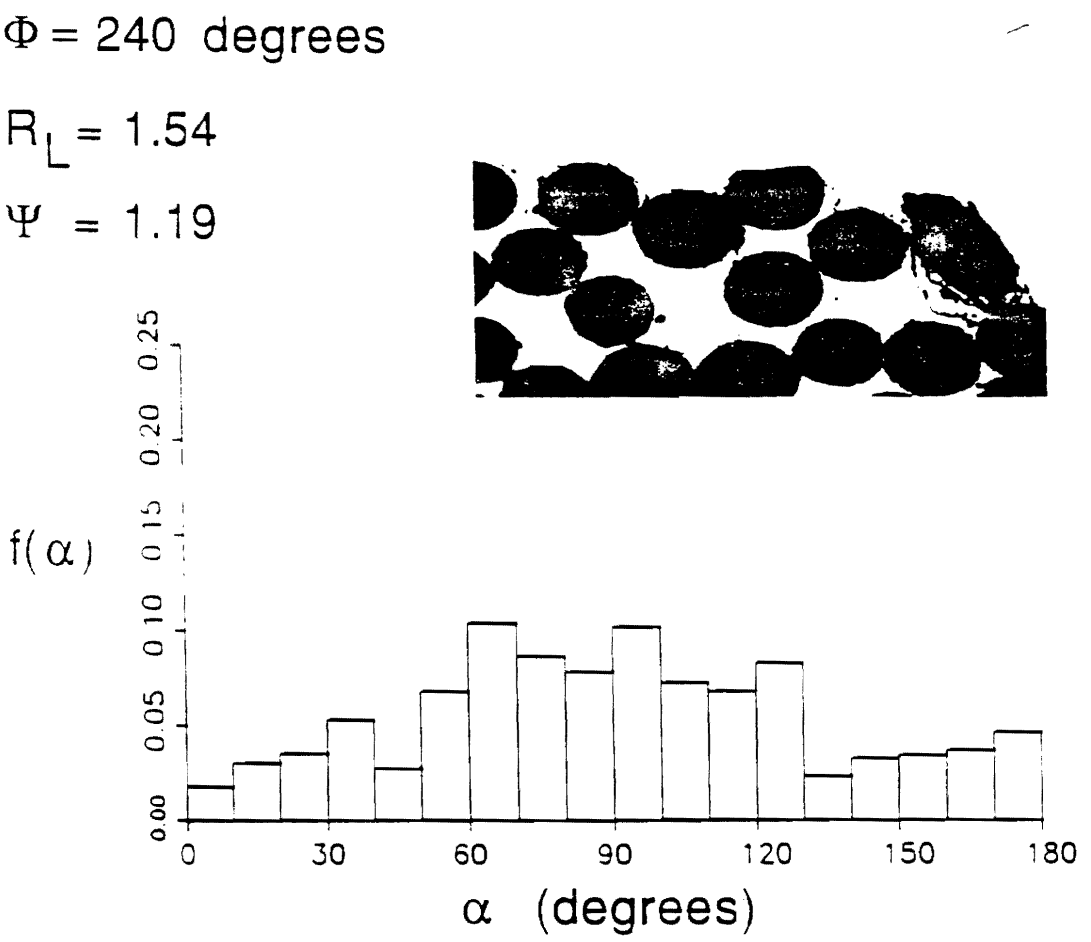

Figure 11 Vertical section fracture profile (ϕ_s = 240°) and corresponding profile frequency function f(α)

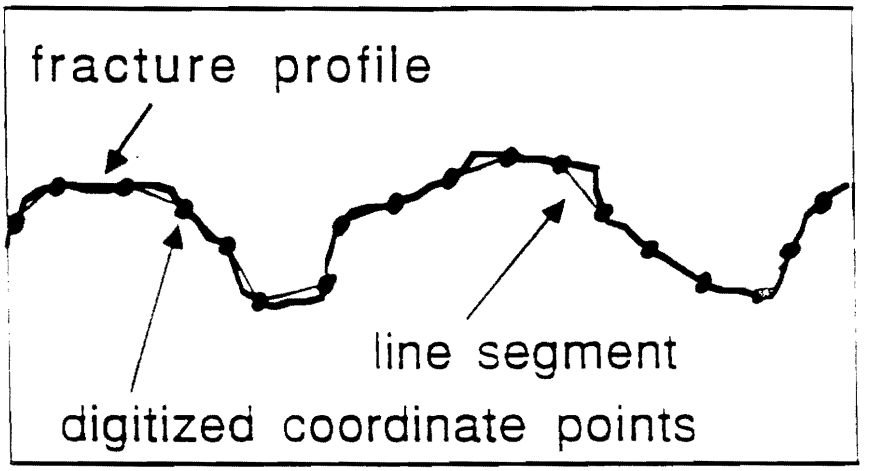

Figure 12 Digitization of fracture profile

Journal of Microscopy
(in press)

:UNBIASED ESTIMATION OF CURVE LENGTH IN 3D USING VERTICAL SLICES:

by

Arun M. Gokhale
School of Materials Engineering
Georgia Institute of Technology
Atlanta, GA 30332-0245 U.S.A.

Keywords: *Anisotropy, vertical sections, line length, projected images, efficient sampling, stereology.*

SUMMARY

An efficient sampling procedure is presented for estimation of total line length per unit volume L_v. It involves the following steps: (1) choose a vertical axis in the specimen, and cut the specimen to obtain VUR vertical slices of thickness Δ such that parallel planes of the slices contain the vertical direction, (2) observe the <u>projected</u> image of a vertical slice using transmission microscopy such that beam direction is perpendicular to the slice, (3) count the number of intersections of the projected images of the lineal features of interest with cycloid shape test lines whose minor axis is <u>perpendicular</u> to vertical axis. The expected value of the number of intersections per unit length $[I_L^c]_{prj}$ is related to L_v as follows:

$$L_v = \frac{2}{\Delta} \cdot [\overline{I_L^c}]_{prj}$$

Thus, L_v can be estimated from the measurements performed on the projected images of VUR vertical slices.

1 INTRODUCTION

One dimensional lineal features are often present in microstructures. For example, dislocation lines, grain edges, edges of faceted precipitates, etc. are important geometric features in metallurgical microstructures. In biological structures, fibres, capillaries, tubules, etc. can be regarded as lineal features. It is of interest to estimate the total line length per unit microstructural volume L_v. It can be shown that (Smith and Guttman, 1953):

$$L_v = 2 \bar{Q}_A \qquad (1)$$

where, $\bar{Q}_A$ is the expected value of the number of intersections of the lineal features of interest contained in a reference volume, with an IUR test plane of unit area placed in the reference volume. If the distribution of the lineal features is isotropic and homogenous, then the measurements on only one sectioning plane can yield a reliable estimate of L_v. However, the lineal features in microstructures often exhibit anisotropy, and in such cases it is necessary to perform the measurements on a number of sectioning planes of different isotropic orientations to obtain an estimate of $\bar{Q}_A$, and hence L_v; such measurements are tedious and time consuming. In this context it is necessary to point out that for a valid application of equation (1), the only requirement is IUR sampling of the structure with a two dimensional test surface; the test probe need not be a plane! For example, the result is applicable, if one counts the number of intersections of the lineal features with the surface of a test sphere (the orientations of surface elements on sphere are truly isotropic, which automatically takes care of 'I' in IUR!). However, such a test probe is not convenient in practice, at least at present. It is the purpose of this paper to <u>design</u> a test probe which is convenient in practice, and to derive a fundamental equation which relates L_v to the corresponding design based

measurements. The present work draws significantly from the elegant concept of vertical section sampling due to Baddeley, Gundersen, and Cruz Orive (1986). It is shown that the intercept count performed on projected images of lineal features in vertical slices using a design based test line shape yields an efficient estimate of L_v in an unbiased manner; the result is assumption free, and it is applciable to any arbitrary ensemble of lineal features contained in a reference volume of any arbitrary shape.

2 THEORY:

In the present context, a slice is defined as the microstructural volume contained between two parallel planes separated by distance Δ; the quantity Δ is the thickness of the slice. For the analysis which follows, it is necessary to adopt a convention for specifying the angular orientations of lines and planes in three dimensional space; this is illustrated in Figure 1. The concept of vertical slices can be developed as follows.

(i) Consider an ensemble or a set of lineal features C of any arbitrary shapes and sizes contained in a reference space of any aribtrary shape. Let V_o be the volume of the reference space. Let L_t be the total length of all the lineal features C of interest contained in the reference space. Hence,

$$L_v = \frac{L_t}{V_o} \tag{2}$$

(ii) Choose any arbitrary direction in 3D space as reference direction or vertical axis, and let this direction be the Z axis of the frame of reference.

(ii) Once the vertical axis is specified, cut the reference volume (specimen) exhaustively into a number of slices of thickness Δ, such that parallel planes of all the slices contain the vertical axis; these are called

vertical slices. Figure 2 shows one such vertical slice. There is absolutely no restriction on the magnitude of the vertical slice thickness Δ, in principle. There is no restriction on physical direction of the vertical axis, but once the vertical axis is selected, parallel planes of all the vertical slices must contain the vertical axis. The angular orientation of a vertical slice is specified by the normal $\vec{N}_s$ to its parallel planes. Obviously, for all vertical slices $\vec{N}_s$ lies in the xy plane (see Figure 2). For all vertical slices, the θ orientation angle (say, θ_s) is equal to $\pi/2$ and the ϕ orientation angle (say, ϕ_s) admits different values ranging from 0 to 2π.

Observe the projected image of a vertical slice of orientation ϕ_s along the projection direction $\vec{N}_s$. The lineal features in the vertical slice project as lines of different shapes and sizes in the projected image. The vertical axis can be identified in the projected image because it is a known direction in the slice and it is perpendicular to the projection direction $\vec{N}_s$. Now superimpose a cycloid shape test line (see Baddeley et. al., 1986 for geometry of cycloid test lines) of length ℓ on the observed projected image of the vertical slice, such that the cycloid minor axis is <u>perpendicular</u> to the vertical axis. This cycloid test line placed on the projected image is identical to the <u>projection</u> of a cycloid test surface of area $(\ell.\Delta)$ contained in the vertical slice as shown in Figure 3. This cycloid test surface is generated by placing our cycloid test line on the top face of the slice and moving it in the projection direction $\vec{N}_s$ till the bottom face of the slice is reached (see Figure 3), <u>without</u> any rotation or tilting of the generating cycloid curve, or any translation in the plane of the curve. The inspection of Figure 3 immediately leads to the following: the total number of intersections of the cycloid test surface with the lineal

features contained in the slice $Q^{cys}(\phi_s)$ is precisely equal to the total number of intersections of the corresponding cycloid test line with the projections of the lineal features of interest in the projected image, $[I^c \quad \phi_s)]_{prj}$.

$$Q^{cys}(\phi_s) = [\, I^c(\phi_s)]_{prj} \tag{3}$$

The cycloid test surface has the following interesting geometric properties.

(a) The surface area of cycloid surface in any orientation range θ_p to $(\theta_p + d\theta_p)$ is directly proportional to $\sin\theta_p \; d\theta_p$, as illustrated in Figure 4.

(b) The ϕ orientation angle of all the surface elements on the cycloid test surface is same, and it is equal to $(\phi_s + \pi/2)$.

follows that $Q^{cys}(\phi_s)$ represents the $\sin\theta_p$ weighted average value of the number of intersections of test planes having θ_p orientations ranging from o to $\pi/2$ and ϕ_p orientation equal to $(\phi_s + \pi/2)$, with the lineal features of interest in the vertical slice ϕ_s. Let $\bar{Q}^{cys}$ be the expected value of $Q^{cys}(\phi_s)$ obtained by averaging $Q^{cys}(\phi_s)$ over all the locations of cycloid test surface in vertical slice, all the orientations ϕ_s of vertical slices, and all the locations of vertical slices in the reference volume. It follows that;

$$\bar{Q}^{cys} = [\overline{I^c}]_{prj} \tag{4}$$

where, $[\overline{I^c}]_{prj}$ is the corresponding average of the number of intersections of projected images of lineal features in the vertical slices with corresponding cycloid test lines. The quantity $[\overline{I^c}]_{prj}$ can be estimated by performing the measurements on VUR vertical slices. It follows that;

$$\bar{Q}^{cys} = [\bar{I}^c]_{prj} = \left[\overline{\int_o^{\pi/2} Q\,(C \cap E)\, \sin\theta_p d\theta_p} \right] \tag{5}$$

where, $Q\,(C \cap E)$ is number of intersections of lineal features C with plane E. The quantity on the right hand side of equation (5) is the $(\sin\theta_p)$ weighted

average value of the number of intersections of test planes of average area ($\ell.\Delta$) contained in the reference volume with the set of lines C, averaged over all possible locations and orientations of test planes in the reference volume V_o. It is now necessary to relate $\bar{Q}^{cys}$ to the total length of lineal features L_v in reference volume V_o or total line length per unit volume L_v. This can be done in a rigourous manner by utilizing some integral geometric concepts.

The density of planes dE in three dimensional space is given by (Santalo, 1976);

$$dE = \sin\theta_p \, d\theta_p \, d\phi_p \, dP \tag{6}$$

where, $0 \leq \theta_p \leq \pi/2$; $0 \leq \phi_p \leq 2\pi$; $-\infty < P < \infty$ (θ_p, ϕ_p) specify the angular orientation, and P specifies the location of the plane E; P is equal to the signed distance of the plane E from a fixed reference point. Let $A\,(V_o \cap E)$ be the area of intersection of plane E with the reference volume V_o; if the plane does not intersect V_o then $A\,(V_o \cap E)$ is equal to zero. For the planes which intersect V_o, $A(V_o \cap E)dP$ is a volume element in the reference space, and hence the integral $(\int A(V_o \cap E)dP)$ for planes of fixed θ_p and ϕ_p is equal to the magnitude of the reference volume V_o; its value is independent of θ_p and ϕ_p. Thus, one can write:

$$V_o = \frac{1}{2\pi} \int_o^{2\pi} \int_o^{\pi/2} \left(\int A\,(V_o \cap E)dP \right) \sin\theta_p d\theta_p \, d\phi_p \tag{7}$$

or

$$2\pi V_o = \int A\,(V_o \cap E)dE \tag{8}$$

It is useful to write equation (8) in an alternate form.

$$2\pi\, V_o = \int_p \int_{\phi_p} \left(\int_o^{\pi/2} A\,(V_o \cap E)\, \sin\theta_p d\theta_p \right) d\phi_p \, dP \tag{9}$$

The total length L_t of set of lines C contained in the reference volume V_o satisfies the following integral geometric equation

$$\pi L_t = \int Q(C \cap E) dE \tag{10}$$

where, $Q(C \cap E)$ is the number of intersections of lines C with plane E. Substituting equation (6) into equation (10) yields;

$$\pi L_t = \int Q(C \cap E) \cdot \sin\theta_p \, d\theta_p \, d\phi_p \, dP \tag{11}$$

or

$$\pi L_t = \int_P \int_{\phi_p} \left(\int_o^{\pi/2} Q\,(C \cap E) \sin\theta_p d\theta_p \right) d\phi_p \, dP \tag{12}$$

Equations (9) and (12) yield;

$$\frac{1}{2}\left(\frac{L_t}{V_o}\right) = \frac{1}{2} L_v = \frac{\int_P \int_{\phi_p} \left(\int_o^{\pi/2} Q\,(C \cap E) \sin\theta_p d\theta_p \right) d\phi_p \, dP}{\int_P \int_{\phi_p} \left(\int_o^{\pi/2} A\,(V_o \cap E) \sin\theta_p d\theta_p \right) d\phi_p \, dP} \tag{13}$$

or

$$\frac{1}{2} L_v = \frac{\overline{\left[\int_o^{\pi/2} Q\,(C \cap E) \sin\theta_p \, d\theta P\right]}}{\overline{\left[\int_o^{\pi/2} A\,(V_o \cap E) \sin\theta_p d\theta P\right]}} \tag{14}$$

The integral in the denominator in the right hand side of equation (14) is precisely the $\sin\theta_p$ weighted average value of area of sectioning planes resulting from intersection with V_o; the quantity is averaged over all θ_p, ϕ_p and P. As mentioned earlier cycloid surface represents ($\sin\theta_p$) weighted average of area of planes, and the integral in the numerator is precisely equal to $\overline{Q^{cys}}$ (see equation (5)). Hence;

$$L_v = 2 \frac{\overline{Q^{cys}}}{\overline{A^{cys}}} = 2 \frac{[\overline{I^c}]_{prj}}{\overline{A^{cys}}} \tag{15}$$

or

$$L_v = 2 \frac{\overline{[I_L^c]}_{prj}}{\overline{\Delta}} \tag{16}$$

where, $[\overline{I_L^c}]_{prj}$ is the expected value of the number of intersections of cycloid test line with projected images of lineal feature of interest per unit test line length. The result is completely assumption free; it is applicable to any ensemble of lineal features contained in any arbitrary shape reference volume. The result is design based, and the following experimental conditions must be satisfied for its valid application:

(a) The slices must be vertical slices, i.e., all the slices must be obtained such that parallel planes of each slice contain the vertical axis. The locations of slices must be uniform or random.

(b) The projection direction must be perpendicular to parallel faces of slice.

(c) In the projected image, the cycloid test line must be oriented such that the cycloid minor axis is perpendicular to the vertical axis.

Note that the above requirements only concern the experimental design, and they do not constitute any assumption concerning the geometry of microstructure.

3. DISCUSSION

The steps involved in the application of the present result for estimation of total length of lineal features per unit volume L_v are as follows:

(i) Choose a vertical axis in the specimen and let this be the Z-axis of the frame of reference. Any direction can be specified as vertical axis, just like for estimation of S_v from vertical sections. If the anisotropy of lineal features has rotational symmetry and microstructure is homogenous, then obviously the best choice for the vertical axis is the symmetry axis. In such a case just one vertical slice may yield a reliable estimate of L_v.

(ii) Once the vertical axis is specified, cut the sample into a number of VUR vertical slices, such that the parallel planes of each slice contain the vertical axis. There is no restriction, in principle, on the magnitude of Δ.

(iii) Observe the projected image of the microstructure contained in the slice; the projection direction must be perpendicular to the parallel planes of the slice.

(iv) Identify the vertical axis in the projected image of the slice. This should be always possible because the vertical axis is a known direction in the vertical slice and it is perpendicular to the projection direction.

(v) Super impose a number of cycloid shaped test figures on the observed projected image such that the minor axis of cycloid is <u>perpendicular</u> to the vertical axis, but the <u>locations</u> of the cycloids should be uniform or random (see Figure 5).

(vi) Count the number of intersections of the projected images of lineal features observed with the test lines and calculate $[I_L^c]_{prj}$ the number of intersections per unit line length of cycloid test lines.

(vii) Measure $[I_L^c]_{prj}$ in a number of VUR vertical slices and calculate its average value $[\overline{I_L^c}]_{prj}$.

(viii) Calculate L_v by using equation (16).

The whole procedure is analogous to the estimation of surface area per unit volume S_v using vertical sections. However, there are the following important differences:

(a) In the present case vertical slices are required rather than vertical sections.

(b) The measurements are performed on the projected image rather than a two dimensional section.

(c) In the present case, the cycloid test line must be oriented such that the minor axis of cycloid is <u>perpendicular</u> to the vertical axis, whereas for estimation of S_v from vertical sections, the cycloid minor axis must be <u>parallel</u> to the vertical axis.

The choice of vertical axis determines the variations in $[I_L^c]_{prj}$ values from one vertical slice to another, and hence it determines the variance of the measurements. Thus the number of vertical slices necessary to reduce the sampling error to the desired level depends on which direction is chosen as vertical axis, although the expected value $[\overline{I_L^c}]_{prj}$ is independent of the choice of vertical axis. For example, if the anisotropy of the lineal features has a rotational symmetry, then VUR vertical slices containing the symmetry axis can yield more efficient estimate of L_v than any alternative VUR slices.

It is important to emphasize that the projection direction must be perpendicular to the parallel planes of the slice, in order to uniquely identify the vertical axis in the projected image. The interpretation of the stereological measurements performed on the projected images is often complicated due to the overlap and truncation effects. However, in the case of lineal features, the probability of overlapping is extremely small. Further, the intersections of the lineal features with parallel planes of the slice are points and hence there is no truncation effect either. However, there can be another type of overlap effect which can lead to significant error. For example if the microstructure contains precipitate particles and the lineal features, some segments of lineal features may not be observed in the projected image as these segments may 'hide' behind the projected images of precipitates; this may lead to an underestimation of L_v. The extent of such underestimation depends on the presence and extent of other microstructural features present in the specimen;

if the problem can lead to significant error, then L_v should not be estimated from the projected image measurements. In order to apply the present technique, it is necessary to measure the slice thickness Δ. A number of experiment of slice thickness; the choice of the method depends on the material under investigation. In many practical cases, all the slices obtained from the given specimen may not be of the same thickness. The present technique is applicable in such a case provided the thickness variation is appropriately accounted $[I_i^c]_{prj}$ be the number of intersections of the lineal features with the cycloid test lines of total length ℓ_i in the i^{th} slice of thickness Δ_i. Equation (15) can be recast in the following form.

$$L_v = \frac{2 \sum [I_i^c]_{prj}}{\sum \Delta_i \ell_i} \tag{17}$$

In some cases, a cycloid test line may intersect the edge of the frame of observation or the edge of the slice. In such a case, the cycloid test line is "partly in - partly out," and the test line length is equal to that portion of cycloid which is in the reference area. This 'effective' test line length can be measured as follows. Draw a tangent to the cycloid test line, where it intersects the frame edge. The angle α between the tangent and the vertical ais can be measured. Since the incrmental length of our cycloid is directly proportional to the cosine of the angle between the tangent and the vertical axis, the fraction of the cycloid length inside reference area can be easily calculated via integration of the cosine function between the appropriate limits.

The present technique should be applicable for estimation of total length of tubules or fibers in a specimen provided their cross sectional area is very small. Dislocations in a single phase crystalline material present an ideal

situation for the application of the present procedures because (a) these features are truly one dimensional, (b) their orientations are often anisotropic, and (c) in a single phase material, there are no other phases or particles and hence no overlaps.

4 CONCLUSIONS

A sampling procedure is developed for efficient estimation of the total length of lineal features per unit volume from the measurements performed on the projected images of the vertical slices. It is shown that the line intercept count performed on the projected images of the lineal features using a test figure of specific shape can yield an efficient estimate of L_v.

ACKNOWLEDGEMENT

The author thanks Professor L.M. Cruz Orive for extremely useful suggestions and comments on the manuscript. This work was supported by NSF sponsored project DMR-8504167; the financial support is gratefully acknowledged.

REFERENCES

1) Baddeley, A. J., Gundersen, H. J. G. and Cruz-Orive, L. M., (1986), Estimation of Surface Area from Vertical Sections, J. Microsc., 142, pt. 3, pp. 259-276.

2) Smith, C. S. and Guttman L., (1953), Measurement of Internal Boundaries in Three Dimensional Strutures, Trans. A.I.M.E., 197, pp. 81-90

3) Santalo L.A., (1976), Integral Geometry and Geometric Probability, Addison-Wesley, Reading, Mass.

LIST OF FIGURE CAPTIONS

Figure 1. (a) Angular orientation of a plane specified by angles θ_p and ϕ_p pertaining to its normal $\vec{N}_p$
(b) Angular orientation of a line is specified by angles θ_L and ϕ_L pertaining to tangent vector $\vec{T}$; orientation of curved line is different at different locations.

Figure 2. Concept of vertical slice and specification of its orientation.

Figure 3. Geometric interpretation of cycloid shape test line placed on projected image of vertical slice.

Figure 4. Geometry of cycloid test surface.

Figure 5. Design based intercept count on projected image.

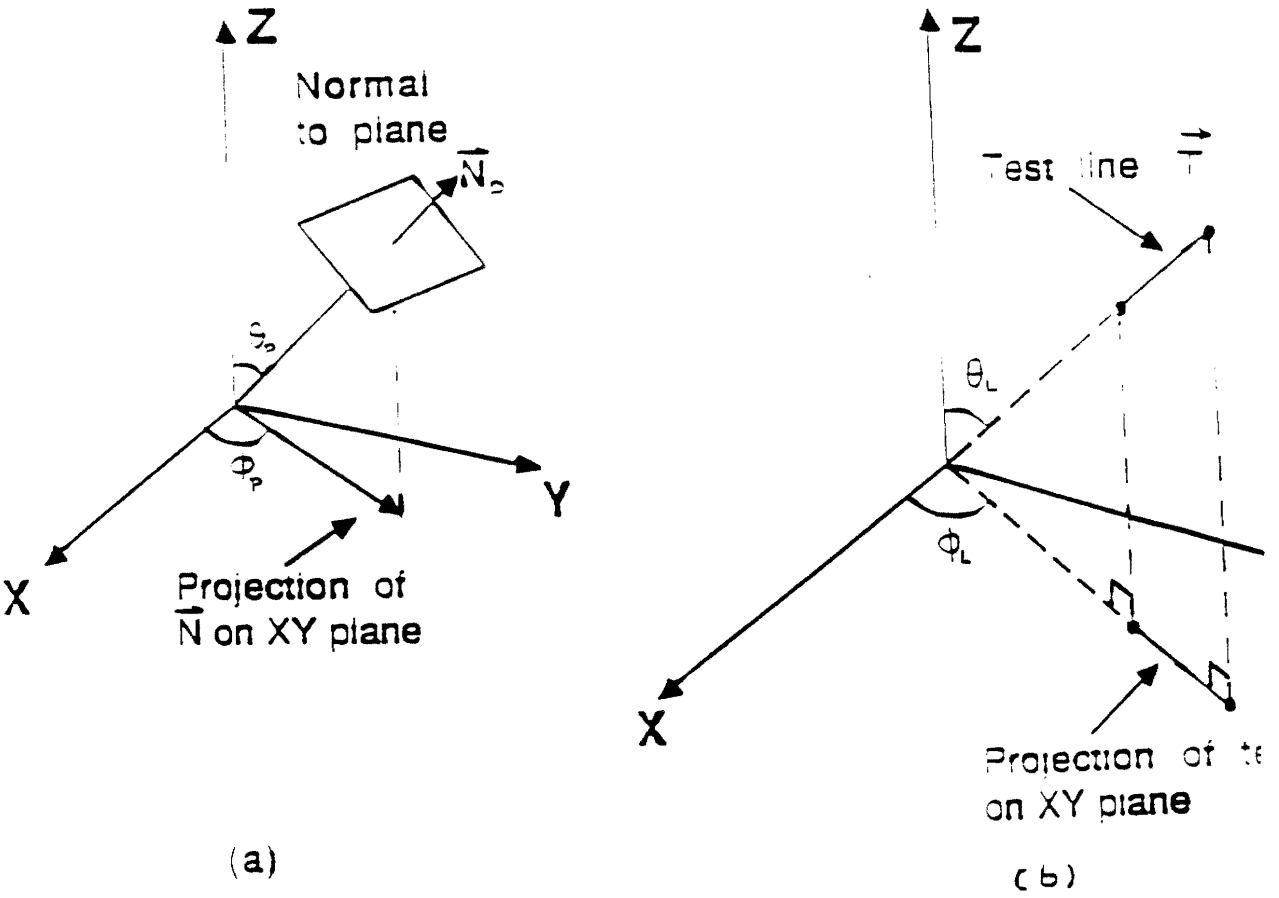

Figure 1. (a) Angular orientation of a plane specified by angles θ_p an pertaining to its normal $\vec{N}_p$
(b) Angular orientation of a line is specified by angles θ_L an pertaining to tangent vector $\vec{T}$. Orientation of curved line different at different locations.

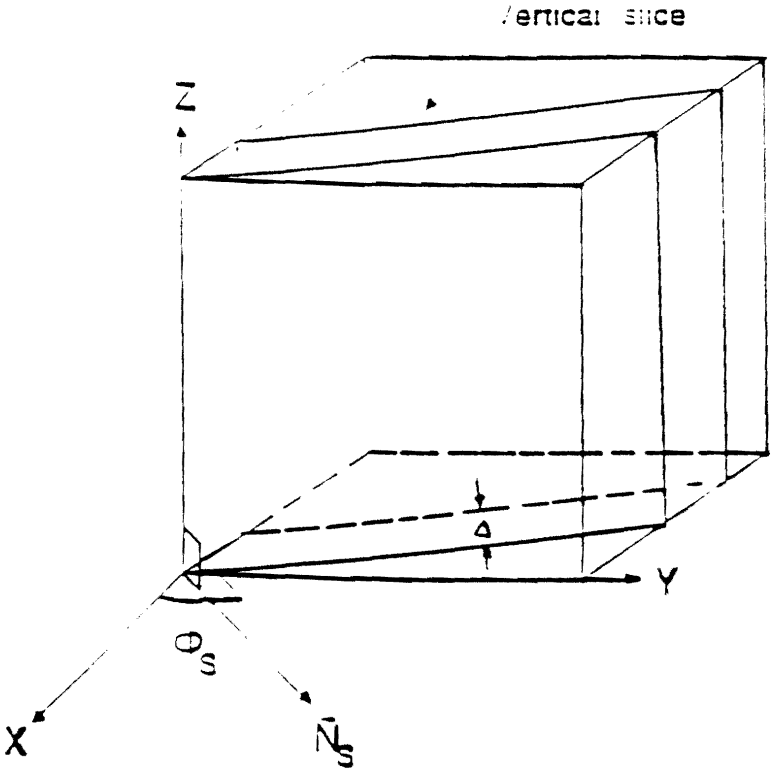

Figure 2. Concept of vertical slice and specification of its orientati

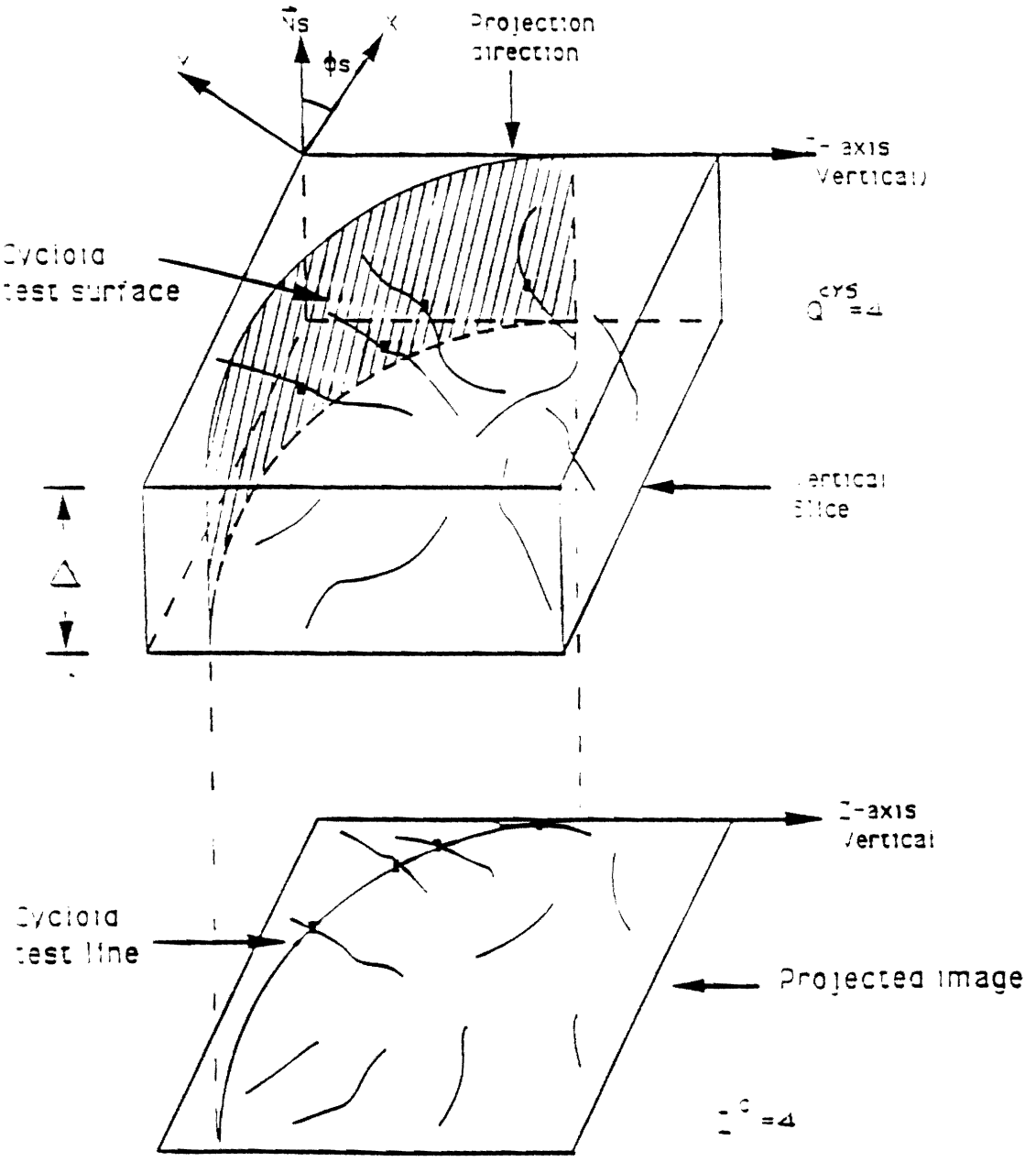

Figure 3. Geometric interpretation of cycloid shape test line placed on projected image of vertical slice.

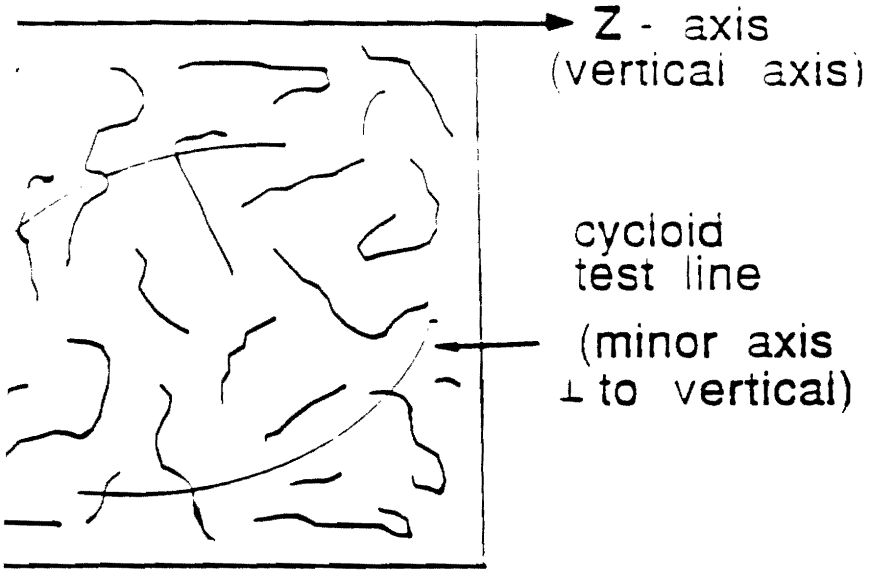

Design based intercept count on projected image.

(I) $\delta A\ (\theta_p) = \Delta\ .\ \delta L\ (\theta_L)$

$\theta_L = \theta_p + \pi/2$

$\delta L\ (\theta_L)\ \alpha\ |\cos\ \theta_p|\ d\theta L_1$

(property of cycloid having minor axis $\perp$ to Z-axis)

$\therefore \delta A\ (\theta_p)\ \alpha\ \text{Sin}\ \theta_p\ d\theta_p$

for $o \leq \theta_p \leq \pi$

(II) All normals $\vec{N}_p$ project on same line op

$\therefore$ all surface elements on cycloid surface have same ϕ_p orientation

$\phi_p = \phi_s + \pi/2$

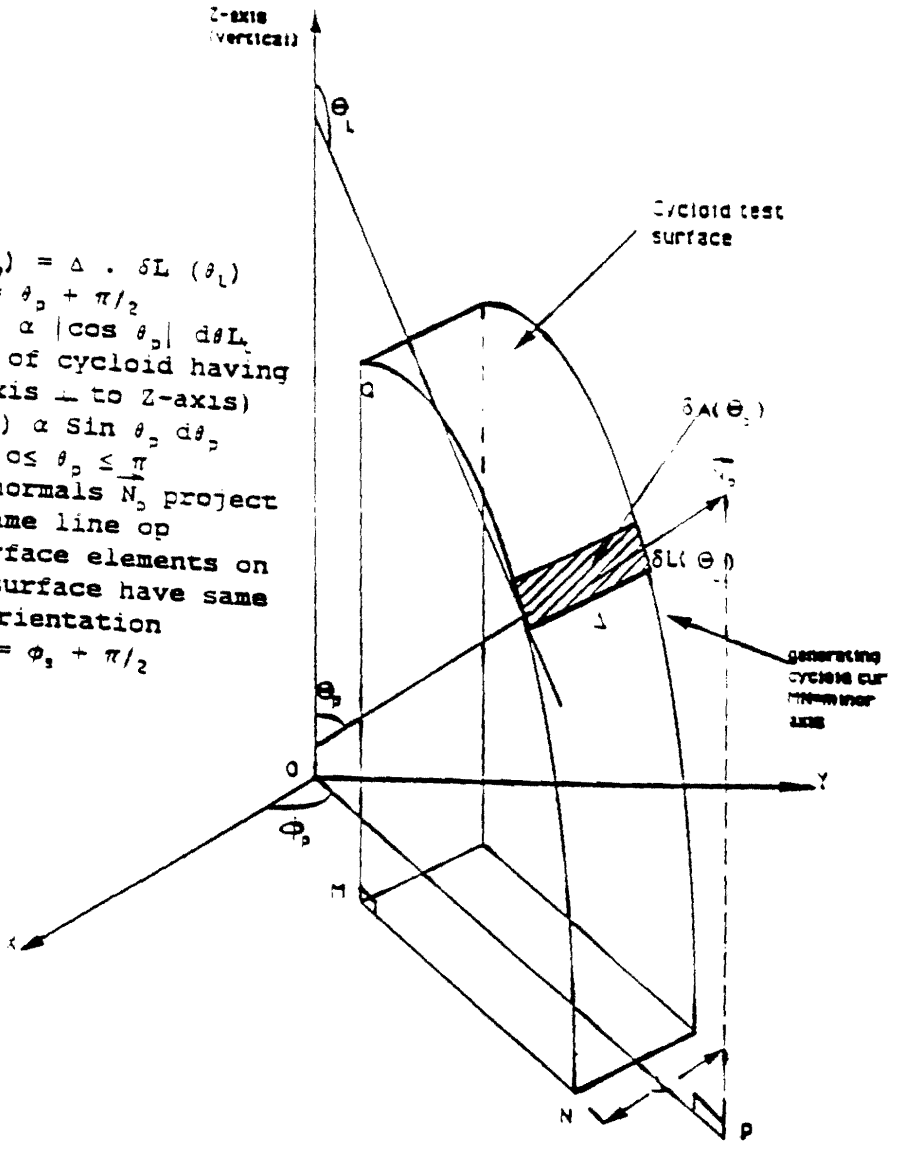

Figure 4. Geometry of cycloid test surface.

Journal of Microscopy
(Submitted)

Efficient Vertical Sections: The Trisector

by

Arun M. Gokhale and William J. Drury
School of Materials Engineering
Georgia Institute of Technology
Atlanta, Georgia 30332-0245
U.S.A.

ABSTRACT

It is shown that just three systematic vertical sections can yield most efficient and reliable estimate of the total surface area per unit volume S_v in homogenous materials microstructures having arbitrary anisotropy and geometry, provided the following conditions are satisfied.

(a) The vertical axis must be selected such that most of the surface area of interest is <u>not</u> parallel to the vertical axis.

(b) The three vertical sections must be mutually at an angle of 120°.

(c) The intersection counts on each sectioning plane must be performed by using cycloid test lines having minor axis parallel to the vertical axis.

To emphasize these design requirements the composite test probe is called "trisector". S_v can be estimated with a maximum error of ±5% by using the following equation.

$$S_v = 2.012\ [I_L^c]_3$$

where, $[I_L^c]_3$ is the expected value of the intersection count per unit test line length when the measurements are performed on three planes of trisector.

It is also shown that independent random vertical sections have little practical utility for estimation of S_v in anisotropic materials microstructures, in general. Further, two perpendicular systematic vertical sections do not contain sufficient structural information for estimation of S_v in anisotropic materials microstructures, in general.

INTRODUCTION

Microstructures usually contain internal surfaces or boundaries. The total area of the internal surfaces of interest per unit volume S_v is a stereological attribute of considerable practical importance. S_v can be estimated from vertical sections by utilizing the following relationship (Baddeley, Gundersen, and Cruz-Orive, 1986).

$$S_v = 2 \overline{I_L^c} \qquad (1)$$

$\overline{I_L^c}$ is the expected value of the number of intersections of oriented cycloid test line of unit length with the traces of the internal surfaces of interest observed in a set of vertical sections (see Baddeley et.al, 1986 for details). The estimation of S_v from the vertical sections requires VUR (vertical, uniform, and random) sampling of the structure: the measurements must be performed on the vertical sections of different angular orientations (rotation around the vertical axis), and at different locations in the specimen, with statistical uniformity. In practice, however, the measurements are performed only on a limited number of vertical sections and the number of placements of cycloid test lines are also limited. It follows that the experimentally estimated value of S_v has a sampling error associated with it. This statistical sampling error is determined by the number of placements of the test line, the number and orientations of the vertical sections sampled, and the uniformity with which the structure is sampled on parallel vertical sections at different locations in the specimen.

The total statistical sampling error and the relative contributions from these factors depend on the choice of the vertical axis, anisotropy of microstructure, and homogeneity of microstructure. For example, in the case of homogenous microstructure having rotationally symmetric anisotropy, all the vertical sections containing the symmetry axis (chosen as vertical axis) are statistically similar, and hence any one such vertical section contains sufficient information for a reliable estimation of S_v; the sampling error is then primarily determined by the number of placements of test lines and statistical uniformity with which the test lines are placed on the vertical section. On the other hand if the anisotropy of microstructure is not rotationally symmetric, then a reliable value of S_v can <u>not</u> be obtained no matter how many measurements are performed on one vertical section or on a set of parallel vertical sections at different locations; it is imperative to perform the measurements on the vertical sections of different angular orientations.

In the case of microstructures encountered in materials science, a significant amount of time and effort goes into metallographic sectioning, polishing, and etching to reveal the structure present in the sectioning plane. The effort necessary for the metallographic preparation often exceeds the effort involved in performing the stereological counting measurements, even when the measurements are performed manually! Thus, at least for applications in materials science, it is desirable to develope an efficient stereological procedure which can yield a reliable

estimate of S_v from the measurements performed on <u>few</u> sectioning planes (preferably three or less, certainly not more than five), without involving any assumptions concerning the geometry or anisotropy of microstructure. Such a procedure need <u>not</u> yield an absolutely precise estimation of S_v, however, it must <u>ensure</u> that the sampling error can be always kept below a few percent (typically, $\pm$ 5% or less). It is the purpose of this paper to develope such a sampling procedure. In this context it is necessary to point out that the materials microstructures can be regarded as homogenous for all the practical purposes. The parallel sectioning planes at different locations reveal the structures that are statistically similar. Thus, the sampling of structure on parallel sectioning planes is inefficient as compared to performing the same total number of measurements on one section of that orientation, with uniform placements of the test probe. However, the materials microstructures are often anisotropic and hence it is imperative to perform the measurements on the vertical sections of different angular orientations. Thus, it is the purpose of this paper to develope an efficient sampling procedure for estimation of S_v, from the measurements performed on few vertical sections, in homogenous microstructure of any arbitrary anisotropy and geometry. The present analysis utilizes the full potential of the concept of vertical sections. It is shown that just three vertical sections can yield a reliable value of S_v, provided the following conditions are satisfied.

(a) The three vertical sections must be mutually at an angle

of 120°.

(b) The vertical axis must be chosen such that most of the surface elements of interest are <u>not</u> parallel to the vertical axis (i.e. the surface element normals are not perpendicular to the vertical axis).

(c) The intersection count on each sectioning plane must be performed by using cycloid test lines, such that cycloid minor axis is parallel to the vertical axis, as in Baddeley et.al, 1986.

To emphasize the above three conditions, the composite test probe is called "trisector". It is shown that one application of trisector is sufficient to keep the sampling error below $\pm$ 5% for estimation of S_v in any homogenous microstructure having any arbitrary anisotropy and geometry.

THEORETICAL DEVELOPMENT

Consider a homogenous microstructure containing internal surfaces of any arbitrary geometry and anisotropy. Specify the angular orientation (θ,ϕ) of a surface element as shown in Figure 1; Z-axis of the reference frame is the vertical axis. Let $dS_v(\theta,\phi)$ be the total area of the surface elements per unit volume, having angular orientation in the range θ to $(\theta + d\theta)$ and ϕ to $(\phi + d\phi)$. Let $dB_A(\theta, \phi, \phi_p)$ be the expected value of the total trace length per unit area resulting from intersections of the surface elements $dS_v(\theta,\phi)$ with the vertical sectioning plane of angular orientation ϕ_p (see Figure 2 for specification of orientation of the vertical sectioning plane, obviously $\theta_p = \pi/2$). As the microstructure is assumed to be homogenous, the expected value dB_A

(θ,ϕ,ϕ_p) is same for all parallel vertical sections of orientation ϕ_p. Simple geometric considerations yield;

$$d\ B_A(\theta,\phi,\phi_p) = [1 - \sin^2\theta \cos^2 (\phi - \phi_p)]^{\frac{1}{2}} dS_v\ (\theta,\phi) \qquad (2)$$

Let α be the angle between tangents to the trace elements dB_A (θ,ϕ,ϕ_p) and the vertical axis, in the vertical section ϕ_p. The angles α, θ, ϕ, and ϕ_p are related as follows.

$$\cot\alpha \ .\ \cot\theta = \sin(\phi-\phi_p) \qquad (3)$$

Let $dI_L^c\ (\theta,\phi,\phi_p)$ be the expected value of the number of intersections of a cycloid shape test line (cycloid minor axis parallel to the vertical axis) with the trace elements $dB_A\ (\theta,\phi,\phi_p)$ per unit test line length. The incremental length of our cycloid is directly proportional to $\sin\theta'$, where θ' is the angle between the tangent to an arc element on the cycloid and the vertical axis (see Baddeley et.al, 1986). Hence,

$$dI_L^c(\theta,\phi,\phi_p) = \left\{ \frac{1}{2}\int_0^{\pi} \sin\theta' .\ |\cos(\theta' + \frac{\pi}{2} - \alpha)|\ d\theta' \right\} .\ dB_A(\theta,\phi,\phi_p) \qquad (4)$$

The integration yields;

$$dI_L^c\ (\theta,\phi,\phi_p) = \frac{1}{2}\left[\sin\alpha + (\frac{\pi}{2} - \alpha)\ \cos\alpha\right]\ dB_A\ (\theta,\phi,\phi_p) \qquad (5)$$

where, $o \le \alpha \le \pi$

Equations (2), (3), and (5) give the following result.

$$dI_L^c\ (\theta,\phi,\phi_p) = f(\theta,\phi,\phi_p)\ .\ dS_v\ (\theta,\phi) \qquad (6)$$

where,

$$f(\theta,\phi,\phi_p) = \frac{1}{2}\left[\cos\theta + \sin\theta \cdot \left|\sin(\phi - \phi_p) \cdot \cot^{-1}\left\{ \frac{\cot\theta}{\sin(\phi-\phi_p)} \right\}\right| \right] \quad (7)$$

and

$$o \le \theta \le \pi/2;\ o \le \phi \le 2\pi, \text{ and } o \le \phi_p \le 2\pi$$

Let $[dI_L^c\ (\theta,\phi)]_m$ be the expected value when the measurements are performed on m vertical sections of orientations ϕ_p^1, ϕ_p^2, ..., ϕ_p^n,..., ϕ_p^m. It follows that;

$$[dI_L^c\ (\theta,\phi)]_m = f_m(\theta,\phi) \cdot dS_v(\theta,\phi) \quad (8)$$

where,

$$f_m(\theta,\phi) = \frac{1}{2}\left[\cos\theta + \frac{\sin\theta}{m} \sum_{n=1}^{m} \left|\sin(\phi-\phi_p^n) \cdot \cot^{-1}\left\{ \frac{\cot\theta}{\sin(\phi-\phi_p^n)} \right\}\right| \right] \quad (9)$$

Let $g(\theta,\phi)$ be the orientation distribution function of the surface elements of interest in the microstructure, such that $g(\theta,\phi)d\theta d\phi$ is equal to the fraction of the surface area in the orientation range θ to $(\theta + d\theta)$ and ϕ to $(\phi + d\phi)$. For randomly oriented microstructure $g(\theta,\phi)$ is equal to $\sin\theta/2\pi$. In general,

$$dS_v(\theta,\phi) = S_v \cdot g(\theta,\phi)d\theta d\phi \quad (10)$$

where,

$$o \le \theta \le \pi/2;\ o \le \phi \le 2\pi$$

obviously,

$$\int_o^{2\pi} \int_o^{\pi/2} g(\phi,\theta)\, d\theta d\phi = 1 \quad (11)$$

Let $[I_L^c]_m$ be the expected value of the total intersection count on m vertical sections of orientations ϕ_p^1, ϕ_p^2, ... ϕ_p^n, ..., ϕ_p^m. Combining equations (8) and (10) gives the following result.

$$[I_L^c]_m = e_m \cdot S_v \tag{11}$$

where,

$$e_m = \int_0^{2\pi} \int_0^{\pi/2} f_m(\theta,\phi)\, g(\theta,\phi)\, d\theta d\phi \tag{12}$$

The quantity e_m is essentially an average value of $f_m(\theta,\phi)$ obtained by averaging it over $g(\theta,\phi)$. For an isotropic microstructure e_m is alway equal to 1/2 and it does not depend on m or the orientations of the vertical sections. As m approaches a very large value, e_m approaches 1/2, irrespective of the nature of anisotropy (i.e. $g(\theta,\phi)$). However, in practical cases, m is small, and microstructure is often anisotropic, and hence e_m depends on m and the vertical section orientations ϕ_p^1, ϕ_p^2, ... ϕ_p^n, ..., ϕ_p^m on which the measurements are performed. The quantity $[I_L^c]_m$ is estimated from the experimental measurements, but the value of e_m is unknown because $g(\theta,\phi)$ is unknown. Thus, for experimental estimation of S_v, e_m is approximated by 1/2 (i.e., its expected value). The estimated value of S_v then differs from its true value by a factor $(2e_m)$, irrespective of how many measurements are performed on the vertical sections ϕ_p^1, ϕ_p^2, ... ϕ_p^n, ..., ϕ_p^m. In the homogenous anisotropic microstructures, this is the main source of the error. Recall that $f_m(\theta,\phi)$ depends on m, the vertical section orientations ϕ_p^1, ϕ_p^2, ... ϕ_p^n, ..., ϕ_p^m, and the choice of the vertical axis. Our

aim is to identify orientations ϕ_p^1, ϕ_p^2, ... ϕ_p^n, ..., ϕ_p^m, and the choice of the vertical axis, for which $f_m(\theta,\phi)$ does not vary significantly with θ and ϕ for reasonably small value of m. Suppose $f_m(\theta,\phi)$ is always in the range $f_o(1 \pm \epsilon_o)$ for all θ and ϕ, then one can write;

$$[I_L^c]_m = f_o\,[1 \pm \epsilon_o] \int_o^{2\pi} \int_o^{\pi/2} g(\theta,\phi)\,d\theta d\phi \;.\; S_v \qquad (13)$$

or

$$S_v = \frac{1}{f_o[1 \pm \epsilon_o]}\,[I_L^c]_m \qquad (14)$$

The quantity $\frac{1}{(1 \pm \epsilon_o)}$ gives the <u>maximum</u> possible error, when S_v is estimated from the following equation (note that $g(\theta,\phi)\,d\theta d\phi < 1$, by definition):

$$S_v = \frac{1}{f_o}\,[I_L^c]_m \qquad (15)$$

Note that f_o need not be equal to 1/2. Our goal is now as follows:

(a) Identify orientations ϕ_p^1, ϕ_p^2, ... ϕ_p^n, ..., ϕ_p^m

(b) Calculate f_o

(c) Calculate ϵ_o

If ϵ_o is small (i.e. ≤ 0.05) for a small value of m then our problem is solved. In such a case, equation (15) should provide an estimate of S_v for any arbitrary homogenous anisotropic microstructure, with an estimate of maximum possible sampling error $\frac{1}{(1 \pm \epsilon_o)}$, apriori, provided sufficient number of measurements are performed with a statistical uniformity. The method for obtaining the solution to our problem now reduces to a set of numerical computer calculations.

COMPUTER CALCULATIONS

The systematically chosen ϕ_p values are expected to lead to smaller value of ϵ_o for given m as compared to m independent random vertical sections (this will be demonstrated later). Let the orientation of the first vertical section be ϕ_p^1. Choose the remaining (m-1) orientations as follows.

$$\phi_p^n = \phi_p^1 + \frac{2\pi}{m} \cdot (n-1) \qquad (16)$$

where,

$$n = 2, 3, \ldots m, \text{ and } m > 2$$

Note that sampling scheme m = 4 is equivalent to sampling on <u>two</u> mutually perpendicular vertical sections. The sampling scheme m = 3 consists of three vertical sections mutually at 120°, and m = 5 consists of five vertical sections, where consecutive sections are at an angle of 72°. Let us calculate the values of $f_m(\theta,\phi)$ as follows.

(1) Initialize the values of ϕ_p^1, θ, and ϕ

(2) Choose m = 3,4, or 5

(3) Calculate vertical section orientations ϕ_p^n using equation (16)

(4) Calculate $f_m(\theta,\phi)$ using equation (9)

(5) Repeat (1) to (4) for all the values of ϕ_p^1 in the range 0° to $\left(\frac{360}{m}\right)°$ at intervals of 1°

(6) Repeat (1) to (5) for all the values of θ in the range 0° to 90° at intervals of 5°

(7) Repeat (1) to (6) for all the values of ϕ in the range 0° to 360° at intervals of 5°

Thus, steps (1) to (7) involve calculation of (4,66,560/m) values

of $f_m(\theta,\phi)$ for each value of m. These calculations were performed on CYBER main frame computer at Georgia Institute of Technology. The calculations lead to the following observations and conclusions.

(I) Five Sectioning Planes: The systematic sampling scheme m=5 consists of five vertical sections, such that consecutive sections are at an angle of 72°. In this case, all the values of $f_m(\theta,\phi)$ were in the range 0.483 to 0.508, i.e., (0.4955 ± 0.0125); see Figure 3. Thus, f_o is equal to 0.4955 and ϵ_o is equal 0.025. Hence, equation (15) takes the following form.

$$S_v = 2.018\ [I_L^c]_5 \qquad (17)$$

The maximum possible error associated with the estimation of S_v using equation (17) is $\pm$ 2.5%. Note that equation (17) is applicable to: (1) any arbitrary choice of vertical axis, (2) any arbitrary anisotropy $g(\theta,\phi)$, and (3) any arbitrary choice of the orientation of the first vertical section ϕ_p^1. Thus, if sufficient number of measurements are performed on these design based vertical sections with statistical uniformity then the total sampling error can be always kept below $\pm$ 2.5%. Interestingly, the value of $f_m(\theta,\phi)$ averaged over all ϕ_p^1 was found to be exactly equal to 0.500, for all the values of θ and ϕ, as expected. This provided cross check on the calculations. Thus, the total surface area per unit volume S_v can be estimated in any homogenous microstructure of arbitrary anisotropy by performing the design based intersection count on five design based vertical sections, with the total

sampling error of less than ± 2.5%, provided the sufficient number of measurements are performed with statistical uniformity; the five vertical sectioning planes must be such that the consecutive planes are at an angle of 72°. This provides a practical solution for applications in materials science. However, it is of interest to investigate if less than five vertical sections can yield a reasonable practical solution.

(II) Three Sectioning Planes: Configuration m=3 consists of three vertical sections that are mutually at an angle of 120°. In this case all the values of $f_m(\theta,\phi)$ were in the range 0.453 to 0.524, i.e., 0.488 ± 0.036. Figure 4 shows the frequency of occurance of $f_m(\theta,\phi)$ values. Thus, $f_m(\theta,\phi)$ varies about ± 7.4% around the value 0.488. For an acceptable solution it is necessary to reduce the variation of $f_m(\theta,\phi)$ to ± 5% or less around some value f_o. Figure 5 shows the distribution of $f_m(\theta,\phi)$ for all θ values less than 85°: $f_m(\theta,\phi)$ is always in the range 0.476 to 0.518, i.e., 0.497 ± .021, a variation of ± 4.2% around f_o equal to 0.497. Figure 6 shows distribution of $f_m(\theta,\phi)$ values for θ in the range 85° to 90°; these values are in the range 0.453 to 0.524. Inspection of Figures 5 and 6, and these data point to a criterian for clever choice of the vertical axis. Note that θ is the angle between the normal to a surface element and the vertical axis. Suppose the vertical axis is chosen such that most of the surface elements are not parallel or almost parallel to the vertical axis (i.e. most of the θ values are less than 85°). To be more precise, let us say that the vertical axis is chosen such that at least 90%

of the surface area corresponds to orientations θ less than 85° (for an isotropic structure 91.3% of the surface area is oriented such that $\theta < 85°$, for any arbitrary vertical axis). In such a case, a simple calculation shows that e_m (see equations (11) and (12)) must be in the range 0.497 ± 0.024. Hence,

$$S_v = 2.012 \overline{[I_L^c]_3} \tag{18}$$

The maximum possible error involved in using equation (18) for estimation of S_v is ± 5%. Thus, the total surface area in any homogenous anisotropic microstructure can be estimated from just three vertical sections with a maximum sampling error of ± 5%, provided sufficient number of measurements are performed on these vertical sections. The sampling error of ± 5% is quite acceptable in most applications. Thus, equations (18) provides an efficient procedure for estimation of S_v in homogenous anisotropic microstructures. However, for a valid application of this result, the following conditions must be satisfied.

(1) The vertical axis must be chosen such that at least 90% of the surface elements are not parallel to the vertical axis (i.e. surface element normals are not perpendicular to the vertical axis).

(2) The measurements must be performed on three vertical sections mutually at 120°.

(3) On each of the three vertical sections, the intersection count must be performed using cycloid shape test lines having cycloid minor axis parallel to the vertical axis.

In order to emphasize these three design requirements, the composite test probe having these characteristics is called "trisector". The geometry of trisector is illustrated in Figure 7. The trisector yields most efficient procedure for the measurement of S_v in homogenous anisotropic materials microstructures; the metallographic polishing and etching is required only on three sections irrespective of anisotropy or geometry of microstructure. It is necessary to utilize equation (18) for estimation of S_v. Note that in trisector all the aspects of sampling are designed; the metallographer does not have the choice for vertical axis, vertical section orientations, or test line shape and orientation.

(III) Two Sectioning Planes: It is of interest to explore whether two perpendicular vertical sections contain sufficient information for a reliable estimation of S_v in homogenous anisotropic microstructures. Figure 8 shows the distribution of $f_m(\theta,\phi)$ values for this case; the values range from 0.393 to 0.555. Thus, there is $\pm$ 17% variation around f_o equal to 0.474, which is clearly not acceptable. Even if the vertical axis is chosen such that most of the surface elements are not parallel to the vertical axis, the variation of $f_m(\theta,\phi)$ for $\theta < 85°$ is still quite significant. It may be concluded that, in general, two perpendicular vertical sections do not contain sufficient microstructural information for a reliable estimation of S_v. This conclusion (although a negative one) is important because metallographers often perform measurements on perpendicular sectioning planes!

(IV) Random Vertical Sections: It is of interest to explore whether a reliable value of S_v can be obtained from the measurements performed on few independent random vertical sections.

the independent random vertical sections are. The steps involved

nputer calculations are as follows:

(1) Pick m random number integers in the interval 0 to 360 by using random number generator, representing the orientations of m vertical sectioning planes.

(2) Calculate $f_m(\theta,\phi)$ for given θ and ϕ using equation (9).

(3) Repeat calculation for all θ in the range 0° to 90° at intervels of 5° and for all ϕ in the range 0° to 360° at intervels of 5°.

(4) Repeat the calculations 1000 times, for m independent random sections; each of the 1000 simulations representing sectioning by m independent random vertical sectioning planes.

Figure 9 shows that frequency of occurrence of $f_m(\theta,\phi)$ values when θ = 60° and ϕ = 30° for 3 independent random vertical sections. Interestingly, $f_m(\theta,\phi)$ varies from 0.258 to 0.702. Figure 10 shows the distribution for seven independent random sections when θ = 60° and ϕ = 30°; the spread in $f_m(\theta,\phi)$ values does not decrease significantly. The over all frequency distribution (all θ and ϕ included) for m = 3 and m = 5 is shown in Figures 11 and 12, respectively. For m = 3, $f_m(\theta,\phi)$ values range from 0.014 to 0.785. Thus, depending on the orientation distribution function $g(\theta,\phi)$, the estimated value of S_v from

measurements performed on three independent random sections may differ from its true value by an order of magnitude even if a very large number of measurements are performed on the three sections! Increasing the number of independent random sections to five does not improve the state of affairs any significantly (see Figure 11). It is interesting to compare Figures 10 and 11 with the corresponding Figures 3 and 4 for systematic vertical sections. It must be concluded that independent random vertical section orientations can not yield a reliable value of S_v in anisotropic microstructures, in general.

DISCUSSION

The analysis presented in the last section concerns estimation of surface area per unit volume in the homogenous anisotropic microstructures encountered in materials science. As mentioned earlier, to clearly reveal the structure present in the sectioning plane a significant amount of tedious, time consuming (and boring) work in necessary for metallographic sectioning, polishing, and etching. These efforts are absolutely necessary before any quantification can be attempted. Thus, it is desired to develope the sampling procedures which can yield reliable values of the stereological attributes from the measurements performed on few sectioning planes; the present analysis provides such a procedure for estimation of S_v using trisector. This sampling procedure involves the following steps:

(1) Choose the vertical axis such that at least 90% of surface area of interest is <u>not</u> parallel to the vertical axis.

(2) Generate three vertical sections which are mutually at an angle of 120°.

(3) On each plane of the trisector generated by steps (1) and (2) perform intersection count using cycloid test lines, keeping cycloid minor axis parallel to vertical axis. Perform these intersection counts with statistical uniformity on all three planes of trisector.

(4) Calculate average number of intersections per unit test line length $\overline{[I_L^c]}_3$ from the measurements performed, and estimate S_v using the following equation.

$$S_v = 2.012\ \overline{[I_L^c]}_3 \qquad (18)$$

If sufficient number of measurements are performed with statistical uniformity on the three planes of the trisector, then using equation (18) S_v can be estimated with an error of at the most ± 5%. It is important to emphasize that a three planes of the trisector have equal 'weightage.' Thus, the number of placements of test lines and the total test line length utilized should be the same on all three planes. For example, if test line is placed 100 times on one plane of trisector at different locations and it is placed only 10 times each on other two planes, then the resulting $\overline{[I_L^c]}_3$ value will be biased, and then equation (18) can <u>not</u> give a reliable value of S_v.

The S_v value estimated using trisector can have an error of ± 5%, (maximum), no matter how many measurements are performed.

Hence it is futile to estimate $\overline{[I_L^c]_3}$ with a standard error lower than ± 5% with 99% confidence. If a value of S_v with an error less than ± 5% is desired (not very likely) then the measurements should be performed on five vertical sectioning planes such that consecutive planes are at an angle of 72°. For such sampling scheme, the choice of vertical axis is absolutely arbitrary, and S_v can be estimated using equation (17) with an error of only ± 2.5%. However, the amount of effort involved increases by at least 66%.

An important question which remains to be analyzed is "How practical is the use of trisector?" In trisector, the vertical axis must be oriented such that at least 90% of the surface area is not parallel or almost parallel to the vertical axis. Can such a choice of vertical axis lead to practical difficulties in sectioning? Fortunately, the vertical axis choice dictated by trisector, is most simple to adopt in practice! Consider grain boundaries or inclusions in a cold rolled metal or alloy. The grain boundaries and inclusions tend to elongate along the rolling direction. The trisector dictates that vertical axis should be perpendicular to the plane of the rolled sheet. It is always simple to cut a rolled sheet along vertical sections perpendicular to the plane of the rolled sheet as required in trisector (see Figure 13). It would be difficult to section parallel to sheet or along different planes containing the rolling direction. Consider the microstructure of an extruded or wire drawn material where the

internal surfaces tend to be parallel to the wire axis or extrusion direction. It is easier to cut such a material along planes where vertical axis is perpendicular to the wire axis or extrusion axis, as compared to sectioning on three planes containing the wire axis or extrusion axis. One can draw similar conclusions for other anisotropic microstructures. Thus, the choice of the vertical axis dictated by trisector is quite suitable from the practical considerations.

The use of trisector requires sectioning on three planes mutually at 120°. This is not difficult in practice. It is easy to fabricate a fixture with three slots mutually at 120° to hold the specimen mounted in a resin, which can be then sectioned along the slots. Thus, the vertical sectioning required for trisector is practically feasible.

An important outcome of the present work is a very clear demonstration of how useless independent random sections are. For all practical purposes, independent random vertical sections can not yield a reliable estimate of S_v in anisotropic microstructure, unless the measurements are performed on very large number of sections. In materials microstructures it is not practical (and in some cases it is not even possible!) to section a specimen along more than five planes of different orientations. Thus, in general, independent random vertical sections have no practical utility for estimation of S_v in anisotropic materials microstructures. In contrast, just three systematic vertical sections mutually at 120° can yield a reliable value of S_v with much less effort.

CONCLUSIONS

A practically feasible efficient sampling procedure is developed for the measurement of the total area of internal boundaries in homogenous anisotropic microstructures encountered in materials science. It is shown that three vertical sections (with specifically chose.. vertical axis) mutually at an angle of 120° contain sufficient structural information for a reliable estimation of S_v.

ACKNOWLEDGEMENT

This research work is part of NSF sponsored project (DMR-8504167) on "Quantitative Analysis of Fracture Surfaces Using Stereological Methods"; this financial support is gratefully acknowledged.

REFERENCE

1) Baddeley A. J., Gundersen H.J.G., and Cruz-Orive L.M., (1986), Estimation of Surface Area from Vertical Sections, J. Miscrosc., 142, pt. 3, pp 259-276.

LIST OF FIGURE CAPTIONS:

Figure 1 Specification of angular orientation of a surface element.

Figure 2 Specification of angular orientation of a vertical sectioning plane

Figure 3 Frequency of occurrence of $f_m(\theta,\phi)$ values when m = 5, and consecutive vertical sections are at an angle of 72°

Figure 4 Frequency of occurrence of $f_m(\theta,\phi)$ values for three systematic vertical sections mutually at 120°

Figure 5 Frequency of occurrence of $f_m(\theta,\phi)$ values for θ < 85° and sampling on three vertical sections mutually at 120°

Figure 6 Frequency of occurrence of $f_m(\theta,\phi)$ values for θ in the range 85° to 90° and sampling on three vertical sections mutually at 120°

Figure 7 Geometry of trisector. The vertical axis is such that at least 90% of surface area is not parallel to vertical axis

Figure 8 Frequency of occurrence of $f_m(\theta,\phi)$ values for sampling on two perpendicular vertical sections

Figure 9 Frequency of occurrence of $f_m(\theta,\phi)$ when θ = 60° and ϕ = 30°, sampling on three independent random vertical sections

Figure 10 Frequency of occurrence of $f_m(\theta,\phi)$ when θ = 60° and ϕ = 30°, sampling on seven independent random sections

Figure 11 The overall frequency of occurrence of $f_m(\theta,\phi)$ for three independent random sections

Figure 12 The overall frequency of occurrence of $f_m(\theta,\phi)$ for five independent random sections

Figure 13 Sectioning by trisector planes

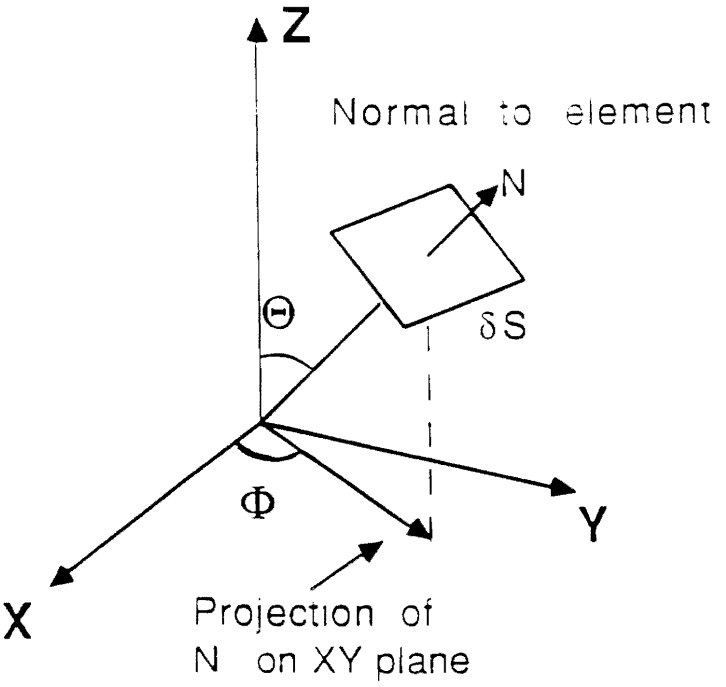

Figure 1 Specification of angular orientation of a surface element.

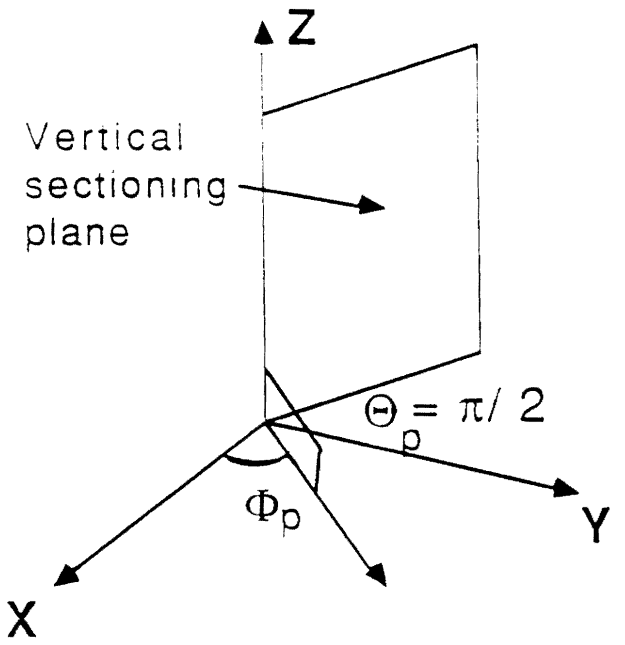

Figure 2 Specification of angular orientation of a vertical sectioning plane

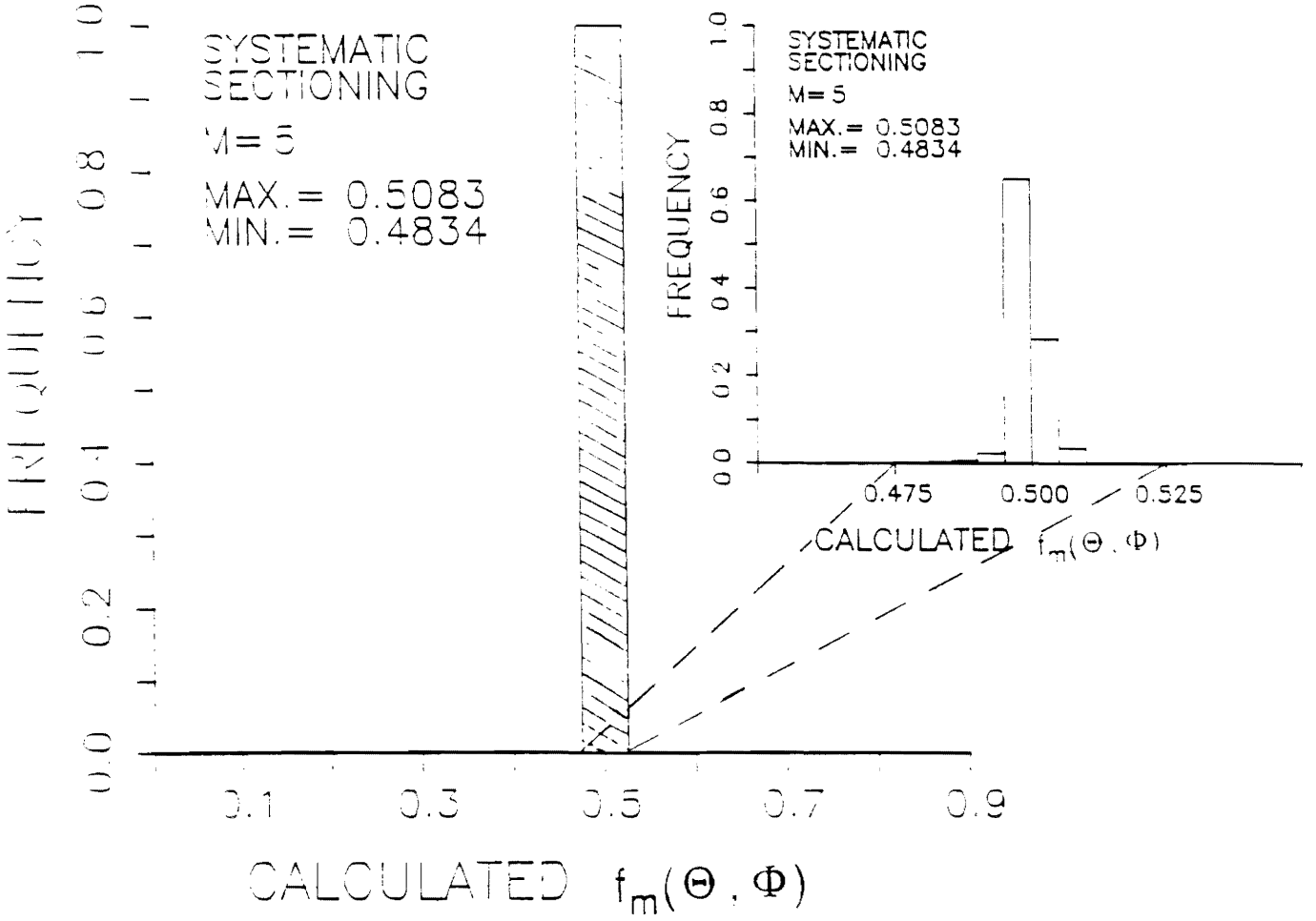

Figure 3 Frequency of occurrence of $f_m(\theta,\phi)$ values when m = 5, and consecutive vertical sections are at an angle of 72°

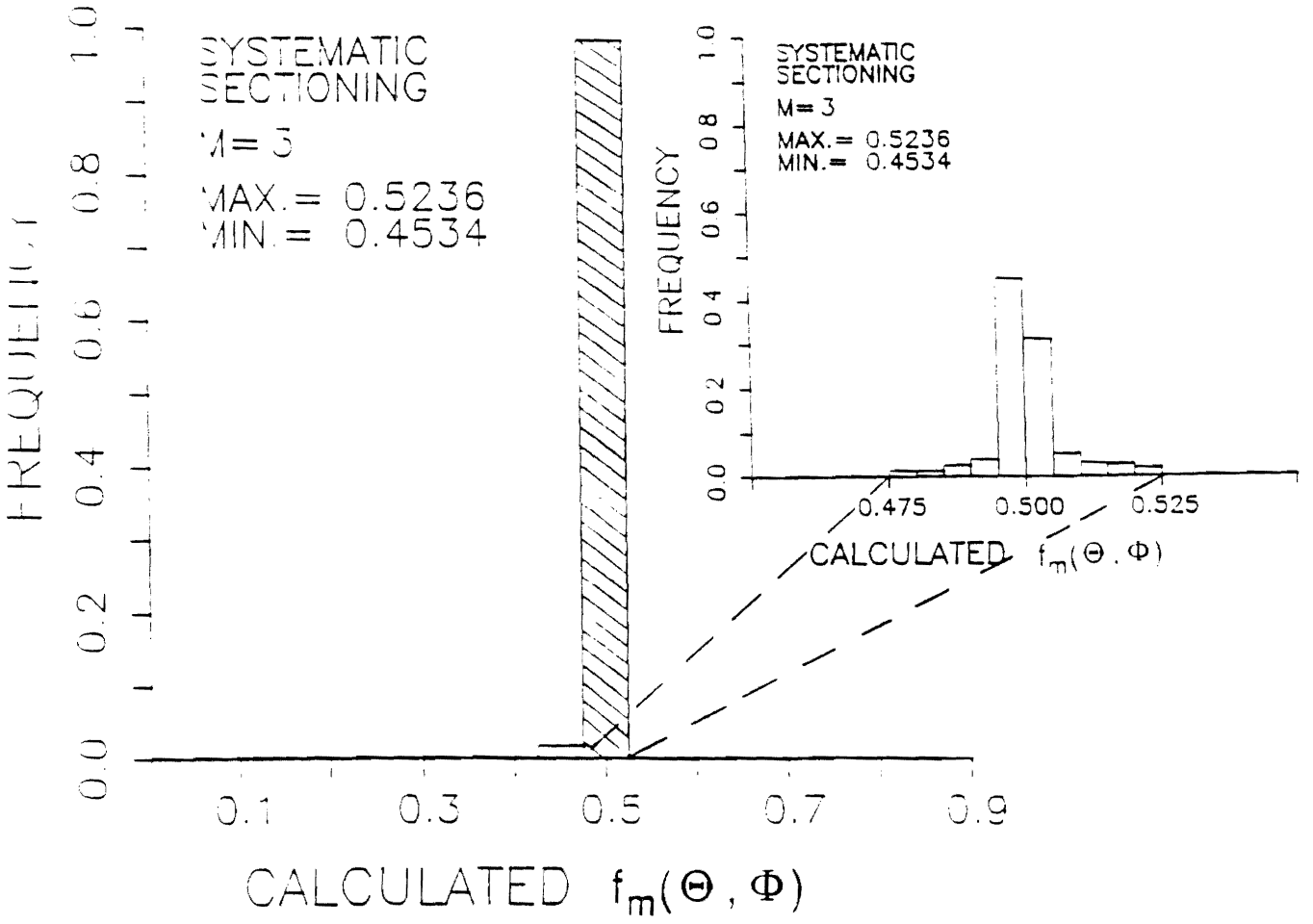

Figure 4 **Frequency of occurrence of f_m (θ,ϕ) values for three systematic vertical sections mutually at 120°**

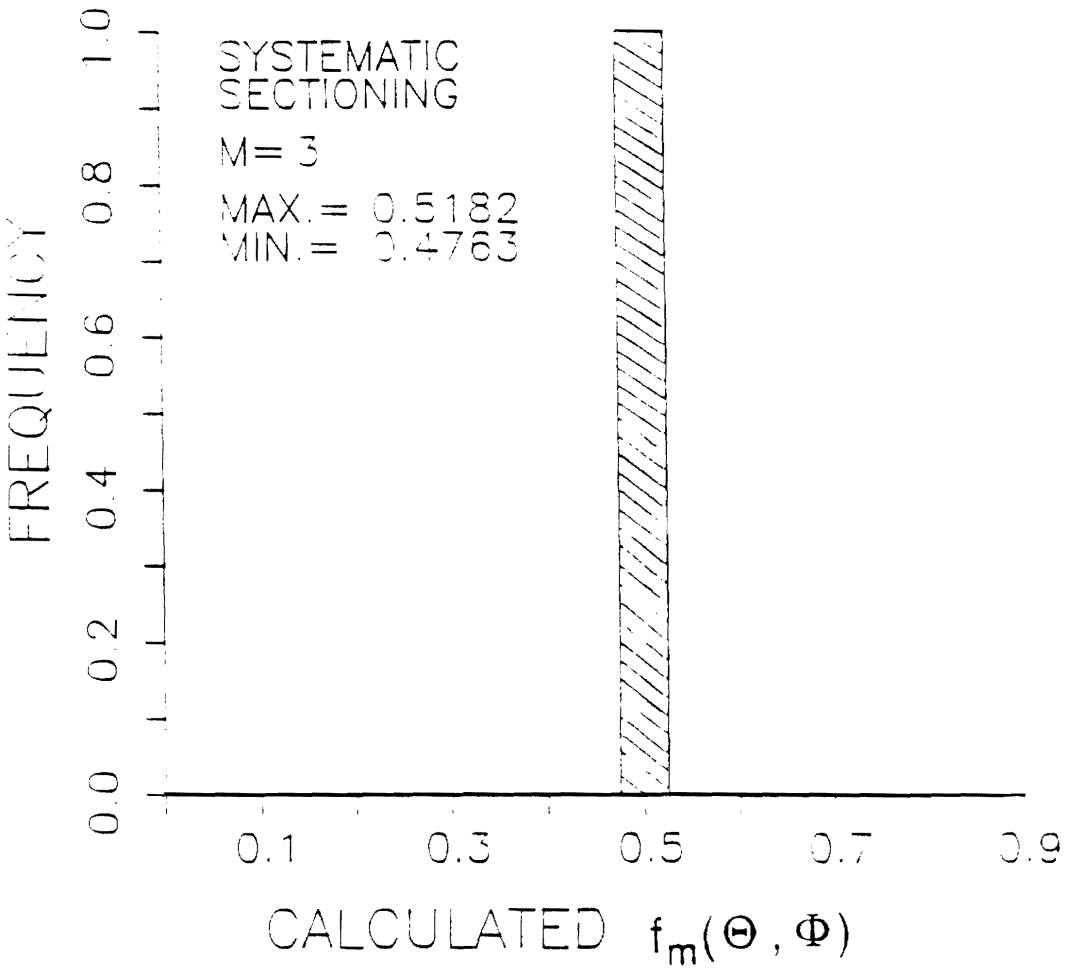

Figure 5 Frequency of occurrence of $f_m(\theta,\phi)$ values for $\theta < 85°$ and sampling on three vertical sections mutually at 120°

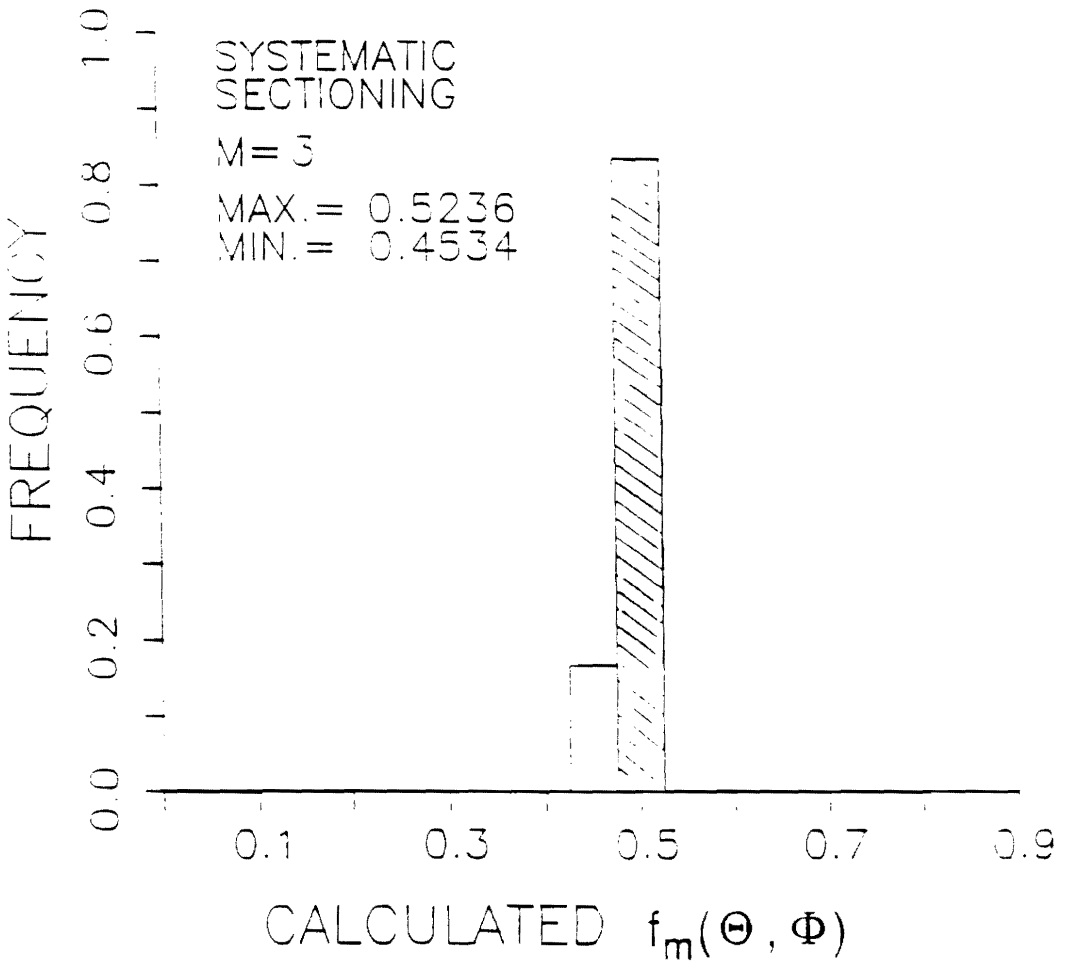

Figure 6 Frequency of occurrence of $f_m(\theta, \phi)$ values for ϑ in the range 85° to 90° and sampling on three vertical sections mutually at 120°

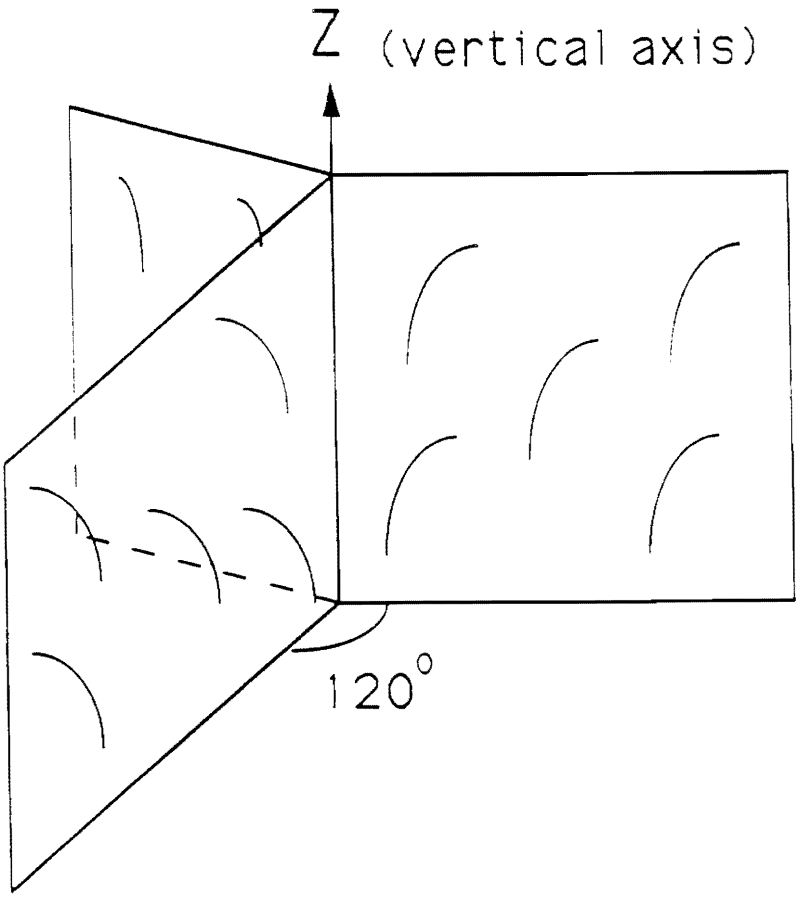

Figure 7 Geometry of trisector. The vertical axis is such that at least 90% of surface area is not parallel to vertical axis

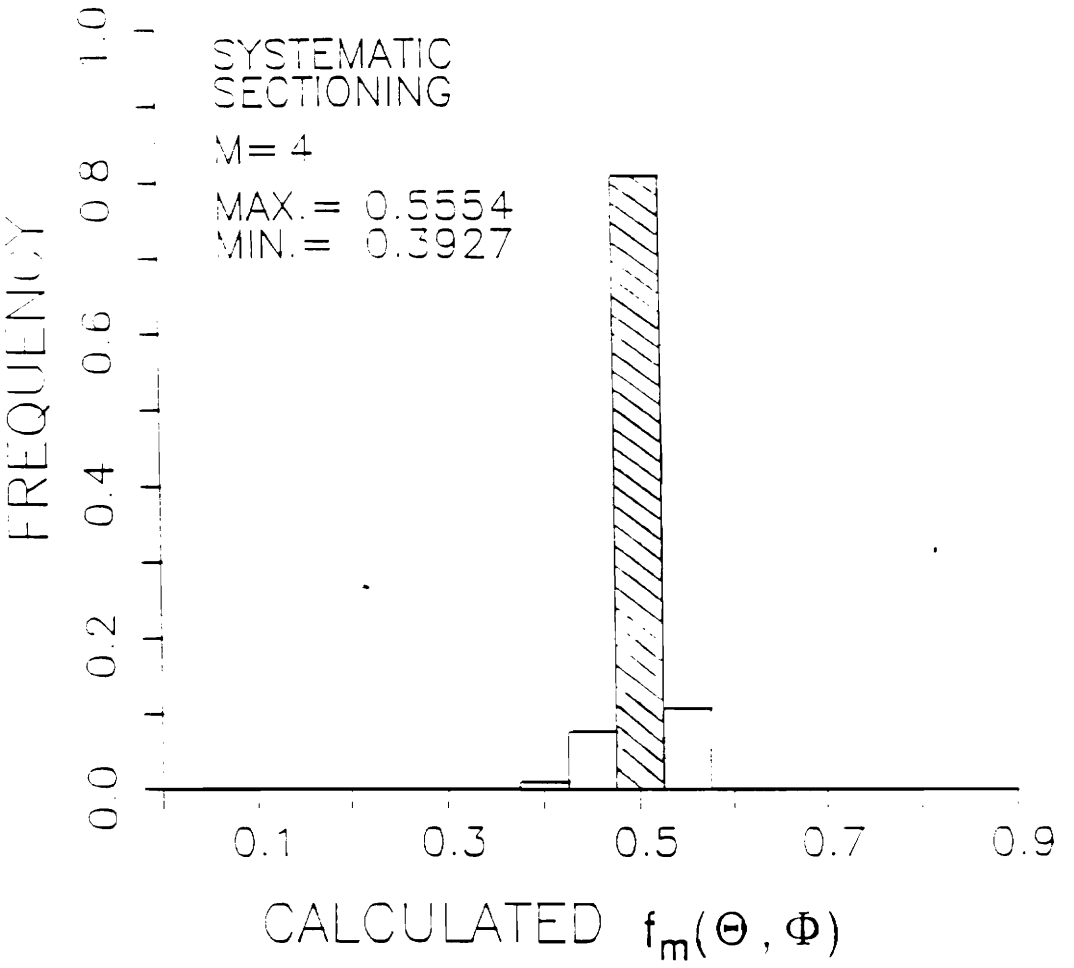

Figure 8 **Frequency of occurrence of f_m (θ,ϕ) values for sampling on two perpendicular vertical sections**

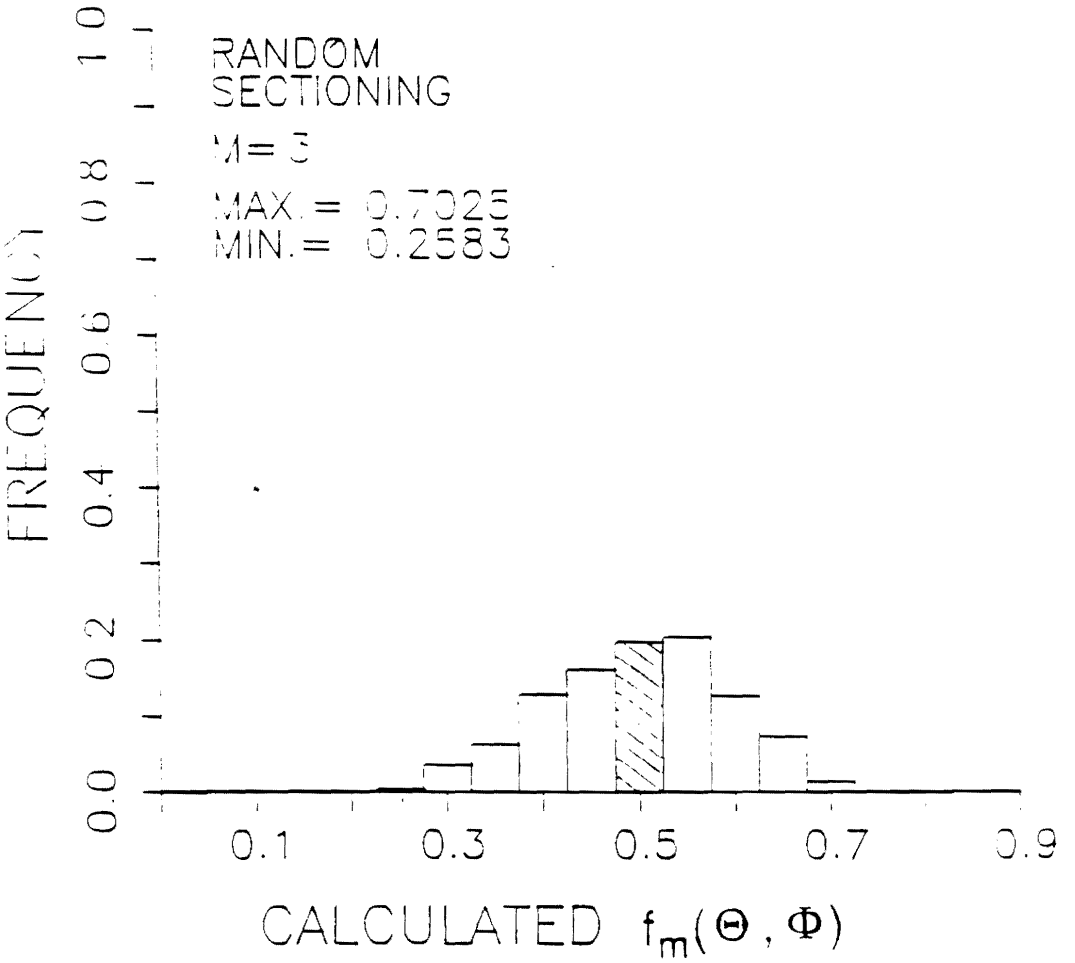

Figure 9 Frequency of occurrence of $f_m(\theta, \phi)$ when $\theta = 60°$ and $\phi = 30°$, sampling on three independent random vertical sections

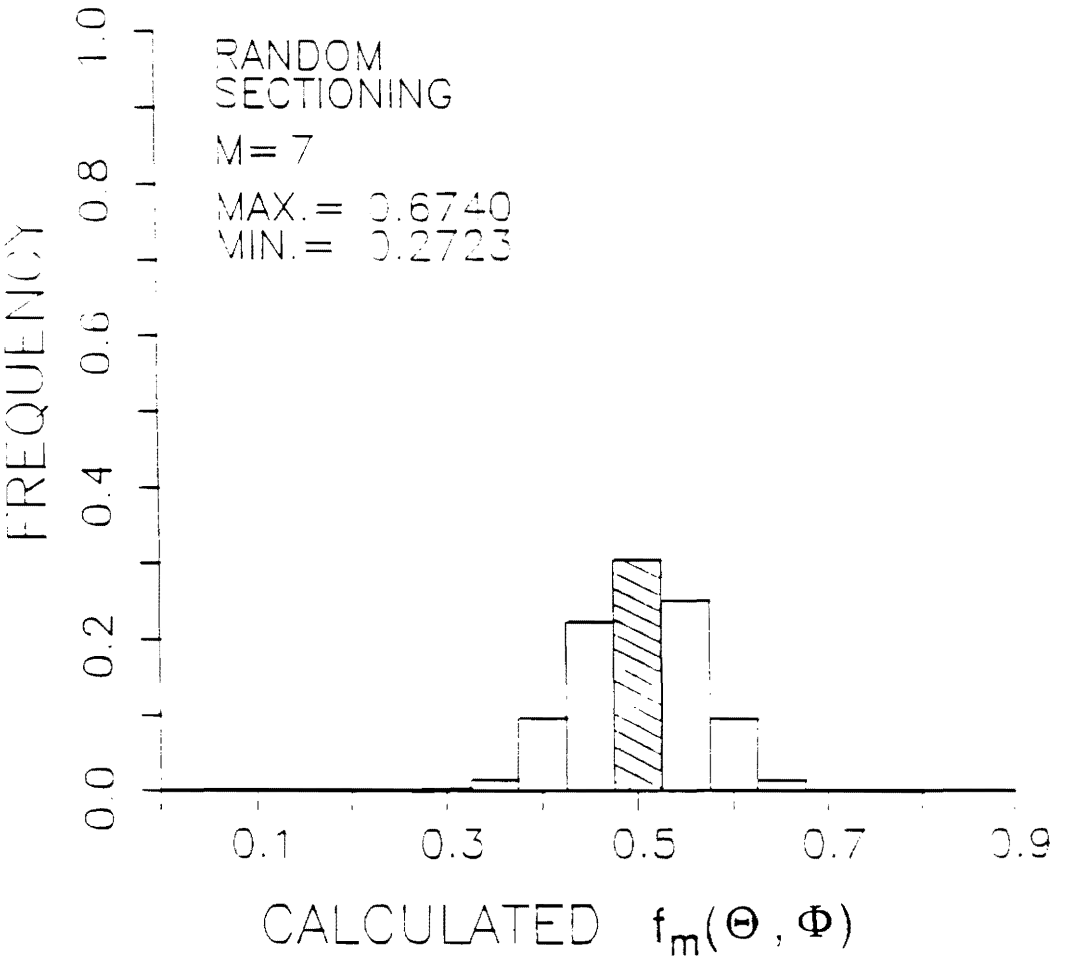

Figure 10 Frequency of occurrence of $f_m(\theta,\phi)$ when $\theta = 60°$ and $\phi = 30°$, sampling on seven independent random sections

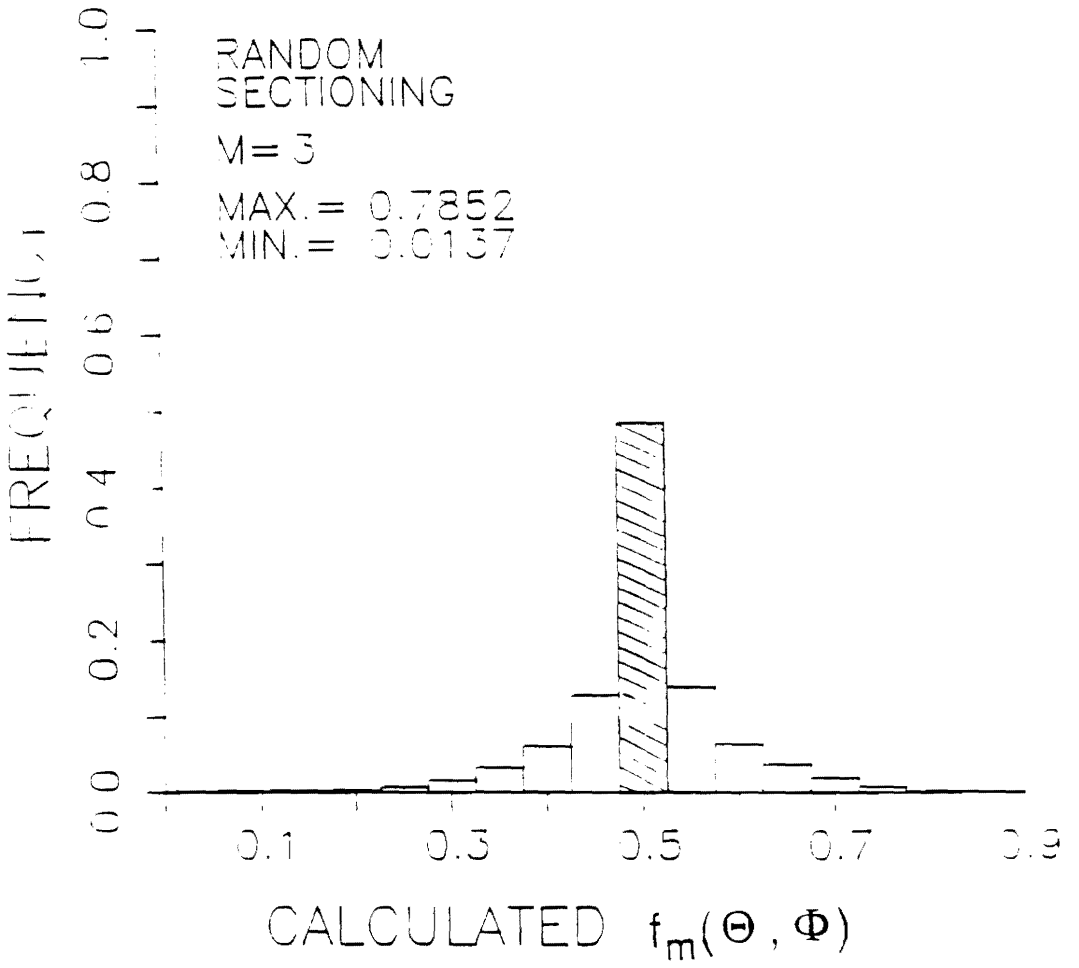

Figure 11 The overall frequency of occurrence of $f_m(\vartheta, \phi)$ for three independent random sections

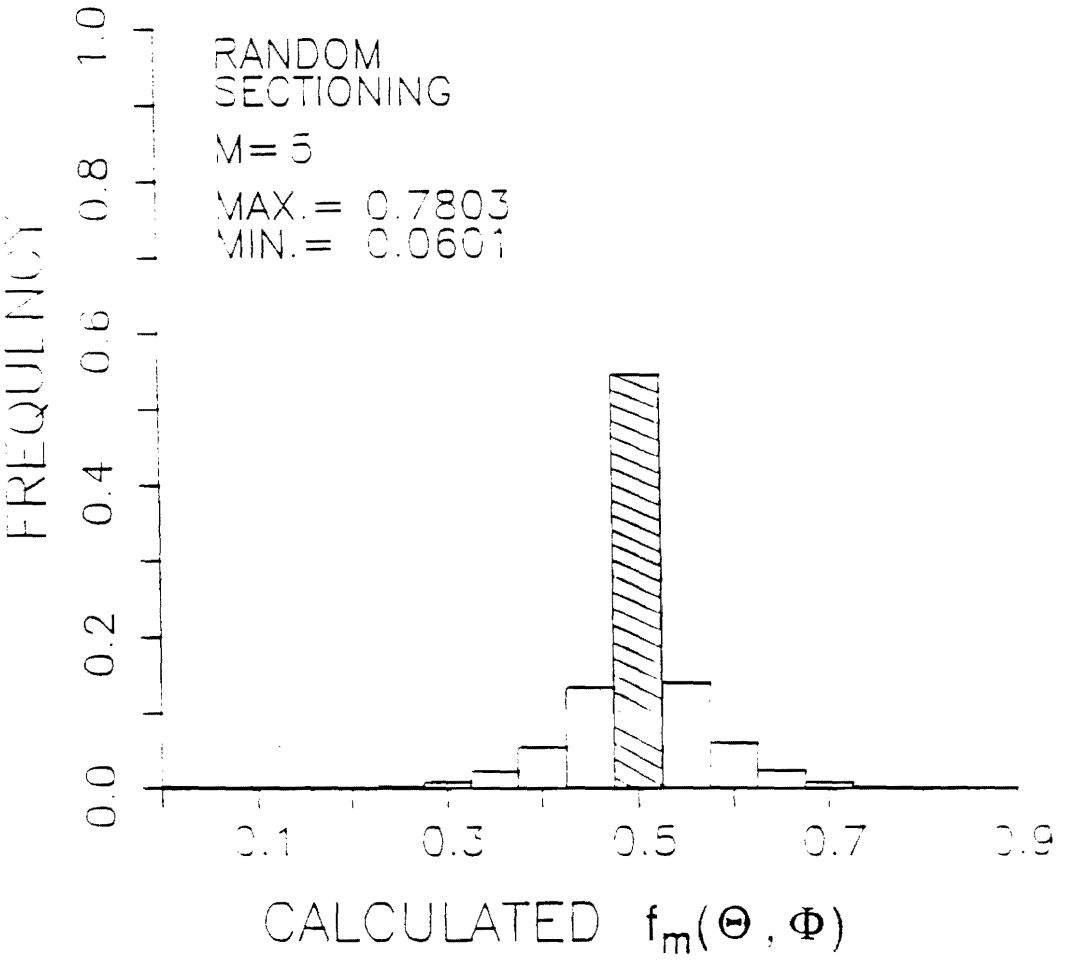

Figure 12 The overall frequency of occurrence of $f_m(\vartheta, \varphi)$ for five independent random sections

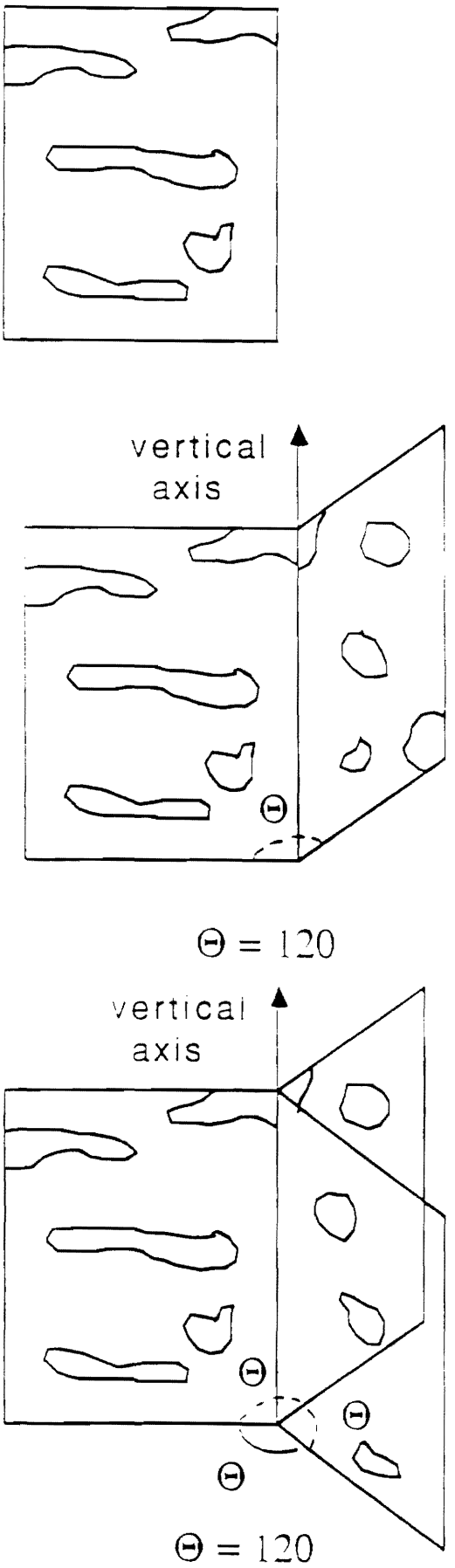

Figure 13 Sectioning by trisector planes

Journal of Microscopy
(submitted)

DESIGN BASED TEST LINES FOR EFFICIENT MEASUREMENT OF ANISOTROPY

by

Arun M. Gokhale
School of Materials Engineering
Georgia Institute of Technology
Atlanta, Georgia 30332-0245
U.S.A.

Key words: Anisotropy, stereology, design based test lines, intersection count, anisotropic microstructures

ABSTRACT

Line intersection count $I_L(\theta)$ in a two dimensional section through a three dimensional anisotropic microstructure depends on the test line orientation θ. If $I_L(\theta)$ is represented by a Fourier series, then each coefficient of the series is uniquely related to the intersection counts pertaining to two design based test lines in a simple manner. Thus, the Fourier coefficients can be estimated directly via design based intersection counting. This provides an efficient procedure for quantification of anisotropy in two dimensions, as a few terms of the series can yield reasonably accurate representation of $I_L(\theta)$. This input can be utilized for estimation of anisotropy in three dimensions using the established stereological procedures.

INTRODUCTION:

Physical processes often generate microstructures that are anisotropic. The properties of such materials are sensitive to the nature and the extent of the microstructural anisotropy. For example, the mechanical properties are influenced by the anisotropy of the internal surfaces in microstructure. However, assumption free experimental measurements of anisotropy are scanty, although the required stereological equations are available for more than twenty years (see, Hilliard, (1967)). This is due to the fact that very significant amount of measurement effort is necessary for the characterization of microstructural anisotropy.

During pa five years or so, efficient design based stereological procedures have been developed for estimation of global microstructural properties such as number per unit volume (Sterio (1984), Cruz-Orive (1986)), surface area per unit volume (Baddeley et. al, (1986)), and total length per unit volume (Gokhale, (1989)). To the best knowledge of the author efficient design based stereological procedure is not available in the literature for assumption free characterization of anisotropy. It is the purpose of this contribution to develope simple design based intersection count technique for quantification of anisotropy in a two dimensional section: the necessary basic input for characterization of anisotropy in three dimensions.

Hilliard (1967) developed the mathematical frame work for calculation of the orientation distribution function of internal surfaces in microstructure from the measurements of line intersection counts as a function of test line orientation in the

three dimensional space. In practice, the number of intersections can be measured as a function of test line orientation in a sectioning plane of known angular orientation; the procedure is then repeated on the sectioning planes of different known orientations. It is interesting to note that a set of vertical sections contains test lines of all possible orientations in the three dimensional space (see, Baddeley et. al. (1986)), and hence it contains sufficient information for quantification of anisotropy of internal surfaces in microstructure. Similarly, a set of vertical slices (Gokhale (1989)) contains all the angular orientations of test planes for quantification of anisotropy of lineal features from similar intersection counts performed on the projected images. The orientation distribution function of internal surfaces or lines can be thus calculated from the measurements performed on vertical sections, or the projected images of vertical slices, respectively. The necessary procedure is given by Hilliard (1967). The present analysis is concerned with obtaining the required intersection count data in a two dimensional section in an efficient manner by using design based test line shapes.

THEORETICAL DEVELOPMENT

Consider a two dimensional section through a three dimensional microstructure containing internal surfaces. The two dimensional section contains line traces of the internal surfaces resulting from the intersections of the surfaces with the sectioning plane. This set of lines (or line traces) is of interest for the characterization of anisotropy. Let θ be the angle between a

straight test line and the reference direction (vertical axis, if the sectioning plane is vertical). Let $I_L(\theta)$ be the expected number of intersections of a straight test line of orientation θ with the line traces of interest per unit test line length. For an anisotropic set of line traces in the two dimensional section $I_L(\theta)$ varies with θ. The aim is to estimate the function $I_L(\theta)$ experimentally without any assumptions. The traditional procedure involves the estimation of $I_L(\theta)$ at 10° intervals of θ to cover the range 0° to 180°, i.e., intersection counts pertaining to eighteen straight test lines of different known orientations. This discrete data forms the input to calculate the analytical form for $I_L(\theta)$ using a suitable numerical procedure. Typically, $I_L(\theta)$ is expanded in terms of a series, and the unknown coefficients of the series are calculated from the experimental data. We shall now develope design based test line shapes such that the corresponding intersection counts directly give the required coefficients, there by decreasing the measurement effort and eliminating the processing of the raw data. Let us represent $I_L(\theta)$ in terms of a Fourier series as follows.

$$I_L(\theta) = a_o + \sum_{m=1}^{\infty} a_m \cos(m\theta) + \sum_{n=1}^{\infty} b_n \sin(n\theta) \qquad (1)$$

where, a_o, a_m, and b_n are the unknown coefficients. In general, these coefficients depend on the orientation of the sectioning plane. Note that the units for all the coefficients are number per unit length. The orientations θ and $(\theta + \pi)$ represent the same

test lines. It follows that;

$$I_L(\theta) = I_L(\theta + \pi) \tag{2}$$

Hence, all the odd coefficients in equation (1) must be equal to zero. Thus, one can write;

$$I_L(\theta) = a_o + \sum_{m=1}^{\infty} a_{2m} \cos(2m\theta) + \sum_{n=1}^{\infty} b_{2n} \sin(2n\theta) \tag{3}$$

Further,

$$\pi a_o = \int_o^{\pi} I_L(\theta)\, d\theta = \pi\, [I_L]_{cir} \tag{4a}$$

or

$$a_o = [I_L]_{cir} \tag{4b}$$

where, $[I_L]_{cir}$ is the expected number of intersections of the line traces with a circular test line of unit length. Thus, the intersection count pertaining to a test line of circular shape is equal to the coefficient a_o. The Fourier coefficients a_{2m} and b_{2n} are given as follows.

$$a_{2m} = \frac{2}{\pi} \int_o^{\pi} \cos(2m\theta) \cdot I_L(\theta)\, d\theta \tag{5}$$

and,

$$b_{2n} = \frac{2}{\pi} \int_o^{\pi} \sin(2n\theta) \cdot I_L(\theta)\, d\theta \tag{6}$$

Write equations (5) and (6) in following useful alternate forms.

$$a_{2m} = 2 \left[\frac{1}{\pi} \int_o^{\pi} [1 + \cos(2m\theta)] I_L(\theta)\, d\theta - [I_L]_{cir} \right] \tag{7}$$

and,

$$b_{2n} = 2 \left[\frac{1}{\pi} \int_0^{\pi} [1 + \sin(2n\theta)]\ I_L(\theta) d\theta - [I_L]_{cir} \right] \qquad (8)$$

All that is required now is the interpretation of the integrals in equations (7) and (8) in terms of intersections counts pertaining to the test line of specific shapes. Consider a test line shape such that the infinitesimal test line length $dL_m(\theta)$ in the orientation range θ to $(\theta + d\theta)$ is given as follows.

$$dL_m(\theta) = \frac{L_m}{\pi} [1 + \cos(2m\theta)]\ d\theta \qquad (9)$$

where, L_m is the total test line length covering all the orientations $o \leq \theta \leq \pi$. Let $[I_L]_{a2m}$ be the expected number of intersections of this test lines with the line traces of interest per unit test line length. It follows that;

$$[I_L]_{a2m} = \int I_L(\theta)\ dL_m(\theta) \Big/ \int dL_m(\theta) \qquad (10)$$

Equations (9) and (10) give the following result

$$[I_L]_{a2m} = \frac{1}{\pi} \int_0^{\pi} [1 + \cos(2m)\theta]\ I_L(\theta)\ d\theta \qquad (11)$$

Combining equations (7) and (11) gives the following interesting result.

$$a_{2m} = 2\ [[I_L]_{a2m} - [I_L]_{cir}] \qquad (12)$$

The Fourier coefficient a_{2m} is precisely equal to two times the difference between the design based intersection counts pertaining

to two test lines of specific shapes. In a similar manner, the following result can be derived.

$$b_{2n} = 2\ [\,[I_L]_{b2n} - [I_L]_{cir}\,] \tag{13}$$

where, $[I_L]_{b2n}$ is the intersection count pertaining to a test line whose shape is such that its length $dL_n(\theta)$ in the orientation range θ to $(\theta + d\theta)$ is given by the following equation.

$$dL_n\ (\theta) = \frac{L_n}{\pi}\ [1 + \sin\ (2n\theta)]\ d\theta \tag{14}$$

L_n is the total line length covering orientations $o \leq \theta \leq \pi$. Equations (12) and (13) are assumption free, i.e., they are <u>not</u> model based. In most of the practical cases few terms of the Fourier series yield reasonably accurate representation of $I_L\ (\theta)$. In other words, the measurements of intersection counts using few design based test line shapes is sufficient to characterize the anisotropy in two dimensions. The present procedure reduces the measurement effort significantly and it eliminates the traditional processing of raw data to recover $I_L\ (\theta)$ from the experimental information. It remains to determine the equations of the necessary design based test lines.

<u>Design Based Test Line Shapes</u>: Consider a curved test line of total length L, such that;

$$dL(\theta) = \frac{L}{C}\ G(\theta)\, d\theta \tag{15}$$

where, $dL(\theta)$ is the test line length in the orientation range θ to $(\theta + d\theta)$, L is the total test line length covering all orientations

range $o \leq \theta \leq \pi$, and,

$$C = \int_o^{\pi} G(\theta)d\theta \tag{16}$$

any continuous function of θ in the interval $o \leq \theta \leq \pi$, at $G(\theta) \geq o$, and $G(\theta)$ is finite in the interval $o \leq \theta \leq \pi$. axis be the reference axis. A curve represented by the ng parametric equation satisfies equations (15) and (16).

$$\begin{aligned} Y &= Y_o + \frac{L}{C} \int_o^{\theta} \cos\theta \; . \; G(\theta)d\theta \\ X &= X_o + \frac{L}{C} \int_o^{\theta} \sin\theta \; . \; G(\theta)d\theta \end{aligned} \tag{17}$$

) is any arbitrary point in XY - plane, and it only specifies cation of the line in XY plane. Equation (17) provides a l algorithm for determination of design based test line shape ed by equations (15) and (16).

or determination of cosine Fourier coefficients, the test hape must be such that $G(\theta)$ is equal to $[1 + \cos(2m\theta)]$. for determination of the coefficients a_{2m} the design based ines have the following parametric equations.

$$Y_{2m} = Y_o + \frac{L_m}{\pi} \int_o^{\theta} \cos\theta \; [1 + \cos(2m\theta)]d\theta$$

$$X_{2m} = X_o + \frac{L_m}{\pi} \int_o^{\theta} \sin\theta \; [1 + \cos(2m\theta)]d\theta \tag{18}$$

$o \leq \theta \leq \pi$

$_{2m})$ are the co-ordinate points of the required lines.

Similarly, the parametric equations of the test lines for measurements of Fourier sine coefficients b_{2n} are as follows.

$$Y_{2n} = Y_o + \frac{L_n}{\pi} \int_o^{\theta} \cos\theta \, [1 + \sin(2n\theta)]d\theta$$
$$X_{2n} = X_o + \frac{L_n}{\pi} \int_o^{\pi} \sin\theta \, [1 + \sin(2n\theta)]d\theta \qquad (19)$$

and $o \leq \theta \leq \pi$

without any loss of generality, one can set x_o and Y_o equal to zero in equations (17) to (19). The specific equations for test line shapes necessary for measurements of first few Fourier coefficients are as follows.

Test line for $Y = \frac{2L}{3\pi} [3\sin\theta - \sin^3\theta]$

measuring a_2 $x = \frac{2L}{3\pi} [1 - \cos^3\theta]$ (20)

Test line for $Y = \frac{2L}{15\pi} [15\sin\theta - 20\sin^3\theta + 12\sin^5\theta]$

measuring a_4 $X = \frac{2L}{15\pi} [7 - 15\cos\theta + 20\cos^3\theta - 12\cos^5\theta]$ (21)

Test line for $Y = \frac{L}{\pi} [\frac{2}{3} + \sin\theta - \frac{2}{3}\cos^3\theta]$

measuring b_2 $X = \frac{L}{\pi} [1 - \cos\theta + \frac{2}{3}\sin^3\theta]$ (22)

Test line for $Y = \frac{L}{\pi} [\sin\theta + \frac{1}{6}\{1 - \cos3\theta\} + \frac{1}{10}\{1 - \cos4\theta\}]$

measuring b_4 $x = \frac{L}{\pi} [1 - \cos\theta + \frac{1}{6}\sin3\theta - \frac{1}{10}\sin4\theta]$ (23)

Figures 1 and 2 depict the test line shapes for measurements of, a_2, a_4, b_2, and b_4. In all the cases Y-axis is the reference direction. The test line shapes for higher coefficients can be easily generated from equations (18) and (19). As shown in Figures 1 and 2 the total test line length is directly related to the length of the test figures along x-axis.

DISCUSSION

The main results of the present work are contained in equations (12) and (13). It is shown that if $I_L(\theta)$ is represented by a Fourier series, then each Fourier coefficient is uniquely related to two design based intersection counts. Although, the Fourier series is utilized in the present work, the function $I_L(\theta)$ can be also represented by a series of a set of any orthogonal functions; the same logic can be utilized to estimate the unknown coefficients via intersection counts pertaining to some other design based test line shapes.

The Fourier coefficients a_{2m} and b_{2n} are expected to depend on the orientation of the sectioning plane in which the intersection counts are performed. However, if the anisotropy is rotationally symmetric, then $I_L(\theta)$ estimated on a single two dimensional section (or in a set of uniformly spaced parallel sections if microstructure is inhomogenous) containing the symmetry axis (chosen as reference direction) contains sufficient information for calculation of the orientation distribution function of the surfaces of interest in the microstructure (see Hilliard, (1967)). This is because in such a case all the sectioning planes containing the symmetry axis contain statistically equivalent structural

information, and hence $I_L(\theta)$ is same on all such planes.

Recently, Benes (1989) has proposed a model based procedure for measurement of $I_L(\theta)$ represented in the following model form.

$$I_L(\theta) = a_o + a_2 \cos 2\theta + b_2 \sin 2\theta \qquad (24)$$

To estimate the anisotropy in a two dimensional section, Benes measured $I_L(\theta)$ for twelve different straight test line orientations at intervals of 15° in the range $o° \leq \theta \leq 180°$, and utilized a sophisticated regression analysis for estimating a_o, a_2 and b_2 from these data. However, using the present analysis, it is necessary to measure the intersection counts pertaining to only three design based test lines (circle for a_o, test line shape in Figure 1(a) for a_2, and test line shape in Figure 2 (a) for b_2) for the direct estimation of the coefficients a_o, a_2 and b_2. This reduces the amount of measurement effort by a factor of four and eliminates the need for any regression analysis! Further, in the case of Benes' (1989) specimens of extruded aluminium alloy, the anisotropy is expected to be rotationally symmetric with respect to the extrusion direction (see Figure 3 in Benes (1989), further, calculated coefficients $\hat{a}$ and $\hat{b}$ are almost an order of magnitude smaller than $\hat{c}$ and $\hat{d}$ in his calculations of anisotropy in three dimensions). In such a case, the model proposed by Benes reduces to the following form.

$$I_L(\theta,\phi) = c \cos 2\theta + d \qquad (25)$$

Thus, the intersection counts pertaining to just two design based test lines (circle for estimating d, and Figure - 1a for estimating

c) on just one sectioning plane containing the extrusion direction is sufficient for direct estimation of the model parameters c and d!

ACKNOWLEDGEMENT:

This research work is part of NSF sponsored project (DMR-8504167) on "Quantitative Analysis of Fracture Surfaces Using Stereological Methods"; this financial support is gratefully acknowledged.

REFERENCES

Baddely A.J., Gundersen H.J.G., and Cruz-Orive L.M. (1986), Estimation of surface area from vertical sections, Journal of Microscopy, vol. 142, Pt. 3, PP. 259-276

Benes Viktor (1989), A Practical approach to stereology of anisotropic microstructures, Journal of Microscopy, vol. 154, Pt. 154, PP. 165-175

Cruz-Orive L.M. (1986), Particle number can be estimated using disector of unknown thickness: selector, Journal of Microscopy, vol. 145, PP. 121-142

Gokhale Arun M. (1989), Unbiased estimation of curve length in 3D using vertical slices, Journal of Microscopy, accepted for publication

Hilliard J.E. (1967), Specification and measurement of microstructural anisotropy, Trans. Met. Soc. AIME, vol. 224, PP. 1201-1211.

Sterio D.C. (1984), The unbiased estimation of number and sizes of arbitrary particles using the disector, Journal of Microscopy, vol. 134, pt. 2, pp. 127-136

LIST OF FIGURE CAPTIONS

Figure 1 Test line shapes for estimating the fourier cosine coefficients a_2 and a_4: figure (a) is for a_2 and figure (b) is for a_4

Figure 2 Test line shapes for estimating the fourier sine coefficients b_2 and b_4: figure (a) is for b_2 and figure (b) is for b_4

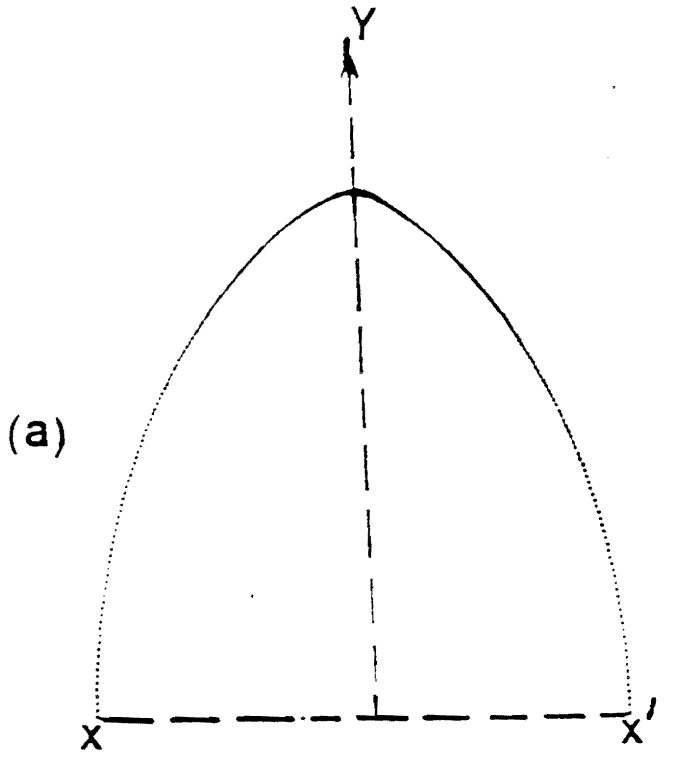

$$\text{Test line length} = \frac{3\pi}{4} \cdot x\,x'$$

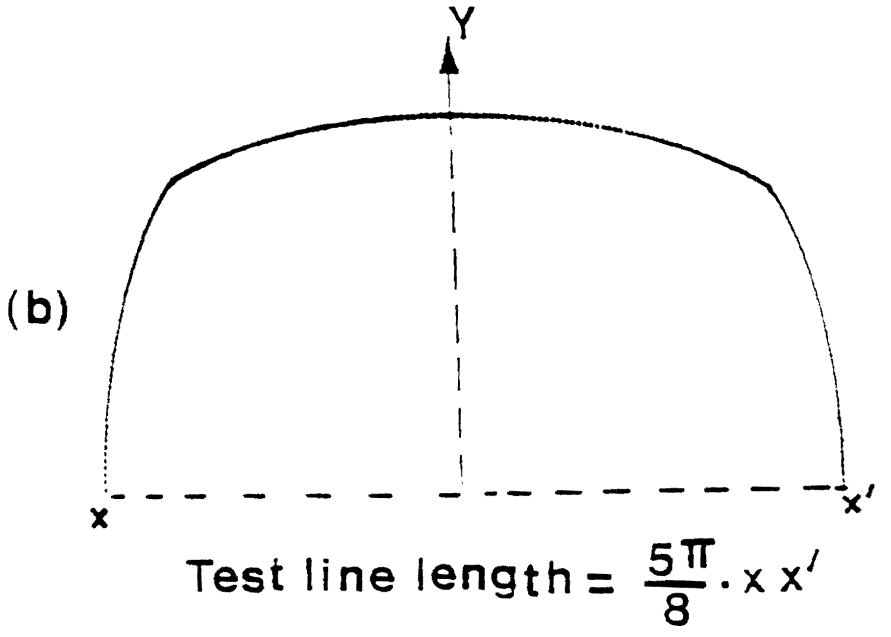

$$\text{Test line length} = \frac{5\pi}{8} \cdot x\,x'$$

Figure 1 Test line shapes for estimating the fourier cosine coefficients a_0 and a_1: figure (a) is for a_0 and figure (b) is for a_1

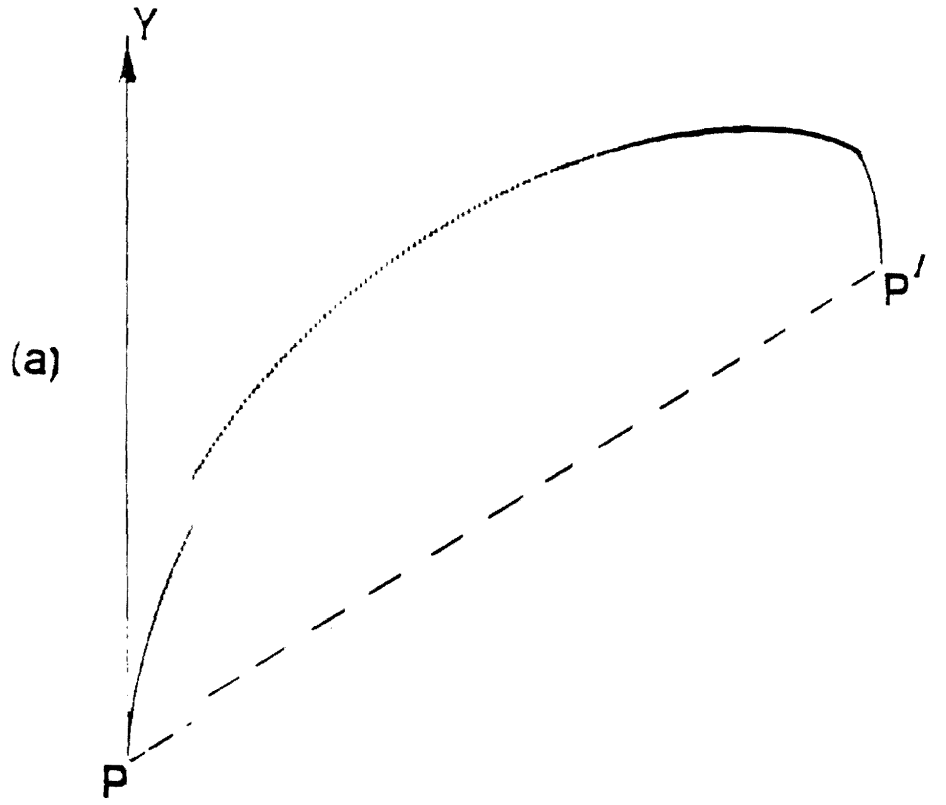

Tes line length = 1·307P P′

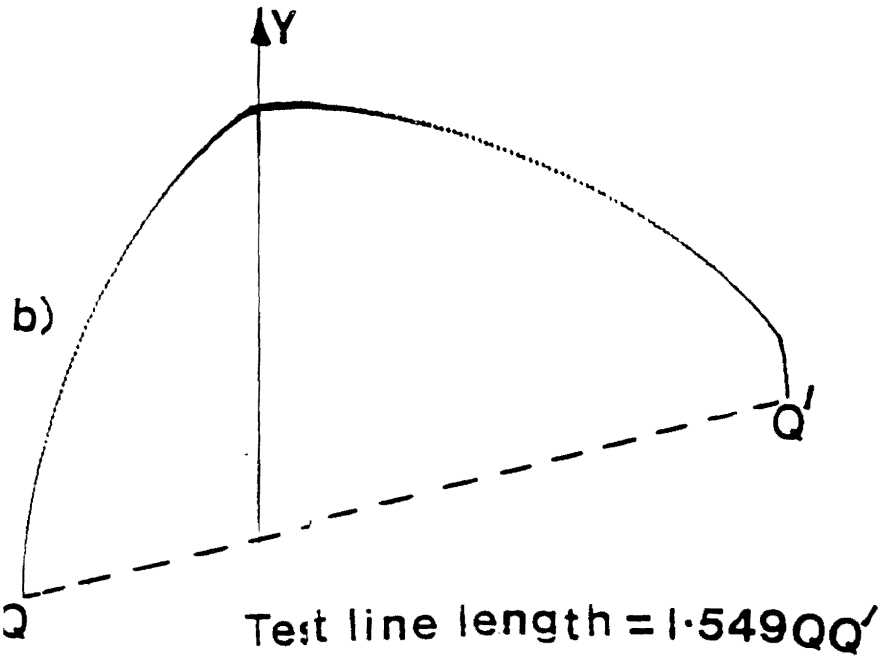

Test line length = 1·549QQ′

:e 2 Test line shapes for estimating the fourier sine coefficients b_2 and b_4: figure (a) is for b_2 and figure (b) is for b_4

2

PROGRESS REPORT

The objective of this research project is the development of general techniques for the quantitative characterization of the geometry of the fracture surfaces and the microstructural features involved in the deformation and fracture processes. This involves the applications and development of unbiased and assumption free stereological relationships. The research consists of analytical theoretical work, computer simulations and calculations, and the experimental measurements. We have made very significant progress during the last one year. These results are reported in nine publications in the scientific journals and conference proceedings. The research efforts have resulted in twelve presentations in the conferences and seminars. These presentations include four invited lectures; one of these presentations was the invited theme lecture in the 8th International Congress for Stereology. One student has completed his M.S. thesis work, and another student is close to the completion of his Ph.D. thesis work. Our results are equally useful for the quantification of biological structures; our publications are cited in the papers published by other research workers in the journals such as Experimental Physiology, and American Journal of Physiology. The following is the summary of the progress.

THEORETICAL DEVELOPMENTS

(1) A new stereological technique is developed for the estimation of the length density of lineal microstructural features from the projected images of the slices (or foils) of unknown and variable thickness. The result is assumption-free

and yields unbiased estimates. It is useful for the estimation of dislocation density from TEM foils of unknown and variable thickness.

Publications: No. 1; Presentations: No. 1

(2) A technique has been developed for the calculation of the evolution of bivariate size distributions from the given models for growth/shrinkage rate and nucleation/annihilation rate. The result is useful for modelling size distributions of cavities and voids during creep or creep-fatigue processes. The procedure can be also used to calculate bivariate particle growth rates from experimentally measured bivariate size distributions.

Publications: No. 3, and 7; Presentations: No. 5

(3) A simple technique is developed to measure the growth rates of thermally induced microcracks resulting from thermal cycling of composites.

Publications: No. 5; Presentations: No. 2 and 6

(4) Statistical analysis of fracture profiles is carried out to determine efficient sampling procedures for profilometry of fracture profiles.

Presentation: No. 11

(5) Theoretical analysis is carried out for interpretation of experimentally measured 'fractal dimension' obtained from different techniques.

Publication: No. 2; Presentations: No. 4,7

EXPERIMENTAL WORK

(1) Stereological techniques were utilized to quantify the damage evolution during the thermal cycling of metal-matrix composite

consisting of aligned alumina fibers distributed in Al-Li alloy matrix. The evolution of microcracks was monitored as a function of the number of thermal cycles. The volume fraction, surface area and number density of microcracks were stereologically measured. These data were utilized to calculate microcrack growth rate.

Publication: 5; Presentations: 2,6

(2) The creep experiments were completed. The stereological properties of creep cavities were measured as a function of time and applied stress.

(3) The creep fracture surfaces were quantified. A simple quantitative test is developed to distinguish between the creep fracture surfaces and the tensile fracture surfaces. These observations are useful for failure analysis.

Publication: No. 4; Presentation: No. 12

(4) A series of fracture surfaces of low alloy AISI 4340 steel were generated by different types of tests (impact, tensile) on the samples having different microstructures. The fracture surfaces have been quantified by measuring fractal dimension, surface roughness, etc. The correlations of these fractographic data with the mechanical properties and fracture mechanisms are investigated.

Publication: 2; Presentations: 4, 7, 9, 10, and 11

RESEARCH PLAN FOR THE NEXT YEAR

It is proposed to focus the research efforts on the following aspects during the third year of the project.

(1) Development of stereological procedures to calculate anisotropy of the lineal microstructural features from their

projected images. The results should be useful to describe geometric anisotropy of dislocation lines.

(2) Applications of fractal plot, i.e. roughness vs. ruler length, to obtain quantitative spatial characteristics of the features observed by SEM fractography.

(3) Analysis of microstructural data obtained from the creep experiments.

(4) Further analysis of creep fracture and tensile fracture surfaces with the goal to generate additional information for failure analysis.

(5) To complete the analysis of fractographic data on 4340 steel to obtain information concerning the fracture mechanisms.

(6) Additional experimental work on fractography of 4340 steel and also on the thermal cycling and fatigue of metal-matrix composite.

RESIDUAL FUNDS

It is anticipated that there will be no residual funds at the end of the present grant period.

THESIS ACKNOWLEDGING NSF SUPPORT

1. Surendra Mishra, M.S. thesis, January, 1992.

PUBLICATIONS ACKNOWLEDGING NSF SUPPORT

(1) A.M. Gokhale, "Estimation of Length Density L_v From Vertical Slices of Unknown Thickness", Journal of Microscopy (Royal Microsc. Soc.), in press.

(2) W.J. Drury and A.M. Gokhale, "Measurement and Interpretation of Fracture Surface Fractal Dimension", Proceedings of ASTM Symposium: "Metallography: 75 Years Later", ASTM Spec. Tech Pub., in press.

(3) A.M. Gokhale, "Bivariate Growth Path Analysis", Acta Stereologica, in press.

(4) A.M. Gokhale and Surendra Mishra, "Application of Quantitative Fractography to Creep Studies", Proceedings of Fifth International Conference on Creep of Materials, ASM, in press.

(5) A.M. Gokhale and W.J. Whited, "Measurements of the Growth Rates of Thermally Induced Microcracks in a Metal-Matrix Composite", Proceedings of Symposium on "Developments in Ceramics and Metal-Matrix Composites", TMS Annual Meeting, March 1-5, 1992, San Diego, California, published by TMS, K. Upadhya, ed., pp. 273-286.

(6) G.F. Vander Voort and A.M. Gokhale, "Comments on Grain Size Measurements Using the Point Sampled Intercept Technique", Scripta Met., in press.

(7) A.M. Gokhale, "Evolution of Bivariate Particle Size Distributions", Metall. Trans.-A, submitted.

(8) E.E. Underwood, "Directed Measurements and Heterogeneous Structures in Quantitative Fractography", Acta Stereologica, 1991, vol. 10 (no. 2), pp. 149-165.

(9) E.E. Underwood, "Metallography", McGraw-Hill Year Book of Science and Technology, 1992, pp. 246-250.

PRESENTATIONS IN THE CONFERENCES AND SEMINARS

(1) A.M. Gokhale, "Recent Developments in Quantitative Metallography", Symposium on Quantitative Metallography and Computer Aided Microscopy of P/M Processed Materials, TMS Annual Meeting, San Diego, California, March 1-5, 1992 (INVITED LECTURE)

(2) A.M. Gokhale and W.T. Whited, "Measurements of the Growth Rates of Thermally Induced Microcracks in a Metal-Matrix Composites", Symposium on "Developments in Ceramic and Metal-Matrix Composites", TMS Annual Meeting, San Diego, California, March 1-5, 1992.

(3) A.M. Gokhale, "Stereology of Cast Microstructures", Seminar at General Motors, Saginaw, Michigan, February 11, 1992.

(4) A.M. Gokhale, "Recent Developments in Quantitative Fractography", Symposium on "Computational Metallurgy", ALCOA, Pittsburgh, October 13-18, 1991 (INVITED LECTURE).

(5) A.M. Gokhale, "Evolution of Bivariate Particle Size Distributions", 8th International Congress for Stereology, Irvine, California, August 25-30, 1991 (INVITED THEME LECTURE)

(6) A.M. Gokhale and W.T. Whited, "Evolution of Microstructural Damage During Thermal Cycling of Metal-Matrix Composite", ASME Summer Conference on Applied Mechanics and Biomechanics, Columbus, Ohio, June 17-19, 1991.

(7) A.M. Gokhale and W.J. Drury, "Measurement and Interpretation of the Fracture Surface Fractal Dimension", ASTM Symposium on "Metallography: 75 Years Later", Atlantic City, N.J., May 8-10, 1991.

(8) A.M. Gokhale, "Microstructural Evolution During Thermal Cycling of Metal-Matrix Composite" Seminar given at Oak Ridge National Laboratory, Oak Ridge, TN, April 18, 1991.

(9) A.M. Gokhale, "Modern Quantitative Fractography" ASM Educational Symposium on "Image Based Analysis Techniques, ASM, Oak Ridge, TN, April 18, 1991 (INVITED LECTURE).

The following papers have been accepted for presentation in the following conferences scheduled in the near future:

(10) A.M. Gokhale and N.U. Deshpande, "Recent Developments in Quantitative Fractography", ASTM Second Symposium on "Fractography of Modern Engineering Materials, Pittsburgh, May 6, 1992.

(11 W.J. Drury and A.M. Gokhale, "Statistical Considerations in the Digital Profilometry", ASTM Second Symposium on "Fractography of Modern Engineering Materials, Pittsburgh, May 6, 1992

(12) A.M. Gokhale and Surendra Mishra, "Application of Quantitative Fractography to Creep Studies", Fifth International Conference on Creep of Materials, Orlando, Florida, May 18-21, 1992.

CURRENT AND PENDING SUPPORT

A.M. GOKHALE

Source of Support	Project Title	Award	Funding Period	Effort	Location
NSF	1	$292,320	7/90-7/93	2 months (summer)	Ga. Tech
ALCOA	2	$ 65,000	1/91-1/94	1 month	Ga. Tech.

E.E. UNDERWOOD

Source of Support	Project Title	Award	Funding Period	Effort	Location
NSF	1	$292,320	7/90-7/93	2 months (cal.)	Ga. Tech

Project Titles

1. Quantitative Analysis of Fracture Surfaces Using Stereological Methods.
2. Research Grant for Research in the Area of Stereology.

E18609

OMB Number 3145-0058

NATIONAL SCIENCE FOUNDATION
1800 G STREET, NW
WASHINGTON, DC 20550

BULK RATE
POSTAGE & FEES PAID
National Science Foundation
Permit No. G-69

PI/PD Name and Address

Arun Manohar Gokhale
School of Materials Engineering
~~GA Tech Res Corp - GIT~~
Georgia Institute of Technology
Atlanta GA 30332 0245

NATIONAL SCIENCE FOUNDATION
FINAL PROJECT REPORT

PART I - PROJECT IDENTIFICATION INFORMATION

1. Program Official/Org. Bruce A. MacDonald - DMR

2. Program Name METALS, CERAMICS, & ELECTRONIC MATERIALS

3. Award Dates (MM/YY) From: 07/9 To: 12/93

4. Institution and Address
GA Tech Res Corp - GIT
Administration Building
Atlanta GA 30332

5. Award Number 9013696

6. Project Title
Quantitative Analysis of Fracture Surfaces Using Stereological Methods

This Packet Contains
NSF Form 98A
And 1 Return Envelope

PART IV -- FINAL PROJECT REPORT -- SUMMARY DATA ON PROJECT PERSONNEL

(To be submitted to cognizant Program Officer upon completion of project)

The data requested below are important for the development of a statistical profile on the personnel supported by Federal grants. The information on this part is solicited in resonse to Public Law 99-383 and 42 USC 1885C. All information provided will be treated as confidential and will be safeguarded in accordance with the provisions of the Privacy Act of 1974. You should submit a single copy of this part with each final project report. However, submission of the requested information is not mandatory and is not a precondition of future award(s). Check the "Decline to Provide Information" box below if you do not wish to provide the ntormation.

Please enter the numbers of individuals supported under this grant.
Do not enter information for individuals working less than 40 hours in any calendar year.

	Senior Staff		Post-Doctorals		Graduate Students		Under-Graduates		Other Participants[1]	
	Male	Fem.	Male	Fem.	Male	Fem.	Male	Fem.	Male	Fem.
A. Total, U.S. Citizens	1	0	0	0	2	1				
B. Total, Permanent Residents	1	0	0	0	0	0				
U.S. Citizens or Permanent Residents[2]:										
American Indian or Alaskan Native										
Asian	1	0			0	0				
Black, Not of Hispanic Origin					0	0				
Hispanic					0	0				
Pacific Islander					0	0				
White, Not of Hispanic Origin	1	0			2	1				
C. Total, Other Non-U.S. Citizens	0	0	0		2	0				
Specify Country 1. India					2	0				
2.										
3.										
D. Total, All participants (A + B + C)	2	0	0	0	4	1				
Disabled[3]	0	0	0	0	0	0	0	0	0	0

☐ Decline to Provice information: Check box if you do not wish to provide this information (you are still required to return this page along with Parts I-III).

[1] Category includes, for example, college and precollege teachers, conference and workshop participants.

[2] Use the category that best describes the ethnic/racial status fo all U.S. Citizens and Non-citizens with Permanent Residency. *(If more than one category applies, use the one category that most closely reflects the person's recognition in the community.)*

[3] A person having a physical or mental impairment that substantially limits one or more major life activities; who has a record of such impairment; or who is regarded as having such impairment. *(Disabled individuals also should be counted under the appropriate ethnic/racial group unless they are classified as "Other Non-U.S. Citizens.")*

AMERICAN INDIAN OR ALASKAN NATIVE: A person having origins in any of the original peoples of North America and who maintains cultural identification through tribal affiliation or community recognition.

ASIAN: A person having origins in any of the original peoples of East Asia, Southeast Asia or the Indian subcontinent. This area includes, for example, China, India, Indonesia, Japan, Korea and Vietnam.

BLACK, NOT OF HISPANIC ORIGIN: A person having origins in any of the black racial groups of Africa.

HISPANIC: A person of Mexican, Puerto Rican, Cuban, Central or South American or other Spanish culture or origin, regardless of race.

PACIFIC ISLANDER: A person having origins in any of the original peoples of Hawaii; the U.S. Pacific territories of Guam, American Samoa, and the Northern Marinas; the U.S. Trust Territory of Palau; the islands of Micronesia and Melanesia; or the Philippines.

WHITE, NOT OF HISPANIC ORIGIN: A person having origins in any of the original peoples of Europe, North Africa, or the Middle East.

A.M. Gokhale
DMR-9013098

PART - II

SUMMARY OF COMPLETED PROJECT

The basic objective of this research was to develop general, unbiased, efficient, and practical stereological and fractographic procedures for quantitative characterization of fracture surfaces and microstructural features in three dimensional space from the observations on the lower dimensional manifolds such as two dimensional sections and projections. These techniques were utilized to study the processes that govern the deformation and fracture of materials. The resulting information is useful to optimize the properties of the existing materials and for the development of new materials. As our stereological techniques are absolutely general, they are also applicable to biological structures. Some of the stereological methods developed during this project are being currently utilized by biologists to estimate length density of microvessels in brain, lengths of capillaries in heart, etc. The results of our research are reported in 17 technical publications, 10 conference presentations (6 invited papers), a theme lecture in 8th International congress for Stereology, two M.S., and one Ph.D. thesis.

The basic components of this project were analytical theoretical work, computer simulations/calculations, and experimental measurements to demonstrate the utility of the new stereological and quantitative fractographic techniques. The experimental portion of the project involved study of creep fracture and creep damage in copper, fatigue crack closure in inconel-718, impact and tensile fracture surfaces of AISI 4340 steel having different microstructure, and microcrack damage in thermally cycled metal matrix composite. We have developed new stereology based method for estimation of average growth rate of thermally induced microcracks in composite materials. A new method has been developed for estimation of length density of lineal features (e.g. dislocations) from projected images of foils of unknown and variable thickness. We have developed a general method for estimation of fractal dimension of anisotropic surfaces from profilometric data. These results are utilized to correlate fractal dimension to absorbed impact energy in AISI 4340 steel. The stereological measurements were utilized to develop a model for cavity nucleation during creep of copper. The image analysis techniques have been developed to quantify spatial arrangements of microstructural features.

A.M. Gokhale
DMR-9013098

PART-III

TECHNICAL INFORMATION

This project work concerns development of quantitative fractographic and microscopic techniques based on stereological principles, and applications of the new methods to the study of deformation and fracture of monolithic and composite materials to illustrate their utility and demonstrate their practical application. The results are useful for development of quantitative correlations of material microstructure to the operative deformation and fracture processes. The basic components of these research were analytical theoretical work, image analysis and software development, computer simulations and calculations, and experimental studies of fracture processes using the new quantitative techniques. The analytical theoretical research involved applications of stochaistic geometry, fractal geometry, and differential geometry to develop the techniques for the estimation of geometric attributes of nonplanar and rough fracture surfaces, and microstructures, in 3D space from the measurements performed on the random or design based 2D sections and projected images. The digital image profilometric techniques have been developed for acquiring the necessary data on fracture profiles. Computer simulations have been utilized to arrive at efficient sampling procedures for quantification of microstructures and fracture surfaces.

Our research has contributed significantly to the development of quantitative fractography and design based stereology. The results are reported in 17 publications in archival technical journals and conference proceedings (list of publications is enclosed), two M.S., and one Ph.D. thesis. The following is a brief summary of this progress.

(A) Analytical Theoretical Work:

(i) A new stereological equation has been derived to estimate the length density of lineal microstructural features such as dislocation lines, fibers, etc. from the measurements performed on the projected images of foils (slices) of unknown and variable thickness (1); the same data also yields average foil thickness. A new concept of sampling with "horizontal slice" is developed to estimate the total number of lineal feature end points from projected images (2).

(ii) A general and flexible procedure has been developed to calculate the evolution of bivariate size and shape (or orientation) distribution of particles/voids/cavities/microcracks

during an evolution process, from modelled nucleation and growth kinetics of individual features (3). The development will be subsequently utilized to model the evolution of size and orientation distribution of microcracks and voids. A simple and general procedure is also developed to calculate individual bivariate particle/microcrack growth paths and growth rates from a series of experimentally measured bivariate distributions during an evolution process (3,4).

(iii) A general stereological equation has been derived to estimate the fractal dimension of anisotropic fracture surfaces, where profile fractal dimension may vary with the orientation of the sectioning plane (5,6).

(iv) A new fractographic parameter is defined to quantify the extent of overlaps (re-entrant regions) in fracture surfaces (7). These concepts are utilized to clearly distinguish between the topography of creep fracture and tensile fracture surfaces (6).

(v) Some new methods of grain size measurement have been critically analyzed (8).

(B) Computer Calculations and Simulations:

(i) Extensive computer calculations and simulations have been carried out to identify efficient sampling schemes for reliable estimation of fracture profile roughness parameter (and hence fracture surface roughness) when the measurements are performed only on limited number of short profile segments rather than the whole profile (9).

(ii) It is shown that sampling with "trisector" yields reliable estimates of total microstructural surface area per unit volume. Three vertical sections mutually at an angle of 120 deg. and having a common zone axis (called vertical axis) contain sufficient information for a reliable estimation of the total surface area per unit volume in a microstructure having arbitrary and unknown anisotropy and geometry (10). The intersection counting on trisector planes must be performed by using design based cycloid shape test lines. The computer simulations were also utilized to examine the effect of misorientation of the trisector planes on the precision of estimated surface roughness (11), and total microstructural surface area per unit volume (12).

(C) Feature Specific Digital Image Profilometry:

Software has been developed to extract some feature specific

geometric information directly and automatically from set of (X,Y) coordinates of points that describe digitized fracture profile. Further work on feature specific Profilometry and the analysis of resulting data are a part of ongoing research.

(D) Experimental Work:

(i) Charpy impact tests and tensile tests were performed on a series of specimens of AISI 4340 steel having different hardness (produced by different tempering treatment). The profilometric measurements clearly showed that the fractal dimension of impact fracture surfaces decreases systematically with the distance from the initial notch: the correlation between impact energy and fractal dimension thus depends on where on the fracture surface the measurements are performed. The impact energy does not correlate to the average fractal dimension, but it shows strong correlation with the fractal dimension of the region of impact fracture surface adjacent to the charpy notch (5,6). This resolves some contradicting observations reported in the literature.

(ii) A new experimental technique is developed to estimate the average growth rate of microcracks in composites during the processes such as thermal cycling. The technique was applied to measure average growth rate of microcracks formed during thermal cycling of a metal matrix composite containing continuous alumina fibers distributed in the Al-Li alloy matrix (13). Such data should be useful to model microcrack damage evolution in composites.

(iii) The design based efficient stereological techniques were used to quantify evolution of population of cavities formed during high temperature creep of copper. The resulting stereological data were used to estimate cavity nucleation rate and growth rates (14). The fractographic measurements on the creep fracture surfaces were utilized to estimate extent of surface overlap and fractal dimension. It was shown that extent of fracture surface overlap can be used to distinguish between creep fracture and tensile fracture surfaces (6).

A.M. Gokhale
DMR-9013098

LIST OF PUBLICATIONS ACKNOWLEDGING NSF SUPPORT

(1) A.M. Gokhale: "Estimation of Length Density L_V From Vertical Slices of Unknown Thickness", **Journal of Microscopy**, 1992, Vol.167, PP. 1-8.

(2) A.M. Gokhale: "Utility of Horizontal Slice for Stereological Characterization of Lineal Features", **Journal of Microscopy**, 1993, Vol.170, PP. 3-8.

(3) A.M. Gokhale: "Evolution of Bivariate Particle Size Distributions", **Metall. Trans.-A**, 1992, Vol.23A, PP. 2973-2980.

(4)A.M. Gokhale: "Bivariate Growth Path Analysis", **Acta Stereologica**, 1992, Vol.11, Suppl.-1, PP. 255-463.

(5)W.J. Drury and A.M. Gokhale: "Measurement and Interpretation of Fracture Surface Fractal Dimension", **ASTM Standard Tech. Pub. No. 1165 : Metallography: Past, present, and Future**, G.F. Vander Voort, et. al., eds., ASTM, 1993, PP.295-309.

(6)A.M. Gokhale, W.J. Drury, and S. Mishra: "Recent Developments in Quantitative Fractography", **ASTM Standard Tech. Pub. No. 1203: Fractography of Modern Engineering Materials**, J.E. Masters and L.E. Gilbertson, eds., ASTM, 1993, PP. 3-22.

(7)E.E. Underwood: "Evaluation of Overlaps in Fracture Surfaces", **ASTM Standard Tech. Pub. No.1094: Micon-90: Advances in Video Technology for Microstructural Control**, G.F. Vander Voort, ed., ASTM, 1991, PP.340-353.

(8)G.F. Vander Voort and A.M. Gokhale: "Comments on Grain Size Measurements Using Point Sampled Intercepts", **Scripta Met. Mat.**, 1992, Vol.26, PP. 1655-1660.

(9)W.J.Drury and A.M. Gokhale: "Statistical Considerations in the Digital Profilometry of Fracture Surfaces", **ASTM Standard Tech. Pub. No. 1203: Fractography of Modern Engineering Materials,** J.E. Masters L.E. Gilbertson, eds., ASTM, 1993, PP. 125-133.

(10)A.M. Gokhale and W.J. Drury: "Efficient Measurement of Microstructural Surface Area Using Trisector", **Metall. Trans.-A**, in press (to appear in May 1994 issue).

(11)A.M. Gokhale and W.J. Drury: "Surface Roughness of Anisotropic Fracture Surfaces", **Materials Characterization**, 1993, Vol.31, PP. 115-123.

(12)A.M. Gokhale, W.J. Drury, and W.T. Whited: "Quantitative Microstructural Analysis of Anisotropic Materials", **Materials Characterization**, 1993, Vol.31, PP. 11-18.

(13)A.M. Gokhale and W.T. Whited: "Measurements of the Growth Rates of Thermally Induced Microcracks in a Metal Matrix Composite", **Proceedings of Symposium on " Developments in Ceramic and Metal Matrix Composites"**, K. Upadhya, ed., TMS, Warrendale, PA., 1992, PP. 273-286.

(14)A.M. Gokhale: "Utility of Stereological Measurements in the Study of Creep Cavitation", **ASTM Standard Tech. Pub. No. 1094: Micon-90: Advances in Video Technology for Microstructural Control**, G.F. Vander Voort, ed., ASTM, 1991, PP. 332-339.

(15)E.E. Underwood: "Directed Measurements and Heterogenous Structures in Quantitative Fractography", **Acta Stereologica**, 1991, Vol.10, PP. 149-165.

(16)E.E. Underwood: "Metallography", **McGraw-Hill Year Book of Science and Technology**, New York, NY, 1992, PP. 246-350.

(17)E.E. Underwood: "Treatment of Reversed Sigmoidal Curves for Fractal Analysis", **ASTM Standard Tech. Pub. No. 1094: Micon-90: Advances in Video Technology for Microstructural Control**, G.F. Vander Voort, ASTM, 1991, PP. 354-364.